NTNU
Norwegian University of
Science and Technology

2) Cloud Radio Access Networks (C-RAN) and optical Mobile backhaul and fronthaul

Dawit Hadush Hailu

Master of Telematics - Communication Networks and Networked Services
Submission date: June 2016
Supervisor: Steinar Bjørnstad, ITEM

Norwegian University of Science and Technology
Department of Telematics

Title:	Cloud Radio Access Networks (C-RAN) and Optical Mobile backhaul and fronthaul networks
Student:	Dawit Hadush Hailu

Problem description:

TransPacket AS (www.transpacket.com) develops the fusion networking, a packet oriented network implementing the principle of integrated hybrid optical networks/ IHON, for efficiently serving both the circuit switched Guaranteed Service Transport (GST) with absolute priority and packet switched Statistically Multiplexed (SM) best effort traffic. The company addresses the transport using optical networks between the controller of the mobile network and the mobile base-stations. Due to a high demand of bandwidth in mobile networks, the need for higher density of cell sites is increasing to meet this demand. Along with this, a cost efficient technology is required for keeping the costs at the moderate level. Thus, the main objective of this thesis is to evaluate the fusion networking as a mobile fronthaul in terms of latency and packet delay variation (PDV). Further, the student will study the latency and packet delay variation in radio over Ethernet mobile fronthaul networks and how well may this be supported in an IHON Ethernet mobile fronthaul. The thesis consists of the following tasks:

- Background study of different fronthaul optical solutions and the evolution of Cloud Radio Access Network (C-RAN).
- Study the fronthaul requirements of mobile networks.
- Investigate the performance of IHON node and standard Ethernet switch.

The evaluation methodology used to achieve the above mentioned objective will be a Simula based on Discrete Event Modelling On Simula (DEMOS) software, a context class for discrete event simulation.

Responsible professor:	Steinar Bjørnstad, ITEM
Supervisor:	Steinar Bjørnstad, ITEM

Abstract

Increasing mobile data traffic due to the rise of both smartphones and tablets has led to high-capacity demand of mobile data network. To meet the ever-growing capacity demand and reduce the cost of mobile network components, Cloud Radio Access Network (C-RAN) has emerged as a promising solution. In this network, the mobile operator's Remote Radio Head (RRH) and Base Band Unit (BBU) are often separated and the connection between them has very tight timing and latency requirements imposed by Common Public Radio Interface (CPRI) and 3rd Generation Partnership Project (3GPP). This fronthaul connection is not yet provided by packet based network. To employ packet-based network for C-RAN fronthaul, the carried fronthaul traffic are needed to achieve the requirements of fronthaul streams. For this reason, the aim of this study was focused on investigating and evaluating the feasibility of Integrated Hybrid Optical Networks (IHON) and Ethernet networks for mobile fronthaul. The fronthaul requirements used to evaluate and investigate these networks were maximum End to End (E2E) latency, Packet Loss Ratio (PLR) and Packet Delay Variation (PDV).

TransPacket AS (www.transpacket.com) develops a fusion switching that efficiently serves both Guaranteed Service Transport (GST) traffic with absolute priority and packet switched Statistical Multiplexing (SM) best effort traffic. Dedicated wavelength is used to provide a deterministic circuit switched transport and uses the leftover capacity on the wavelength to transport the best effort traffic without affecting the absolute priority packets. We verified how the leftover capacity of fusion node can be used to carry the low priority packets and how the GST traffic can have deterministic characteristics on a single wavelength by delaying it with Fixed Delay Line (FDL). For example, for L_{1GE}^{SM}=0.3 the added SM traffic increases the 10GE wavelength utilization up to 89% without any losses and with SM PLR=$1E^{-03}$ up to 92% utilization.

The simulated results and numerical analysis confirm that the PDV and PLR of GST traffic in IHON network and the PLR of High Priority (HP) traffic in Ethernet network meet the requirements of mobile fronthaul using CPRI. However, the PDV of HP traffic meets the fronthaul network when the number of nodes in the Ethernet network is at most four. For both IHON and Ethernet network, the number of nodes in the network limits the maximum separation distance between BBU and RRH (link length); for increasing the number of nodes, the link length decreases. Consequently, Radio over Ethernet (RoE) traffic should receive the priority

and Quality of Service (QoS) only GST or HP can provide. On the other hand, SM or Low Priority (LP) classes are not sensitive to QoS metrics and should be used for transporting time insensitive applications and services.

Furthermore, we numerically evaluated the performance of active Wavelength Division Multiplexing (WDM) when Optical Transmission Network (OTN) encapsulation is employed and dedicated fronthaul networks in terms of the maximum one-way latency and the maximum separation distance between BBU and RRH provided that the typical values of BBU are known.

Acknowledgment

The success and final outcome of this thesis required a lot of guidance, support, and motivation. I am deeply indebted to my supervisor Steinar Bjørnstad who was always willing to share his deep insights, wide knowledge, and extensive experiences. His suggestions and mind stimulating discussions, leading me to further expand and deepen my knowledge. In a time of losing confidence and facing problems, it was his motivation, guidance, valuable feedback and support that helped me to think in several ways and prompted me to think beyond the obvious. Generally speaking, without him, the completion of this thesis would have been impossible.

I would also like to express my deepest gratitude to Laurent Paquereau and Mona Nordaune for their administrative assistance. My acknowledgment also goes to Raimena Veisllari and Norvald Stol for their support and encouragement during the work. Moreover, I am really thankful to my uncle Abera Hailu for the unceasing encouragement, support, and attention.

Preface

This thesis is submitted as the completion of MSc. degree in Telematics specialized in Networks and QoSs at the Norwegian University of Science and Technology (NTNU). The thesis described herein was conducted under the supervision of Adjunct Associate Professor Steinar Bjørnstad at the Department of Telematics, NTNU and is the product of the master period, between January 2016 and June 2016. It has a workload of 30 European Credit Transfer System (ECTS) credits. Yours truly has a bachelor degree in Electrical and Computer Engineering from Mekelle University (MU).

Contents

List of Figures xi

List of Tables xiii

List of Acronyms xv

1 Introduction 1
- 1.1 Introduction . . . 1
- 1.2 Background and Motivation . . . 1
- 1.3 Statement of the Problem . . . 6
- 1.4 Objectives of the Thesis . . . 6
- 1.5 Methodology . . . 7
- 1.6 Thesis Outline . . . 7

2 Cloud Radio Access Network/C-RAN 9
- 2.1 Introduction . . . 9
- 2.2 Evolution of BS Architecture . . . 10
- 2.3 C-RAN Architecture . . . 11
  - 2.3.1 C-RAN System Architecture . . . 12
  - 2.3.2 C-RAN Components . . . 13
  - 2.3.3 Advantages of C-RAN . . . 14
- 2.4 Optical Networks for C-RAN . . . 15
- 2.5 Fronthaul Transport Options . . . 16
  - 2.5.1 Dedicated Fiber . . . 17
  - 2.5.2 Passive WDM . . . 18
  - 2.5.3 Microwave . . . 19
  - 2.5.4 OTN . . . 19
  - 2.5.5 Ethernet . . . 21
- 2.6 Radio over Ethernet . . . 22

3 Fronthaul Network Requirements 27
- 3.1 Requirements and Challenges of Fronthaul Networks . . . 28
  - 3.1.1 Data Rate . . . 28

3.1.2 Latency . . . 29
3.1.3 Packet Delay Variation . . . 31
3.1.4 Synchronization and Jitter . . . 31

4 Integrated Hybrid Optical Networks/IHON 33
4.1 Introduction . . . 33
4.2 Hybrid Optical Network Architectures . . . 34
4.2.1 Client-server Hybrid Optical Network . . . 34
4.2.2 Parallel Hybrid Optical Network . . . 35
4.2.3 Integrated Optical Hybrid Optical Network . . . 35
4.2.4 OpMiGua . . . 36
4.2.5 Fusion Solution/IHON Network . . . 37
4.3 IHON Node Design . . . 38
4.3.1 IHON Node Operation . . . 39
4.3.2 Delay and Packet Delay Variation in IHON Node . . . 40
4.3.3 Delay and Packet Delay Variation in Ethernet Switch . . . 41
4.3.4 Inter-packet Time Gap Computation in IHON Node . . . 43
4.4 IHON Node Aggregation . . . 44

5 Analytical/ Simulation Model 47
5.1 Maximum End-to-End Latency . . . 47
5.1.1 Maximum E2E Latency and Separation Distance for Active WDM . . . 48
5.1.2 Maximum E2E Latency and Separation Distance for Dedicated Fiber . . . 51
5.1.3 Maximum E2E Latency and PDV for Ethernet Networks . . . 52
5.2 Simulation Model for IHON Node and Standard Ethernet Switch . . . 53
5.2.1 Traffic Pattern . . . 53

6 Results and Discussions 55
6.1 Simulation Parameters . . . 55
6.2 IHON Node Performance . . . 56
6.2.1 GST Traffic Performance . . . 58
6.2.2 SM Traffic Performance . . . 59
6.2.3 Comparison Between GST and SM Traffic Performance in IHON Node . . . 62
6.3 Ethernet Switch Performance . . . 64
6.3.1 HP Traffic Performance . . . 65
6.3.2 LP Traffic Performance . . . 67
6.4 Mobile Fronthaul Networks . . . 69
6.4.1 Evaluation of IHON Network for Mobile Fronthaul Network . 70
6.4.2 Evaluation of Ethernet Network for Mobile Fronthaul Network 72

6.5 Application of Ethernet streams in Fronthaul Network 75

7 Summary and Conclusion **77**
7.1 Summary 77
7.2 Conclusion 78

8 Future Work **81**
8.1 Future Work 81

References **83**

Appendices

A IHON Node and Ethernet Switch Implementation **89**
A.1 IHON Node Implementation 89
A.1.1 GST_Generator Entity 89
A.1.2 SMGenerator 89
A.1.3 GSTPacket Entity 90
A.1.4 SMPacket Entity 90
A.1.5 SM_packet_scheduler Entity 90
A.1.6 SM_Waiting bin 91
A.1.7 SM_pkt_check and GST_pkt_check queues 91
A.2 Ethernet Switch Implementation 91
A.2.1 HP_Generator Entity 91
A.2.2 LP_Generator Entity 91
A.2.3 HPPacket Entity 92
A.2.4 LPPacket Entity 92
A.2.5 HP_packet_scheduler Entity 92
A.2.6 LP_packet_scheduler Entity 92
A.2.7 HP_Waiting Bin 93
A.2.8 LP_Waiting Bin 93
A.3 IHON and Ethernet Source Codes 93
A.4 Input File and Output File 93
A.5 Simulator Validation 95

B QoS Targets for Reference Service Classes **98**

C Example of Input File **99**
C.1 Input File for IHON Code: Input_IHON.txt 99
C.2 Input File for Ethernet Code: Input_Ethernet.txt 100

D Confidence Interval Calculation In the Simulator **101**

List of Figures

1.1 Mobile backhaul and fronthaul network architecture in Long Term Evolution (LTE), extracted from [AWP15]. 4

2.1 Base station architecture for traditional macro Base Station (BS) (no BBU hotelling), extracted from [CCY+15]. 10
2.2 Base station architecture for BS with RRH, extracted from [CCY+15]. . 11
2.3 Base station architecture for C-RAN with RRHs, extracted from [CCY+15]. 12
2.4 Options of C-RAN system architecture including the split functions of RRH and BBU, extracted from [PWLP15]. 13
2.5 RRH components, adopted [LKB09]. 14
2.6 Point to point fiber [PMC15]. 17
2.7 Passive WDM [PMC15]. 18
2.8 Active WDM [PMC15] 19
2.9 OTN based mobile fronthaul solution [PMC15]. 20
2.10 Ethernet packet format, extracted from [For]. 21
2.11 Ethernet packet format to support the Radio over Ethernet(RoE), extracted from [For]. 23
2.12 Radio over Ethernet(RoE) fame structure, extracted from [For]. 24

3.1 Packet stream synchronization. 32

4.1 Client-server hybrid optical networks [GKB+06]. 35
4.2 Parallel hybrid optical networks [GKB+06]. 35
4.3 Integrated hybrid optical networks [GKB+06]. 36
4.4 A hybrid network model illustrating the sharing of the physical fiber layer. The optical cross connects and optical packet switches are co-located, either as separate units or as one integrated unit. The WRON can be a Static or a Dynamic-WRON [BNOS05]. 37
4.5 Fusion network: created by combining the best properties of packet and circuit switching, extracted from [Tra12]. 38
4.6 Schematic diagram of IHON node design, extracted from [VBB13]. . . . 39
4.7 Internal operation of IHON node, adopted from [VBB13]. 40

4.8 a) Inter packet gap and delay experienced by GST packets, b) Scheduling in strict priority QoS in packet switches where packet delay variation (PDV) occurs on high-priority packets, c) Scheduling in fusion node where SM packets are inserted only if there is a suitable gap between the GST packets, extracted from [VBB13]. 42
4.9 First-In First-Out (FIFO) delay on Ethernet switch 42
4.10 Detection of free time gaps with in the time window created by the fixed delay, extracted from [VBB13]. 43
4.11 Aggregation of five GST streams and SM insertion. The figure explains how GST traffic are aggregated in fusion node, and how the insertion of SM packet is achieved [VBB+15]. 46

5.1 The maximum end to end latency in C-RAN network. 48
5.2 Delay contribution of the BBU and RRH along the fronthaul network. . 50

6.1 Diagram illustrating how the IHON node is connected to Packet generators for measuring the performance metrics. 57
6.2 Average latency of SM traffic as function of GST load for SM load=0.1, 0.35 and 0.4(IHON node). 60
6.3 Packet delay variation of SM traffic as function of GST load (IHON node). 61
6.4 PLR of SM traffic as function of GST load (IHON node). 61
6.5 Average latency of SM and GST traffics as function of GST load for SM load=0.1 (IHON node) 62
6.6 Packet delay variation of SM and GST traffics as function of GST load for SM load=0.1(IHON node). 63
6.7 Illustration of Ethernet Switch for measuring the performance of HP and LP traffic. 64
6.8 Average latency of HP traffic as function of HP load for LP load 0.4 and 0.45(Ethernet switch). 65
6.9 PDV of HP traffic as function of HP load for HP load=0.4 and 0.45 (Ethernet switch). 66
6.10 Average latency of LP traffic as function of HP load for LP load=0.4 and 0.45 (Ethernet switch). 67
6.11 Packet delay variation of LP traffic as function of HP load for LP load=0.4 and 0.45 (Ethernet switch). 68
6.12 PLR of LP traffic as function of HP load for LP load=0.4 and 0.45 (Ethernet switch). 69
6.13 Mobile fronthaul network under study. The nodes can be either IHON node or Ethernet switch depending on the network under evaluation. . . 69

List of Tables

2.1 Optical fronthaul/transport options. 16
2.2 Allocated RoE `pkt_type` values where TBD stands for To Be Defined (since RoE frame structure is an ongoing work, some of the packet type values are not yet defined), extracted from [For]. 24

3.1 Detailed CPRI capacity requirement and application in support of mobile broadband where * means no information, extracted [PMC15]. 28
3.2 Latency, PDV and synchronization requirements for Ethernet Fronthaul with symmetry assumption. 30
3.3 Timing requirements for BS, extracted from [CJCB15] 32

4.1 Definition of parameters used in the gap computation. 44

5.1 Delay components of each parts of Figure 5.2, extracted from [HJS]. . . 49
5.2 Typical values of delay components in the fronthaul network, extracted from [HJS]. 49

6.1 Simulation parameters used in the analysis of performance metrics of SM and GST packets (for IHON node). 55
6.2 Notation of parameters used in the simulation result analysis. 56
6.3 Average latency, PLR, and PDV of SM and GST traffic as function of GST load for SM load=0.3 (IHON node). 57
6.4 Average latency and PDV of LP and HP traffics as function of HP load for HP load=0.4 (Ethernet switch). 64
6.5 Maximum link length and number of nodes in IHON network to meet the fronthaul requirements for GST traffic where L_{total}=50μsec, D_T=5μsec/km, and D_{node}=1.2μsec. 71
6.6 Average latency comparison between LP and HP traffics of Ethernet switch and fronthaul requirements for LP load=0.4. 73
6.7 Maximum link length and number of nodes in Ethernet network to meet the fronthaul requirements for HP traffic where L_{total}=50μsec, D_T=5μsec/km, and D_{node}=1.2μsec. 73

6.8 The Number of nodes in Ethernet network to meet the PDV fronthaul requirements for HP traffic where PDV_{total}=5μsec and PDV_{node}=1.2μsec. 74
6.9 PLR comparison between LP and HP traffics of Ethernet switch and Fronthaul requirements for LP load=0.4. 75

B.1 Requirements of demanding services and applications based on ITU-T recommendation Y.1541 [SSR11] 98

List of Acronyms

1G First Generation.

2G Second Generation.

3G Third Generation.

3GPP 3rd Generation Partnership Project.

5G Fifth Generation.

AWG Arrayed Wavelength Grating.

BBU Base Band Unit.

BE Best Effort.

BER Bit Error Rate.

BS Base Station.

BTS Base Transceiver Station.

C/M Control and Management functions.

CDMA Code Division Multiple Access.

CMCC China Mobile Communications Corporation.

CoMP Coordinated Multiple Point transmission and receptions.

CPRI Common Public Radio Interface.

C-RAN Cloud Radio Access Network.

CWDM Coarse Wavelength Division Multiplexing.

DA Destination Address.

DL DownLink.

D-RoF Digital Radio over Fiber.

DWDM Dense Wavelength Division Multiplexing.

E2E End to End.

FCS Frame Check Sequence.

FDD Frequency Division Duplexing.

FDL Fixed Delay Line.

FDMA Frequency Division Multiple Access.

FEC Forward Error Correction.

FIFO First-In First-Out.

GE Gigabit Ethernet.

GPS Global Positioning System.

GSM Global System for Mobile Communication.

GST Guaranteed Service Transport.

HARQ Hybrid Automatic Retransmit reQuest.

HetNet Heterogeneous Network.

HP High Priority.

HSDPA High Speed-Downlink Packet Access.

HSPA High Speed Packet Access.

HSUPA Enhanced High-Speed Uplink Packet Access.

IEEE Institute of Electrical and Electronics Engineers.

IETF Internet Engineering Task Force.

IHON Integrated Hybrid Optical Networks.

IT Information Technology.

ITU International Telecommunication Union.

ITU-T International Telecommunication Union - Telecommunication.

LAN Local Area Network.

LNA Low Noise Amplifier.

LP Low Priority.

LTE Long Term Evolution.

LTE-A Long Term Evolution-Advanced.

MAC Medium Access Control.

MBH Mobile Backhaul.

MFH Mobile Fronthaul.

MIMO Multiple Input Multiple Output.

MU Mekelle University.

NMT Nordic Mobile Telephone.

NTNU Norwegian University of Science and Technology.

OADM Optical Add/Drop Multiplexer.

OAM Operation Administration and Maintenance.

OBS Optical Burst Switched.

OBSAI Open Base Station Architecture Initiative.

OCS Optical Circuit Switched.

ODF Optical Distribution Frame.

OFDMA Orthogonal Frequency Division Multiple Access.

OpEx Operational Expense.

OpMiGua Optical packet-switched Migration-capable networks with service Guarantees.

OPS Optical Packet Switched.

OTN Optical Transmission Network.

OXC Optical Cross Connect.

PDV Packet Delay Variation.

PLR Packet Loss Ratio.

PON Passive Optical Network.

PTP Precision Time Protocol.

PtP Point to Point.

QoS Quality of Service.

RAN Radio Access Network.

RAT Radio Access Technology.

RF Radio Frequency.

RoE Radio over Ethernet.

RRH Remote Radio Head.

RTT Round Trip Time.

RU Radio Unit.

SA Source Address.

SDH Synchronous Digital Hierarchy.

SDR Software Defined Radio.

SFP Small Form-factor Pluggable.

SM Statistical Multiplexing.

SOF Start of Frame.

SONET Synchronous Optical Network.

TACS Total Access Communication System.

TCO Total Cost of Ownership.

TDM Time Division Multiplexing.

TDMA Time Division Multiple Access.

TSN Time-Sensitive Networking.

UDWDM Ultra Dense Wavelength Division Multiplexing.

UE User Equipment.

UL UpLink.

UMTS Universal Mobile Telecommunications System.

VLAN Virtual Local Area Network.

VLSI Very Large-Scale Integration.

WCDMA Wideband Code Division Multiple Access.

WDM Wavelength Division Multiplexing.

WiMAX Worldwide Interoperability for Microwave Access.

WRON Wavelength Routed Optical Network.

Chapter 1
Introduction

1.1 Introduction

Mobile network architectures are usually split into three parts: Radio Access Network (RAN), backhaul network and core network [Gro]. The RAN consists of systems and technologies performing radio-access related functions such as managing radio transmission and reception to/from mobile devices. There is a standard called Radio Access Technology (RAT) that defines the interfaces, protocols, and the architecture and specific functions. An example of RAT includes Wideband Code Division Multiple Access (WCDMA)/High Speed Packet Access (HSPA), LTE, Worldwide Interoperability for Microwave Access (WiMAX) $\cdots$ etc. Traffic aggregation and transport between the core network and the RAN is performed by the backhaul network. Since the architecture and implementation of the backhaul networks are almost agnostic with respect to RAN and core architectures, they are not defined by RAT standards. Eventually, the core network performs all non-radio access related functions and used as the gateway towards all fixed and mobile networks, mainly towards Internet. In most cases, functions and interfaces of core networks are standardized according to the adopted RAT. The User Equipment (UE) are directly connected to the BS of RAN via the radio link, and evolution of this BS undergoes several changes and leads to the new RAN network, C-RAN. The terms BS (for C-RAN) and Base Transceiver Station (BTS) (for traditional network LTE network) are used interchangeably in this context as they are referring to the same concept.

1.2 Background and Motivation

BSs for mobile communication have been evolved from a bulky rack-full of equipment to multiple form factors aimed at different deployment scenarios. Traditionally, the collection of these multiple stand-alone BSs/BTSs has been treated as RANs or cellular networks [LPHL14]. A single BTS had multiple transceivers to serve several different frequencies and different sectors of a cell when a sectorized BS

is considered and covers a small geographical area, whereas a group of BTS may cover a large continuous geographical area. Each BTS was responsible for processing and transmitting its own signal to and from UE, and forwards the data payload to and from the UE and out to the core network through the mobile backhaul. The cellular network has evolved through a series of innovations aimed at unified targets: performance and efficiency in high mobile environment [Msh12], beginning with the analog First Generation (1G) cellular networks to Fifth Generation (5G) (which is expected to be deployed initially in 2020 to provide about 1000 times higher wireless area capacity and save up to 90% of energy consumption per service compared with the current 4G system [ABC+14] [PLJ+14]). The 1G system provided the basic mobile voice service based on analog radio transmission techniques. It employed Frequency Division Multiple Access (FDMA) to multiplex traffic flows. Nordic Mobile Telephones (NMTs) and Total Access Communication Systems (TACSs) were the two most popular analog systems, offered handover and roaming capabilities, but they were unable to interoperate between countries.

Second Generation (2G) mobile systems provided an increased voice capacity delivering mobile to the masses. They are characterized by digitization and compression which allowed the accommodation of many more mobile users in the radio spectrum through either time (Global System for Mobile Communication (GSM)) or code (Code Division Multiple Access (CDMA)) multiplexing [Msh12]. Compared to 1G system, 2G system offered higher spectrum, higher efficiency, better data services, and more advanced roaming. GSM was deployed to provide a single unified standard and enable seamless services throughout Europe by means of international roaming. To support multiple users, GSM uses Time Division Multiple Access (TDMA) technology, and it has been contentiously improved to offer better services. The development of new technologies based on the original GSM technology leads to advanced systems.

In 1G and 2G cellular networks, the BTSs were equipped with its own cooling system, battery backup, monitoring system, and so on. It implies that the BTS had an all-in-one architecture, an architecture where all power, analog, and digital functions are housed in a single container as large as a refrigerator and is commonly found in large cell deployments. Since each BTS is working on its own, it doesn't reduce the interference with other BTSs by using collaboration algorithms such as genetic algorithm [GKB+06]. In addition, it is hard to upgrade and repair because of the all in one BS.

In addition to the shortcoming of the BS architecture, increasing network traffic demand, limited bandwidth availability and mass adoption of mobile broadband were the major challenges of traditional cellular networks. As a consequence, telecom operators were seeking new ways to increase network capacity and coverage while

reducing time to market for new services and achieving lower Total Cost of Ownership (TCO) [Eri15]. To achieve these goals, they needed a cost effective combination of several standards (GSM, LTE, and others), transport technologies, frequency band and cell layers while handling the substantial high capacity demand. To accommodate the substantial high capacity demand in cellular systems, reducing cell size to increase the network capacity by improving the spatial reuse of radio resources could be one possible solution. However, it causes an increased system cost to provide coverage areas with small cells due to construction and operation related problems. As a result, a new RAN architecture based on distributed BS , C-RAN, has been proposed [Ins11] [NMW+12] to address the above mentioned challenges. And the 3GPP has been taken the evolution of radio access technology through High Speed-Downlink Packet Access (HSDPA) and Enhanced High-Speed Uplink Packet Access (HSUPA).

Later, in Third Generation (3G) deployment, a distributed BS was introduced where the RRHs and BBUs are separated using fiber links with digital baseband interfaces, such as CPRI and Open Base Station Architecture Initiative (OBSAI). At this stage, the concept of fronthaul was introduced. Unlike traditional cellular networks that are built with many all-in-one BS architectures, C-RAN can be viewed as an architecture evolution based on distributed BSs. To enable flexible deployment, C-RAN or C-RAN architecture divide the BS into BBU and RRHs. Figure 1.1 illustrates the segment where fronthaul and backhaul are located in the overall mobile network. Fronthaul is a segment that connects RRH and BBU, whereas backhaul accounts for the segment between the core network and the edge of the entire telecommunication network, and the physical medium can be fiber, copper, and microwave. As seen from Figure 1.1, C-RAN is a fronthaul architecture that addresses capacity and coverage issues while supporting mobile xHaul (x can be Fronthaul or Backhaul) solutions. It also provides great benefits in controlling ongoing operational costs, improving network security, network controllability, network agility and flexibility [CPLC+13] [Ins11]. The detailed description of C-RAN is presented in Chapter 2.

As previously mentioned, Mobile Backhaul (MBH) network comprises any of the three listed physical mediums: optical fiber, copper, and microwave radio. Older generation networks rely on leased E1/T1 copper line for backhaul connection between cell sites and BS controller [TZJ11] [ZBJ08]. Because of its low latency, deterministic QoS, and synchronization ability, T1/E1 lines are highly suitable for voice service [TZJ11]. Due to mass adoption of mobile broadband and increasing demand of bandwidth per subscriber, operators must build large numbers of new cell sites. As a result, the leased copper lines would cost a high Operational Expense (OpEx) and is no longer suitable for future MBH. To combat these challenges, carriers are working on transforming from the Time Division Multiplexing (TDM) based

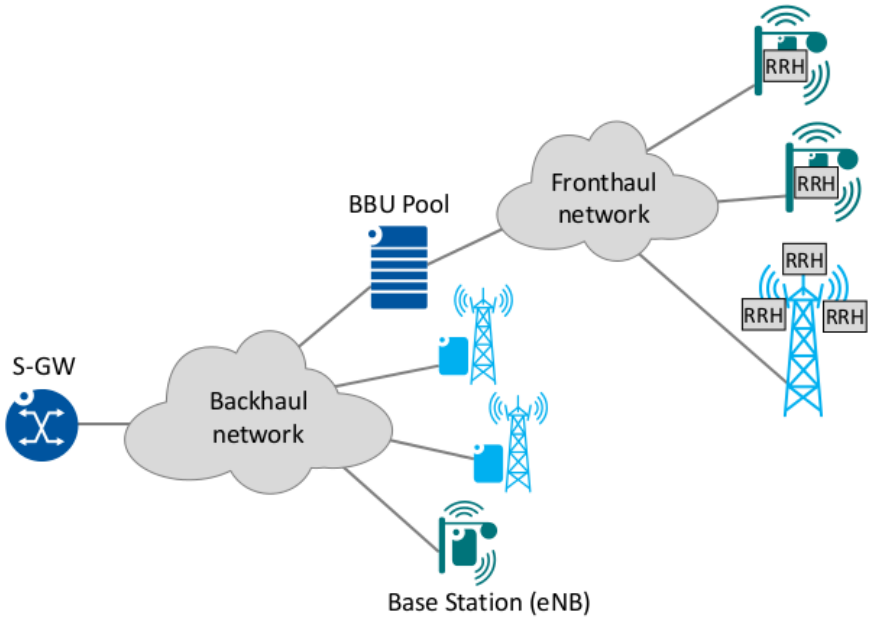

Figure 1.1: Mobile backhaul and fronthaul network architecture in LTE, extracted from [AWP15].

architecture to all packet Ethernet-based architecture. The Ethernet is not originally designed for carrier-class deployment because it doesn't meet certain requirements, such as delay, synchronization and so on [SRV08]. Ethernet-based network with new technologies might be used to accommodate ultra high mobile data traffic with efficient spectrum utilization. It has been suggested a new technology based on coherent Ultra Dense Wavelength Division Multiplexing (UDWDM) [SGR+11] and Orthogonal Frequency Division Multiple Access (OFDMA) [CTH+12] separately for future MBH systems.

In fronthaul network, fronthaul flows have a very high bitrate in the order of gigabits per second; For instance, for an LTE sector configured as 2x2 Multiple Input Multiple Output (MIMO) with 20 MHz carrier bandwidth requires about 2.5 Gb/s, which gives a total of 7.5Gb/s for a typical 3-sector cell sites. Such fronthaul capacity doesn't not scale with time-varying traffic load condition of the cell (i.e. it leads to fully nonelastic traffic). These features constitute a relevant problem to the traditional RAN infrastructure that is designed to carry much lower bitrate. As a result, the common fronthaul solution in C-RAN is the use of an optical access networks. But this transport solution requires consumption of a number optical fiber

links, which are scarce and needs huge investment by operators. For example, in areas where there is dynamic user expectation like clients are engaged in mobile-savvy activities-from texting to video phone calls such as in ultra-modern stadium and dense population area (like China), requires a new emerging technology: the C-RAN. In such scenarios, using fiber as full fronthaul network may not be economically available to the rooftop where the RRH needs to be deployed [Ler14]. In other cases, installing fiber in existing tower may prove to be a challenging problem. And also deploying traditional small cell sites in suburban and road areas (where more capacity is needed to meet fast growing traffic demand) are not realistic solutions for these areas that form a high percentage of an operator's footprint. As a complement to the both traditional small cell and fiber, a new fronthaul network that can extend the existing traditional small sites and enable quick deployment of cell site with much lower TCO is needed. Another technology such as WDM and OTN could save fiber consumption, however, the cost of introducing these additional transport equipment makes economically not viable for operators. Hence, the current Mobile Fronthaul (MFH) solutions are rather short-term approaches and needs improvement in both the topology and technology. As an attempt to address this issue, some of the recent research is focusing on Ethernet-based fronthaul transport network pushed by their lower costs, ability to employ statistical multiplexing, and improved performance.

Using Ethernet in the fronthaul [GCT+15] has been proposed to take some advantages: lower cost equipment, shared use of lower-cost infrastructure with fixed access networks, obtaining statistical multiplexing, and optimized performance. Despite of their attractive advantages, Ethernet also comes with their own challenges: achieving low latency and jitter to meet delay requirements, and ultra high bit rate requirements for transporting radio streams for multiple antennas in increased bandwidth [GCT+15]. For the above reasons, the current fronthaul networks are increasingly integrating more cost-effective packet switched technology, especially Ethernet/Internet technologies. The former disadvantage will be explored in this study, while the latter is studied in detailed in [GCT+15]. In addition to standard Ethernet switch used by Ethernet, there is another node, H1, developed by transpacket [Tra13] employed in IHON fusion solution. Fusion solution/IHON that uses standard Ethernet technology rather than all-optical switching technology provides the fusion properties of circuit and packet switching network in packet network [Tra13]. It enables Ethernet transport and ensures strict QoS for GST traffic, and optimize resource utilization by introducing SM traffic in the unused capacity.

Moving from this background, we intend to study the transport of radio signals over Ethernet technology using the two types nodes: standard switches and IHON nodes, H1. In particular, we focus on three performance metrics to evaluate the radio over Ethernet IHON mobile fronthaul networks (latency, PLR, and PDV) with related target compared to the standard Ethernet network. The main motivation of this

thesis is dealing with the level of timing performance required and studying on how well this timing be supported in an IHON Ethernet mobile fronthaul. Furthermore, It is targeted to find how the IHON hybrid principle may be applied and how it will perform in a network containing only a few, or only a single wavelength channel.

With packet-based C-RAN realization, the MFH issue has been one of the biggest challenges. As a result, several continuous studies/efforts towards an MFH have been made even though they haven't touched the root of the MFH itself. Institute of Electrical and Electronics Engineers (IEEE) 802.1CM [Gro] has begun the development of a potential new work item on Time-Sensitive Networking (TSN) for MFH. ORI [ETS] is studying how to reduce the CPRI data rate using compression technology. In addition, the use of Ethernet to transport the CPRI data traffic is under discussion by the CPRI Forum, while the design of CPRI encapsulation on Ethernet packets has begun by the IEEE 1904.3 Task Force [For].

1.3 Statement of the Problem

Fronthaul network, between BBU pool and RRHs, needs tight requirement of latency, PDV, PLR, jitter, and time and frequency synchronization. To meet these requirements, several transport options have been used and proposed; optical access networks (such as dedicated fiber, passive WDM, active WDM, and OTN), microwave, and Ethernet as a fronthaul solution. Using optical access network requires consumption of a number of optical fiber links which needs a huge investment by operators. In fact, it may employ multiplexing technique to reduce the number of fiber used for transporting the high bit rate fronthaul flows, but still it doesn't apply the concept of statistical multiplexing to further reduce the cost. On the other hand, a microwave is an emerging fronthaul solution for short distance RAN architecture.

In this thesis work, we are motivated to investigate the feasibility of fronthaul networks over IHON network. We believe that the use of these fronthaul transport options can bring several advantages: use of statistical multiplexing, reduced cost, and optimized performance. Given the tight fronthaul requirements, this thesis focuses on the evaluation of IHON networks for fronthaul solution or not. The thesis is further extended to validate and evaluate whether the Ethernet network can fulfill the requirements of fronthaul network. In general, this project will evaluate the Ethernet technology and IHON network for C-RAN fronthaul network. Furthermore, the requirements of fronthaul network are checked against the evaluated results of this work.

1.4 Objectives of the Thesis

The objective of this work is to perform and analyze the following goals:-

- Investigate and identify the possible fronthaul solutions for C-RAN in mobile networks.
- Collect the fronthual requirements for mobile networks with respect to different performance metrics.
- Study the latency and timing required for transporting RoE packets.
- Examine the Ethernet frame format supporting radio signals in mobile networks.
- Study the potential benefits that brings into Ethernet mobile fronthaul.
- Identify the challenges/ parameters difficult to achieve in mobile network fronthaul.
- Evaluation of fusion/IHON network for fronthaul networks in terms of latency, PLR, and PDV.
- Investigate the performance of Ethernet network for fronthaul networks emphasizing on measuring PLR, latency, and PDV.

1.5 Methodology

To achieve the above mentioned objectives, a list of methods were set up: research of scientific papers relevant to this topic and analytical/simulation method were used.

Research methodology

Background research, conference papers, white papers, International Telecommunication Union - Telecommunication (ITU-T), IEEE 1904.3, IEEE 802.1CM (TSN), and Internet Engineering Task Force (IETF) standard recommendations were used to collect the fronthaul requirements and study the overview of CRAN. Different transport options other than Ethernet were studied in order to get acquainted the principles of fronthaul networks.

Analytical and Simulation methods

An analytical model designed to mathematically model the performance metrics has been used to numerically present our results. The programming language chosen to construct the simulation model is **Simula** based on Discrete Event Modelling On Simula (DEMOS) software, a context class for discrete event simulation. Moreover, **Matlab** has been used for post processing of raw data's from the simulator and plotting the data's with error bars. The simulations were ran 10 times by varying simulation seeds for each data points, and the results were reported with **95**% confidence interval.

1.6 Thesis Outline

The rest of this thesis is organized as follows:

Chapter 2: Cloud Radio Access Network(C-RAN) describes the evolution, architectural background, component, advantage, and challenges of C-RAN emphasizing on the BBU and RRHs detail. Several fronthual transport options are also given and discussed. At the end, an overview of Ethernet packet frame format for transporting RoE packets is presented.

Chapter 3: Fronthaul Requirements presents the requirements and challenges of fronthaul networks focusing on the key performance elements: data rate, latency, packet delay variation. It also presents the synchronization of baseband radio signals.

Chapter 4: Integrated Hybrid Optical Network(IHON) describes the three types of hybrid optical network architectures and principle of Optical packet-switched Migration-capable networks with service Guarantees (OpMiGua). It emphasis on the principles, properties and main characterstic of IHON or fusion networking. A detailed insight on the delay and PDV of IHON and Ethernet standard switch, IHON node aggregation, and an algorithm to compute the inter packet gap are also given.

Chapter 5: Analytical/Simulation Model presents the numerical analysis of the different fronthaul options described in Chapter 2. The simulation model for IHON and Ethernet Switch is also described thoroughly.

Chapter 6: Results and Discussions present the results obtained from the simulator. A comparison of the performance of IHON and Ethernet switch is given with the help of figures and tables. A more comprehensive discussion based on the obtained results is dealt. This chapter also presents the latency, PLR, and PDV requirements to achieve the mobile fronthaul requirements.

Chapter 7: Conclusion and Summary wraps up and summarizes the whole thesis work.

Chapter 8: Future work presents some suggestions and ideas for further investigation that weren't covered in this work.

Chapter 2
Cloud Radio Access Network/C-RAN

In this chapter, the focus is on the role of C-RAN architecture in today's mobile networks. In addition, the evolution of BS architecture is discussed, and the critical drawbacks of the fronthaul network transport option are detailed. A clarification of C-RAN architecture, a various component of C-RAN, and the use of an optical network for C-RAN network is described. The motivation behind the use of Ethernet and framing of data's for Ethernet is also explained.

2.1 Introduction

An inevitable use of mobile devices (e.g. smartphones and tablets), which are the source of an explosion traffic, requires some radical changes to the existing mobile network technologies and architecture. A novel LTE RAN is one of the changes which is already introduced, and it is adopted to increase spectrum efficiency and serve high traffic density areas by deploying additional micro-cells in the cell cites. Several other improvements are being performed by academic and industrial research. C-RAN can be regard as one of the ways to evolve the mobile networks and architectures.

C-RAN is a proposed architecture for future cellular networks, which has the potential of combining emerging technologies from both the wireless and the Information Technology (IT) industries by incorporating cloud computing into RANs. Since it was first proposed by China Mobile Communications Corporation (CMCC) in 2011, further research and development have been pursued [Ins11]. The letter 'C's in C-RAN comes from the four main characteristics of C-RAN: Cloud, Centralized processing, Cooperative, and Collaborative or Clean. The main idea in C-RAN is baseband units from multiple BS are pooled into centralized BBU pool so that they can be shared between BSs of several cell sites, statistical multiplexing gains [CCY+15]. This implies that the network architecture is able to adapt to non-uniform traffic and utilizes the pooled BSs more efficiently. Compared to traditional cellular architecture, C-RAN needs fewer BBUs which directly reduces the cost of network operation. In

the following sections, we present the evolution of BS.

2.2 Evolution of BS Architecture

Based on the placement and implementation of BS, the BS has evolved through three main steps. Figure 2.1 illustrates the first traditional generation macro base station, mobile network infrastructure based on all in one BS architecture, in which all BS hardware is located in a radio cite cabinet, and the antennas are driven through coaxial cables. BS hardware like the BBU, Radio Unit (RU), power unit, and battery backup were located at the base of a tower. It doesn't employ the BBU hotelling, also called BBU hostelling. Hence, the BBU is implemented as a single form factor device. As it is seen from Figure 2.1, there is no fronthaul network as both BBU and RRH are located in the same cell site cabinet. The length of the separation between RRH and their respective transmission and reception antenna can be up to some meters or ten meters depending on the topology of the cell site. Consequently, they experience a negligible power loss.

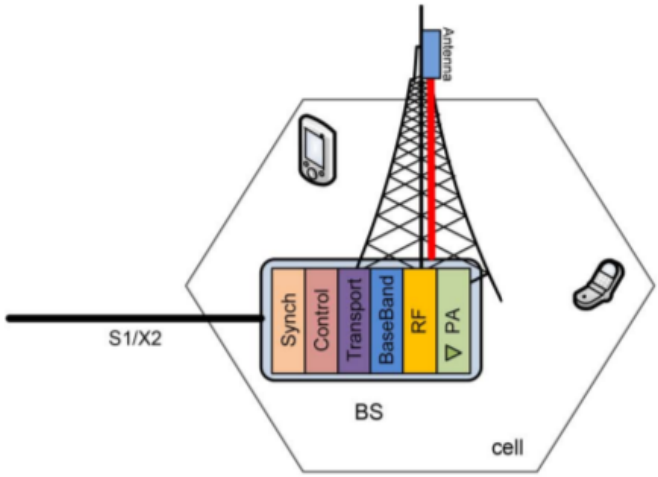

Figure 2.1: Base station architecture for traditional macro BS (no BBU hotelling), extracted from [CCY+15].

In the second step, Figure 2.2, with fiber based interconnection the RRH containing the Radio Frequency (RF) transmit and receive components is collocated with the antenna at the top of the cell site thus only short coaxial jumper are used for the connection to the antennas. The RRH is linked to the BBU in the cabinet using a Digital Radio over Fiber (D-RoF) protocol such as either the CPRI [Int16] or the OBSAI [OBS16]. Using an optical interface allows a much lower power consumption approach at higher data rates within the cell. Thus, this is a first preliminary

step for all BBU hotelling solutions, where BBU an RRHs are separated. RRHs are implemented as a stand-alone devices embedding their own power and cooling subsystems. Since the RRH is placed close to antennas, the power consumption is comparatively (to all-in.one BS) is reduced. This is because the power margin for the coaxial cable connecting RRH and antenna loss is much lower.

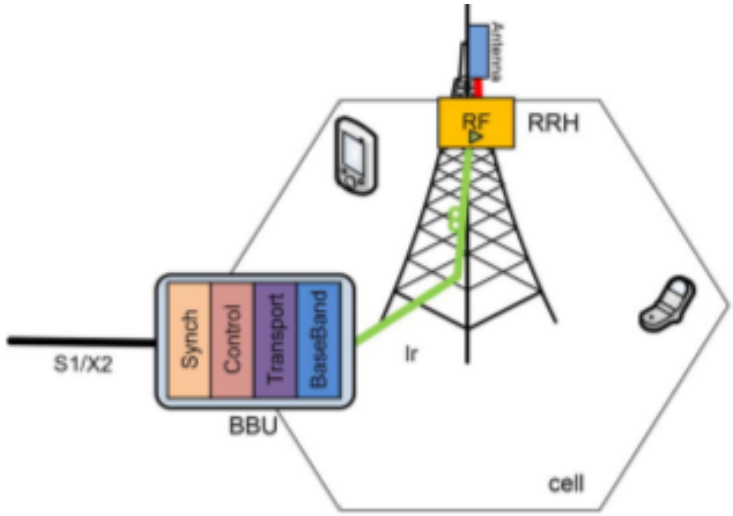

Figure 2.2: Base station architecture for BS with RRH, extracted from [CCY+15].

2.3 C-RAN Architecture

Figure 2.3 shows the third step of mobile network evolution, C-RAN. The concept from which C-RAN moves is the splitting of traditional BSs into RRH and BBU. It introduces centralized, collaborative, and cloud and clean system, to optimize cost and energy consumption in the field of mobile networks [HDCCL14] [WZZ14]. Figure 2.3 presents a simplified overall C-RAN architecture. Furthermore, it centralizes the BBU processing resource together so that the resource could be managed and allocated dynamically on demand. Moving some part the radio network control function from being collocated with the antenna at the cell site to the location deeper into the network introduces a new transmission network into the overall network infrastructure-rMobile Fronthaul. This new C-RAN architecture offers many benefits to operators such as in controlling operational cost, energy saving, improved spectral efficiency and resource efficiency, greatly increases the flexibility of the network, and facilitation of service on edge.

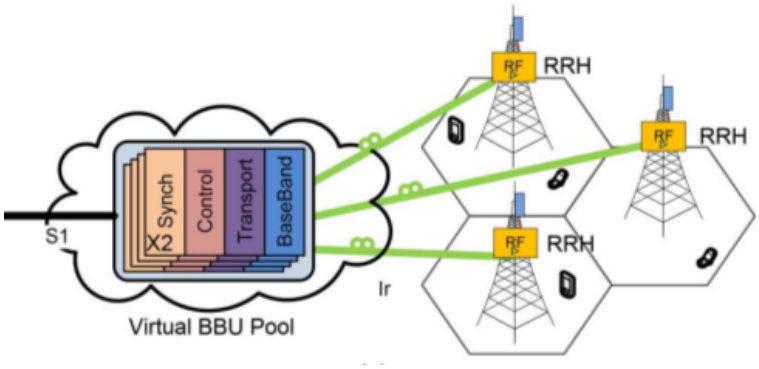

Figure 2.3: Base station architecture for C-RAN with RRHs, extracted from [CCY+15].

2.3.1 C-RAN System Architecture

In [PWLP15], three different architectures are defined according to the constraints on fronthaul and the distribution functions between RRHs and BBUs.

- **Full centralization:** In this system structure, BBU is responsible for baseband processing (i.e., physical layer, layer 1), the Medium Access Control (MAC)(layer 2), and the network layer (layer 3) functions. Due to the high bandwidth of the baseband radio signals, this option has higher requirements in transmitting signals between RRH and BBU [Ins11]. As shown in Figure 2.4, the BBU contains all processing and managing functions of the conventional BS. This structure incurs a high burden on fronthaul. Nonetheless, it makes it clear and simple, benefits in terms of operation and maintenance, and has capabilities to support multi-standards. Thus, the focus of this thesis will be in this kind architecture.

  The RRH, on the other hand, deals with up/down conversions, amplification of RF signals, filtering and interface adaptions.

- **Partial centralization:** In this sort of architecture, the RRH is responsible for RF related baseband processing and integrating RF functions while BBU are responsible for all other functions of layer 1 and the upper layers (layer 1 and layer 2) functions, as shown Figure 2.4. It greatly reduces the burden of fronthaul and the RRH-BBU overhead. Some advanced features; for example in LTE system such as Coordinated Multiple Point transmission and receptions (CoMP) and MIMO, however, can not be efficiently supported [PWLP15]. It creates a complex interaction between layer 1 and layer 2 functions.

•**Hybrid centralization:** Some functions of layer 1 such as the cell-specific signal processing functions and the user specific are removed from BBU and appended into a separate unit. The separate unit can be part of the BBU pool or not [PWLP15]. This structure can be regard as a special case of full centralization and has some benefits: support resource sharing and is capable of reducing energy consumption in BBUs.

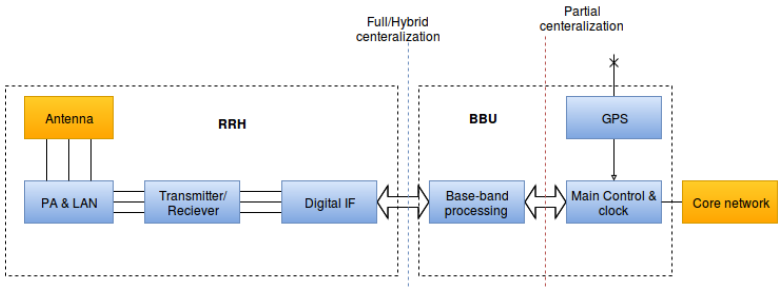

Figure 2.4: Options of C-RAN system architecture including the split functions of RRH and BBU, extracted from [PWLP15].

2.3.2 C-RAN Components

The general architecture of C-RAN consists of three main parts, namely (i) a RRH consisted of antenna system, (ii) a BBU pool, real-time cloud for centralized processing, and (iii) a fronthaul network/transport infrastructure that connects RRH and BBU.

•**RRH:** In [MS12], Figure 2.5, RRH consists of antennas system, power amplifier, A/D converter, and Low Noise Amplifier (LNA) which basically perform analog processing can be mounted on the tower near the antenna. By conducting most baseband processing in BBU pool, these modules have much less complexity and energy consumption which directly lowers their price. RRHs can be distributed in certain areas, first of all in urban areas with high traffic loads with a cost efficient manner. They are mainly used to transmit high data rate RF signals to mobile terminal in the downlink and forward the baseband signals from the mobile terminal to the central processing unit, BBU in the uplink.

•**BBU pool:** The baseband signal processing is conducted in BBU that is linked by means of an optical fiber to RRH by using D-RoF technology. It consists of an element whose purpose would be scheduling and processing the incoming signals from different cell sites to virtual base station and optimizing radio resource allocation. Based on traffic aware scheduling of UEs and time varying

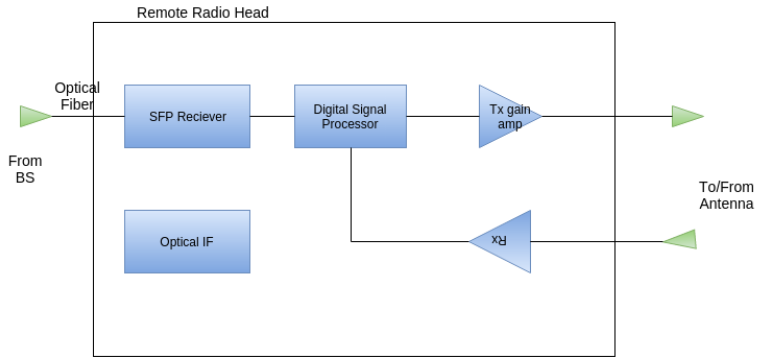

Figure 2.5: RRH components, adopted [LKB09].

channels, the processing capability is adaptively configured and the signal processing resources are dynamically allocated in the software defined BBU. This capability together with its modular design optimizes available space and deployment time.

- **Fronthaul/transport network:** Fronthaul network is a segment which in different topological solutions to provide a connection between RRHs and BBUs with high capacity and low time latency [HDDM13] [PWLP15]. The link between RRHs and BBUs is realized through via different technologies, such as optical fiber networks, cellular communication, and even wave communication. And also, the transmission can be done using two different protocols; CPRI and OBSAI. Both the standards employ radio signal digitisation or D-RoF.

2.3.3 Advantages of C-RAN

In this subsection, the major advantage of C-RAN is given based on [Ins11].

- Resource pooling
- Energy efficient with a centralized processing of the C-RAN, the number of BS and other site equipment's power consumption can be largely reduced. Due to sharing of BBU pool among a large number of virtual BS, higher utilization of processing resources and lower power consumption is achieved by several mechanisms. For instance, an idle virtual BS can be selectively turned off without affecting the service commitment, especially at night where there is no much traffic, to reduce the processing power. Hence, C-RAN is an eco-friendly infrastructure.
- BS visualization: As a result of the visualization of BS in BBU pool, the capacity of the RAN is improved. It also provides an easy sharing channel

information, signaling and traffic data about the active UE in the system. And also, the visualization allows an easy implementation of joint processing and scheduling; for example, CoMP in Long Term Evolution-Advanced (LTE-A), to mitigate inter-cell interference and improved spectral efficiency.

- Adaptability to non-uniform Traffic

  Depending on the movement of UEs, the traffic that can be supported by the serving RRH dynamically changes. Nonetheless, the serving BBU is still in the same BBU pool. The non-uniform traffic generated from the UE can be distributed in a BS of the sameBBU pool because the coverage area of BBU pool is larger than the traditional BS. Hence, the distributed BBU pool has a load balancing capability to adapt the dynamic traffic change.

- Coordination for interference mitigation(ICIC)

- Multi-technology support

  C-RAN supports the multiple access technologies such as GSM, Universal Mobile Telecommunications System (UMTS) and LTE in the same BBU cloud so as to share the BBU. Though the implementation of these technologies differs in their detailed function, the BBU designers should integrate them into a single device for multiple RATs support. Software Defined Radio (SDR) based BBU is one of the possible schemes to process any protocols.

- No Global Positioning System (GPS) in each remote site

2.4 Optical Networks for C-RAN

The new connectivity segment between the centralized BBU and multiple RRHs is based on D-RoF technology over fiber resources. WDM technology can be employed to deal with the high number of digital radio over fiber links per antenna site. Because of its lower cost, Coarse Wavelength Division Multiplexing (CWDM) could be the first approach. Table 2.1 summarizes the several existing optical solutions to achieve transport of fronthaul traffics in C-RAN and are detailed in Section 2.5.

Table 2.1: Optical fronthaul/transport options.

Fronthaul options	**Technology description**	**pros**	**cons**
Dedicated fiber	• Data signals are transported without encapsulation • Passive solution	• No additional cost for transmission equipment • No need for power supply at the radio site	• Requires a lot of fibers • Extra equipment for monitoring
Passive CWDM	Use colored SFP at the BBU and RRH together with CWDM to channelize the fiber	• Use few fibers • No power is needed (high reliability and suited for outdoor deployment) • low cost for CWDM	• No native OAM • Not bidirectional (2 fibers per link)
Active WDM	Use WDM transponders or muxponders to extend the supportable distance	Offer ring or point-to-point with additional protection schemes	Need special attention to synchronization support and latency for correct transportation
OTN	Use OTN maxponders to transport fronthaul flows	• Bidirectional • High efficiency fiber sharing	• Power supply required • Risk on performance (latency and performance)

2.5 Fronthaul Transport Options

In C-RAN architecture, the fronthaul can be transported by possibly reusing existing RAN infrastructure at different levels, for example, cable, wavelength, and sub-wavelength(bitstream). To transport fronthaul over the existing network infrastructure, some technologies can be used; e.g, OTN and Ethernet. In describing fronthaul transport options, terms such as passive and active solutions are used to distinguish whether the transport options require an energy consuming equipment or not. When no additional energy consuming equipment is needed in the intermediate

nodes or end points of the fronthaul network which in turn leads to lower operational cost and less maintenance, it is called a passive solution. On the other hand, an active solution requires an energy consuming intermediate nodes or end points and is less robust than passive solutions.

The following subsections describe the transport options which are potential candidates for CPRI transport, but it is implied that several cases can be obtained by combining some of the transport options.

2.5.1 Dedicated Fiber

With dedicated fiber fronthaul, each RRH is connected to the BBU over a point to point fiber pairs or a single fiber if bidirectional fibers are used [Dav14]. In such scenarios, fronthaul is transported over point to point fiber pairs (each carrying a separate flow for each BBU-RRH CPRI port pairs). Any fronthaul interface can be used even though an already defined public standards are mostly preferred such as CPRI. As a special case, when an intermediate nodes are present in the infrastructure, the Point to Point (PtP) connection is routed via Optical Distribution Frames (ODFs), a passive interconnection fabric. With the above assumptions, the method is categorized as passive solutions. This transport option is important for scenarios where operators have a large installed base of available fiber. However, the cost associated with deploying new fiber and issue of the fiber availability limits the broad applicability of this transport option. It has several advantages: no extra equipment cost for transmission and its simplicity- no additional equipment is added to the network. Because of this, the latency contribution caused by the fronthaul network over lower-layer technology is zero and the fronthaul traffic is transported "as it is". Considering a basic fronthaul implementation, the maximum E2E latency consists of the delay components for uplink BBU and RRH, downlink BBU and RRH, and the propagation delay along the fronthaul link (t_{TR}=0). On the other hand, requiring extra equipment for monitoring and large consumption of fiber are among the major challenges of this approach. Figure 2.6 illustrates dedicated fiber mobile front haul network option in which gray optical modules are used in both the RRH and BBU ,SFP. Due to the above mentioned problems, point to point fiber is not practical for the majority of C-RAN deployments.

Figure 2.6: Point to point fiber [PMC15].

2.5.2 Passive WDM

Passive WDM-based fronthaul deploys WDM networking to a fronthaul network [TMC14]. Traffic flows in the fronthaul network are transmitted on separate wavelength channels using WDM transceivers operating according to WDM technology. This enables multiplexing of several wavelengths into fewer fibers using a passive WDM multiplexer in each cell sites. Figure 2.7 presents a passive WDM in which the incoming wavelengths are split by means of passive demultiplexers and is sent to separate CPRI ports of BBUs. Depending on the specific requirement of the network, CWDM or Dense Wavelength Division Multiplexing (DWDM) technologies are directly deployed in the RRH and BBU with a passive Optical Add/Drop Multiplexer (OADM) to multiplex the colored wavelength onto a single fiber pair. CWDM technology is best suited for outdoor equipment because it doesn't require temperature control and is capable of multiplexing about 16 wavelength channels into a single fiber. In most cases, the maximum number of RRH in cell site (assuming several sectors, RATs, and antennas) is less than this number of wavelengths. Hence, it is possible to aggregate all traffic flows of the whole cell site fronthaul into a single fiber. Comparing to dedicated fiber, this solution is more relevant because it greatly reduces the amount of fiber without affecting the energy consumption. Below is a list of the major drawback and merits of passive based Mobil fronthaul.

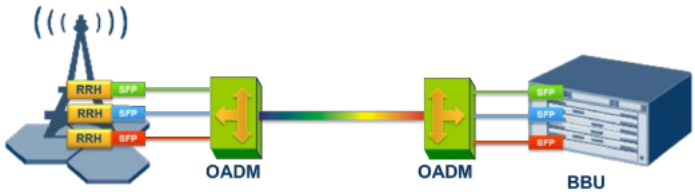

Figure 2.7: Passive WDM [PMC15].

Passive WDM-based fronthaul has the following advantages:

- Potential low cost for CWDM technology. Hence, it is the most practical one.
- No need of active components on the passive multiplexer.Thus, it offers high reliability and is suitable for outdoor deployment.
- Reduce significant use of fiber.
- Provide 16-channels per fiber (CWDM).

Despite their attractive advantages, passive WDM also comes with their own disadvantages:

- Not bidirectional (It requires 2 fibers per link).
- Inventory management required to align optics color with RRH-BBU link.

- Lack of native OAM: fault isolation is operationally challenging and expensive.
- Lack of clear demarcation points between wireless access point and fronthaul equipment.

Similarly, Active WDM enables the use of 1310 nm gray wavelength in the RRH and BBU by employing a separate transponder [TMC14].

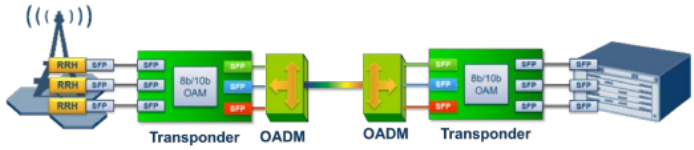

Figure 2.8: Active WDM [PMC15]

Figure 2.8 illustrates active WDM-based mobile fronthaul where an external device is used on the transponder for OAM propose. The active components in the figure introduce an asymmetric latency in the uplink and downlink directions. In addition to this, it requires two WDM optical modules for uplink and downlink CPRI links.

2.5.3 Microwave

Microwave is a potential option for short distance CPRI transport between RRH and BBU where fiber is not available [Dav14]. It is an emerging mobile fronthaul approach for Heterogeneous Networks (HetNets). In HetNets, small cell site is fronthauled to near by macro-site. This transport technology could only support the CPRI line bit rate options.

There are some limitations of this approach:

- Limited area coverage/ reach: typically 1 Km or less.
- Bandwidth: support only up to CPRI option 3.
- Site placement challenges: highly sensitive to weather fading.

2.5.4 OTN

Utilizing OTN as mobile fronthaul brought a new standardized format for carrying different types of protocols across the optical network [TMC14]. This technology is employed in TDM-over-WDM for E2E mapping traffic flows in the fronthaul network into wavelengths. In Figure 2.9, both at the cell site and BBU hotel, there are OTN muxponders which transport fronthaul flows over the OTN signal hierarchy. In OTN signal hierarchy, CPRI signals/data are mapped into OTN low-level containers which in turn are multiplexed into higher layer signals and are transmitted on different

wavelength channels. The architecture of OTN is similar to active WDM but two major differences: OTN based solution is based on standardized technology(though International Telecommunication Union (ITU) G.709) and enables standard based client multiplexing to reduce the number of wavelengths required. Client multiplexing, standard based carrier-grade functions, increases fiber utilization and reduces the use of optical modules.

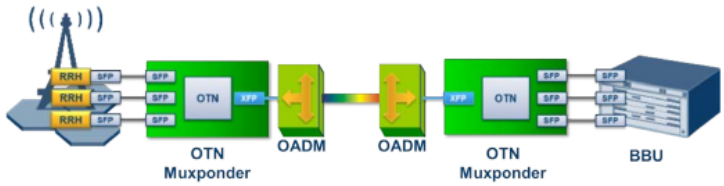

Figure 2.9: OTN based mobile fronthaul solution [PMC15].

OTN also introduced a standard based carrier-grade functions such as per client and line OAM, and Forward Error Correction (FEC), which allows longer reach and low-cost transceivers to be utilized. It offers multiservice support, which combines several interfaces such as CPRI, Gigabit Ethernet (GE), Synchronous Optical Network (SONET)/Synchronous Digital Hierarchy (SDH) ... etc on the same infrastructure. It is also capable of managing DWDM transport in which a single fiber can support up to 40 to 90 wavelengths, possibly with a bidirectional transmission. They automatically endowed Control and Management functions (C/M), without utilizing an external devices. Cross-connect devices can be added to the fronthaul network to get more advanced transport functions in the complete OTN based fronthaul network. The transport functions may include reconfiguration of routes and protection mechanisms which can be implemented either as electronic switches (like OTN wrappers) or in all optical switches (like Arrayed Wavelength Grating (AWG) or OADM). Additional benefits of OTN solution includes: sharing of an underlying infrastructure by several mobile operators, capable of supporting HetNets and carrier aggregation, and offers in-band client and path monitoring.

Like active WDM, the asymmetric latency caused by introducing active equipment have been a key challenge in OTN based solutions. It also places a strict requirement on the trasmit SERDES design of the OTN mapper in order to meet the CPRI 2 ppb and 3GPP 50 ppb requirements. The relevant energy consumption due to OTN devices and, particularly much higher costs, makes OTN unattractive for operators like at least for smaller RAN instances. However, they are a promising future transport options in the long-term.

2.5.5 Ethernet

Ethernet is the most widely deployed Local Area Network (LAN) technology and nearly ubiquitous standard technology in which frames arrive asynchronously because of their burstiness [Gro]. By asynchronously it means that when a frame is completely processed, it is not deterministic when the next frame will arrive. With Ethernet, data are transmitted intermittently rather than in a steady data stream. During the data transmission, an Ethernet link can be idle when there no frame to be processed. Thus, synchronizing nodes over Ethernet link in order to take the advantage of an idle period is more challenging in fronthaul mobile network.

A data packet transmitted on an Ethernet link is sent in something called an Ethernet packet, which transmits an Ethernet frame as its payload. It is chunk of data enclosed in one or more headers that help to recognize the data and route it to the desired destination. The headers and trailers are added to the packet as shown in Figure 2.10.

Figure 2.10 depicts that an Ethernet frame is preceded by a preamble and Start of Frame (SOF). As its first two fields, each Ethernet frame starts with an Ethernet header containing Destination Address (DA) and Source Address (SA) addresses. At the middle of the frame, it contains the payload data and any headers for other protocols carried in the frame. Finally, the frame ends with Frame Check Sequence (FCS). It is also important to note that Ethernet adds 42 bytes overhead to the Ethernet payload assuming that one 802.1Q header and inter-frame gap are included. The description of an Ethernet format fields is described below:

Figure 2.10: Ethernet packet format, extracted from [For].

•**Preamble:** This field is seven octets long, and is used by the receiver to allow it to enable synchronization. It consists of a pattern of all the form 10101010 to inform the receiving station that a frame is starting and establishing a synchronization.

•**SOF:** The SOF delimiter is one byte filed, and it consists of a pattern of alternating ones and zeros but ending in two ones. The purpose of this field is to indicate the start of the frame.

•**Dest. MAC:** This field is a six bytes long which contains the address of station for which the data is intended. By convention, Ethernet addresses are quoted as a sequence of six bytes in hexadecimal. The left most significant bit determines whether the destination is an individual (individual addresses have a most significant bit of 0) or a group address (multicast addresses have a most significant bit of 1). An interesting feature is that the next bit in the destination address indicates whether the address is globally or locally administered. If the bit is zero, the address is globally administered otherwise it is locally administered. Note that the remaining 46 bits are used for the destination address.

•**Src. MAC:** This address contains the address of the sending station. It consists of the address of six bytes and is always an individual address, hence, the left most bit is always zero.

•**802.1Q:** If present, it is a four byte field that indicates Virtual Local Area Network (VLAN) membership. 802.1Q uses an internal tagging mechanism to insert the 4-byte tag field between the SA and length fields in the original Ethernet frame.

•**Packet Length:** This consists of two bytes field to provide the mac information and indicate the number of data types contained in the payload field of the frame.

•**Inter-Frame Gap:** Inter-frame gap is idle time between frames. Before transmitting a new frame, a minimum of 12 bytes of idle line is required.

•**Ethernet Payload:** contains the payload and can be up to 46 bytes payload.

2.6 Radio over Ethernet

In order to enjoy the potential flexibility of BBU-RRH fronthaul, a traffic dependent and packet based topology and an interface is required. The main motivation behind RoE is that it allows mixing of several type of traffics such as radio signal for mobile communication , TV ...etc. Current fronthaul standards like CPRI was originally defined as an internal BS interface to provide dedicated transport protocols for sampled radio waveform transport. In this case, the framing is carried out at the regular intervals by matching the length of frames to the specific slice of the wireless system frames [GCT+15].

According to IEEE 1904.3 Task force, for transporting radio signals between RRH and BBU, either structure-agnostic or structure-aware encapsulation mode can be utilized, and the task group is developing a standard for encapsulating fronthaul digitilized radio samples into Ethernet frames. Structure-agnostic encapsulates digitalized radio sample or data blob without know how about the transported stream/flow whereas structure-aware encapsulates and knows the type of the transported flows. In both modes, the encapsulation header is the same. In this subsection, we present the structure agnostic encapsulation format. Let us consider a fronthaul downlink, a data is encapsulated with the Ethernet header in the BBU pool and the header is decapsulated in the RRH. Conversely, in the uplink, an Ethernet header is encapsulated to the data in the RRH and decapsulated from the Ethernet in BBU. As depicted in Figure 2.11, the structure of Ethernet packet for supporting digitalized radio signal is shown. The Ethernet packet includes the traditional Ethernet header and RoE or Ethernet payload which also contains the RoE header and RoE payload.

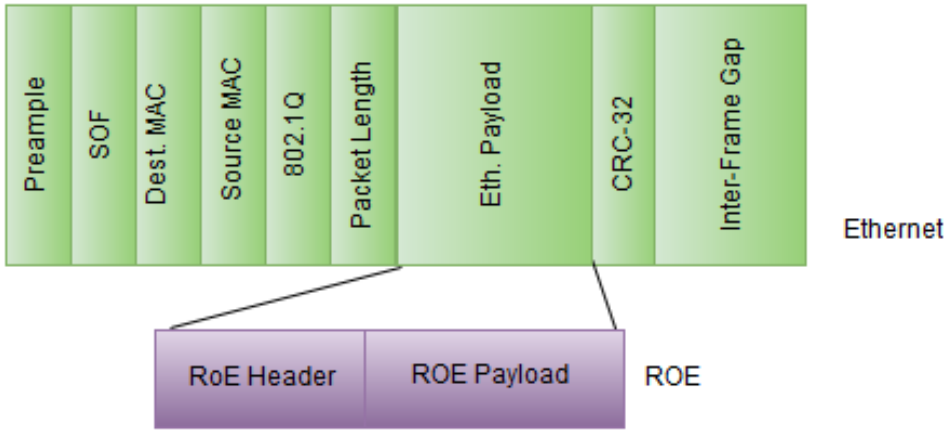

Figure 2.11: Ethernet packet format to support the Radio over Ethernet(RoE), extracted from [For].

RoE added a minimum of 6 bytes to the Ethernet packet. Figure 2.12 illustrates the native RoE encapsulation format with minimal header of 32 bits (it can also be up to 6 octets) per Ethernet packet. The number of frame per Ethernet packets highly affects the size of overhead (i.e when the number of basic frames per packet is greater than small Ethernet packets, there will be a large overhead). Considering both the header added by Ethernet and RoE, a total of 48-98 bytes (depends on the overhead added by RoE) is likely to occur per packet.

Below describes the fields shown in the Figure 2.12.

•**Version(ver):** The version field indicates the version of the RoE header being used.

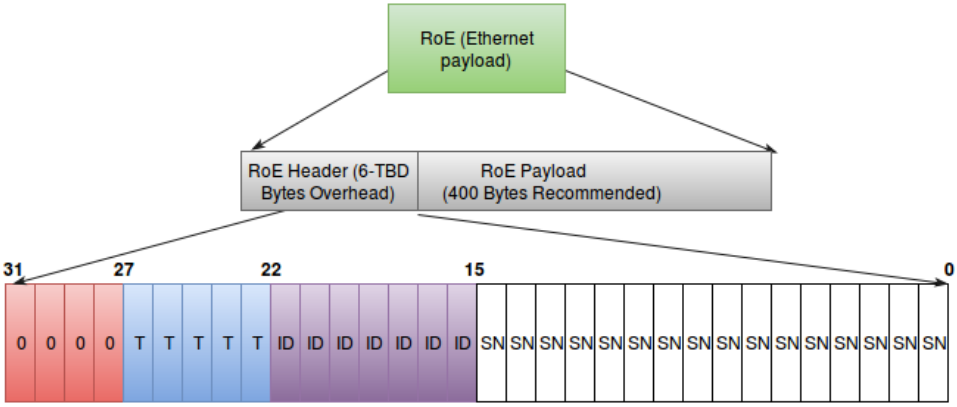

Figure 2.12: Radio over Ethernet(RoE) fame structure, extracted from [For].

This specification defines the value to zero(0b00) as shown in the Figure 2.12 from bit 31 to bit 28. However, new versions of the header may be defined in the future specification.

•**Packet type(`pkt_type`):** This field contains the RoE packet subtype information. For example, the packet type 0X00 is reserved for control packets of RoE. Bits 27 to 23, in Figure 2.12 shows the packet type in which one value is reserved for future extension and one value for structure agnostic payload. There are 32 types available and some of the types may include additional headers. Of the 32 types, some of the packet types and their functions are mentioned in Table 2.2.

Table 2.2: Allocated RoE `pkt_type` values where TBD stands for To Be Defined (since RoE frame structure is an ongoing work, some of the packet type values are not yet defined), extracted from [For].

`pkt_type`(in hexadecimal)	Function	Meaning
0x00	Control packet	Payload carrier TLVs for control purpose
0x01	Structure agnostic packet	Content of the payload is unknown at the RoE protocol
0x02	Antenna flow	TBD
0x03	Vendor specific flow	TBD
0x04	Antenna control	TBD
0x05	Slow C and M	TBD

•**Flow ID(`flow_id`):** The flow identifier field contains an identifier number for the

RoE packet flow. It is represented as unassigned integer between 0x0) and 0x7f. Hence, there are 128 flow id available in the RoE header and is indicated in the bit 15 to 0. The benefit of having this field is for multiplexing individual RoE flows between source and destination address pair: For instance, multiple antennas behind one MAC address. The identifier basically allows splitting the multiplexed RoE flows from the underlying network provided that multiplexing mechanism is used. It has no "routing information" at the Ethernet layer and only interpreted by the end point applications. This means that each SA/DA pair has their corresponding flow id number space. According to [For] discussion, the `flow_id` can identify two types of flows: a single AxC; or a group of AxC. And also, the flow id assignment can be done either out of bound or be using the RoE control channel or protocol.

- **Sequence number(seqnum):** This consists of a 32 bits packets sequence number field. It is initialized to 0 (it would eliminate the need for a start of frame bit) and incremented by one on every sent packet irrespective of the contents of the packet. This implies that the sequence numbers do not hold information about the location of the data within the flow or stream but it would carry the information within the frame. A typical way of defining sequence number is a byte counter in which the counter value relates to the first byte in the packet. Thus, it is a generic way of understanding the data within the frame.

- **Payload:** The content of this field varies depending on the RoE subtype. Its format and the control packet content relies on the control packet type.

Chapter 3
Fronthaul Network Requirements

This chapter presents dimensioning the mobile fronthaul requirements. In order to meet the expected QoS for the end users, mobile fronthaul dimensioning plays an important role. Dimensioning requirement for C-RAN architectures featuring a fronthaul network depends on the BBU and RRH separation distance. Thus, the amount of latency introduced to the fronthaul network must carfully be considered, and the actual timing performance also needs to be accuratly determined. As a result, the fronthaul network of C-RAN architecture imposes very stringent requirements. In the following sections, we focus on the four fronthaul network requirements[1]: data rate, latency, jitter & synchronization, and PDV.

Before moving on, there are various metrics which should be understood before studying the mobile fronthaul requirements which include;

1. **Delay/Latency:** It is the measure of the time taken for traffic to arrive at the destination. This performance metrics consists of processing delay, queuing delay, propagation delay and transmission delay.
2. **Packet loss ratio:** measures the ratio of the number of lost packets to the number of transmitted packets.
3. **PDV:** measures the difference in packet delay between selected packet in a flow.
4. **Queue length:** measures the length of a queue.
5. **Capacity:** refers to the amount of traffic that can be accommodated by the system (in bits/s or other units).
6. **Throughput:** measures the quantity of successful traffic that reaches at the destination.

[1]The requirements discussed in this chapter are based on symmetrical assumptions; the uplink and downlink transmission occupy the same bandwidth.

3.1 Requirements and Challenges of Fronthaul Networks

Enabling the open interoperability between BBU and RRH elements in fronthaul network highly depends on the performance and synchronization requirements. And also, there are a number of challenges when a single BBU is shared by a number of RRH. In the following subsections, the fronthaul requirements and challenges are described throughly.

3.1.1 Data Rate

Traffic flows in the fronthaul network have a very high bitrate, usually on the order of units to tens Gbit/s for a cell site, resulting from the aggregation of flows from one or more antennas. The CPRI data rate depends on the RAT, carrier bandwidth, and MIMO implementation [PCDS14]. It can go from 614.4Mbits/s up to 10.17Gbit/sec and are summarized in Table 3.1 with examples and their corresponding applications. For instance, for LTE-A with 4x4 MIMO and 20MHz carrier require approximately 4.915Gbit/s CPRI rate per sector. Similarly, for one sector LTE with 20MHz and 2x2 MIMO the CPRI rate is 2.457Gbits/s.

Table 3.1: Detailed CPRI capacity requirement and application in support of mobile broadband where * means no information, extracted [PMC15].

CPRI	**CPRI Rate**	**Example Data Capacity**	**Application**
Option 1	614.4 Mbps	37.5 Mbps	– 2G/3G Radios – 10 MHz 1T1R LTE Configuration
Option 2	1,228.8 Mpbs	75 Mbps	– 10 MHz LTE, 2T2R LTE Configuration – 20 MHz LTE 1T1R LTE Configuration – Small Cells

Option 3	2,457.6 Mpbs	150 Mbps	– 10MHz 4T4R LTE Configuration – 20MHz 2T2R LTE Configuration – Majority of LTE Macro Market – Small Cells
Option 4	3,072.0 Mpbs	*	*
Option 5	4,915.2 Mpbs	300 Mbps	– 10MHz 8T8R LTE Configuration – 20MHz 4T4R
Option 6	6144Gpbs	*	*
Option 7	9,830.4 Mpbs	600 Mbps	20MHz 8T8R LTE Configuration
Option 8	10,137.6 Mpbs	750 Mbps	Carrier aggregation of 5x20MHz 2T2R LTE

Such very high data rates results in a fully non elastic traffic when time varying traffic load condition of a cell is considered. For traditional RAN, these features are the major challengs as they are designed to transport much lower bitrates.

3.1.2 Latency

The fronthaul and CPRI/OBSAI protocols requires very stringent latency requirement which is often the overall limiting factors how far the fronthaul network can extend. It is a key factor that also depends on heavily on the MFH technology to be used. Specifically, this is a case for fast transportation and high capacity mobile networks with the higher speed CPRI/OBSAI options. Hence, the designing RAN and adding functionality to the MFH needs special consideration such as selection of MFH technology.

As a consequence of decoupling the traditional BS functions into a centralized BS that will be shared among multiple RRHs (i.e. fronthaul network), strict timing conditions between BS and RRH have been specified by RAT standards. Delay contributions due to the transportation of fronthaul signals along RAN network,

Table 3.2: Latency, PDV and synchronization requirements for Ethernet Fronthaul with symmetry assumption.

Properties	Values	Sources
Latency budget(BBU to RRH, including fiber length, PDV, bridged delays)	50μs(for data rate 1–10 Gbit/s)	[IEA]
Latency budget(excl. cable, BBU to RRH)	5μs(for data rate 1–10 Gbit/s)	[IEA]
Maximum Frequency Error contribution	2 ppb	[EA]
Maximum. Bit Error Ratio	10^{-12}	[Int16], [IEA]
Maximum End to End Latency /RTT(including fiber length, PDV, bridged delays)	100μs- 400μs (250μs for optical networks)	[GCT+15], [IEA]
Maximum. PDV	5μ or 10 % of E2E latency	[Gro]
Geographical distance between RRH and BBU	less than 20 Km (current working assumption) and 25 km for optical networks	[STK+15], [HJS]
PLR caused by bit error, congestion ..etc	10^{-6} - 10^{-9}	[Gro]

"fronthaul latency", is one of the main significant challenges for the BBU-RRH design and has a relevant impact on the total latency in the BS.

In general, given that the total latency is fixed by standard, as shown in the Table 3.2 and the internal processing delays of both BBU and RRH depends on the specific software and hardware implementation, there is a standard upper limit on the latency of fronthaul network. The latency can be further categorized into two parts: namely 1) latency due to the adaptation of fronthaul signals into the RAN infrastructure services, which can be caused by the technology used such as CPRI and OBSAI transmission/reception interfaces, and other functions required by optional layer transport technologies(i.e. multiplexing/demultiplexing, buffering, reframing and error correction), and 2) latency due to the contribution of signal propagation along the RAN. The second contribution imposes a limitation on the maximum geographical distance between BBU hostel and the controlled cell sites. A numerical analysis of this parameter is found in Chapter 5.

3.1.3 Packet Delay Variation

PDV is defined as 2-point packet delay variation. As per ITU Y.1540 "delay variation of an individual packet is naturally defined as the difference between the actual delay experienced by that packet and a nominal or reference delay. ITU Y.1540 6.4.2.1 and RFC 5481 using the minimum delay as a reference. (Use of the average delay as the delay variation reference is depreciated.)"

3.1.4 Synchronization and Jitter

Baseband radio signals are very sensitive to mismatch between transmitter and receiver clock frequencies, bit errors, and variation in clock phase (jitter). The synchronization mechanisms in traditional BS and C-RAN BS are different. Traditional BS feeds a single clock generator to all-in-one BS, whereas in C-RAN BBU is responsible not only to transmit the baseband data in both directions, but also the clock signal generated at the BBU to RRH. In order to reduce the overlap of signals coming from different BS operating in different frequency and meet the requirements imposed by RAT standards on accuracy and stability of radio interface, proper synchronization (keeping the carrier frequency sharp) is needed for mobile network operation. For successful TDD network operation, RRH clock is synchronized to the bit clock of the received CPRI signal. It needs to follow time frames precisely so that the downlink and uplink frames don't overlap. The precision of frequency can be changed if some jitter affects the CPRI signal.

There are two types of synchronization methods in fronthaul [GCT+15]: 1) Frequency synchronization, with which the time between two rising edges of the clock match, and 2) phase synchronization, with which the rising edge must happen in the same time. Table 3.3 summarizes the timing requirement for LTE BSs for various network features.

Generally, fronthaul networks have strict synchronization requirements in terms of maximum tolerable Bit Error Rate (BER), frequency error contribution and phase synchronization as defined in Table 3.2. According to CPRI specification, as an example, the BER must be at most 10^{-12} and the jitter introduced by the CPRI link can contribute quantity not greater than 2ppb to the frequency accuracy budget.

As explained earlier Ethernet-based fronthaul network employs statistical multiplexing in order to efficiently utilize the network capacity by employing SM technology. However, it imposes high bandwidth-delay product and packet delay variation on the traffic thus, buffering is needed for handling the packet delay variation of traffic. Although the high throughput is highly welcomed by data-centric technologies, the delay and PDV characteristics are bottlenecks for transporting real-time applications. When such networks are used for transporting packetized streams of continuous media,

Table 3.3: Timing requirements for BS, extracted from [CJCB15]

Feature	Frequency	Time
LTE-A FDD	±50 ppm (wide area BS) ±100ppb (Local area BS) ±250 ppb (home BS)	-
LTE-A TDD		± 5μs (cell with raduis > 3km), ±1.5μs (cell with radius ≤ 3km)
MIMO		≤ 65ns
eICIC		±1 μs
CoMP		±1.5 μs
CPRI	±2 ppb	± 16.6276 ns

receiver synchronization is required. It is aimed to smooth the transmission packet delay variation between packets arrivals for a given stream. This transmission packet delay variation/jitter can be solved at the receiver by using playout buffers [WAS15] as shown in Figure 3.1. In such approach, the buffers introduce additional delay in order to produce a playout schedule that meets the synchronization requirements. The playout buffer is used for packets whose scheduled playtime is in the future. And, it simply replays packets according to the frequencies of packet streams. In such operation, the jitter can be removed at the expense of increased delay.

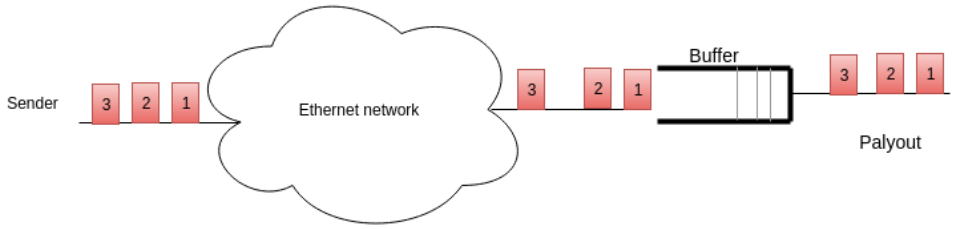

Figure 3.1: Packet stream synchronization.

Chapter 4
Integrated Hybrid Optical Networks/IHON

In this chapter, IHON network (also called fusion solution), a proposed solution for combining the best properties of circuit switching and packet switching into a single architecture is described thoroughly. An overveiw of Optical Migration Capable Networks with Service Guarantees (OpMiGua) networks and an algorithm to compute the free gap between GST packets in IHON node are also explained. Furthermore, the chapter focuses on the concept of aggregation of GST traffics in IHON node, how SM packets are inserted in the computed free gap, and the IHON node design.

4.1 Introduction

Traditionally, infromation have been transported from one place to another place using circuit switched fiber optic networks. Even though guaranteed QoS, low latecny variation, low latency, and synchronization support are the essential and vital features of Optical Circuit Switched (OCS) networks, they are not bandwidth efficient for bursty IP traffic [Bay01]. As a result, the ever increasing IP traffic volume with the resulting demand for capacity leads to the migration of the networks from optical circuit switched networks to optical packet based networks. This inevitable shift brings better bandwidth utilization and lowers cost by introducing statistical multiplexing; however, the low lateny, low PDV, and guaranteed QoS are only offered by OCS technologies and are still essential for mobile fronthaul, backhaul, metro, and transport networks. Both Optical Packet Switched (OPS) [OSHT01] and Optical Burst Switched (OBS) [QY99] networks introduce SM to overcome the inefficient utilization of bandwidth.

In order to support and satisfy the above requirements in multi-service network simultaneously, impovements have been made to the optical packet switched networks to accommodate high throughput and effective QoS capability. The improvements have introduced hardware and software complexity which in turn result in expensive

operational and capital cost of the techniques. Thus, a new concept of hybrid switch networks integrating both OCS and OPS technologies is introduced. It is proposed to provide support for various service requirements and efficiently utilize the bulk capacity of optical networks. In the following sections, the variants of hybrid optical network architecture are detailed.

4.2 Hybrid Optical Network Architectures

Hybrid Optical Network Architectures employ two or more technologies simultaneously to improve the overall network performance by combining the advantage of different network technologies while avoiding their disadvantage [GKB+06]. According to the author [GKB+06], the network architecture combines two or more basic switching technologies at the same time to transport all traffic.

Depending on the degree of interaction and integration of the network technologies, hybrid optical networks can be divided into three [GKB+06]:

1. Client-server optical hybrid optical network
2. Parallel optical hybrid optical network
3. Integrated optical hybrid optical network

In the following subsections, the key characteristics, performance benefits, and the realization complexity of hybrid networks are discussed according to the article [GKB+06].

4.2.1 Client-server Hybrid Optical Network

As shown in Figure 4.1, this class employs a hierarchy of optical networks, where the wavelength-switched server layer (the lower layer) serves as a server layer setting up a virtual topology for the upper client layer. Since the client layer is an OBS or OPS network, it consists of several OBS or OPS nodes. The nodes at the ingress of the core network are responsible for aggregating traffic, and are connected via the direct light path to the server layer. Hence, packets or bursts transparently flow in light paths established in the lower layer and can only be switched at the upper layer. To allow transparent flow of the payloads the server layer allocates lightpaths, where as client-layer performs switching of optical bursts/packets [GKB+06].

Since this particular hybrid archieture uses a virtual topology which only yields less traffic per link, the multiplexing gain is reduced.

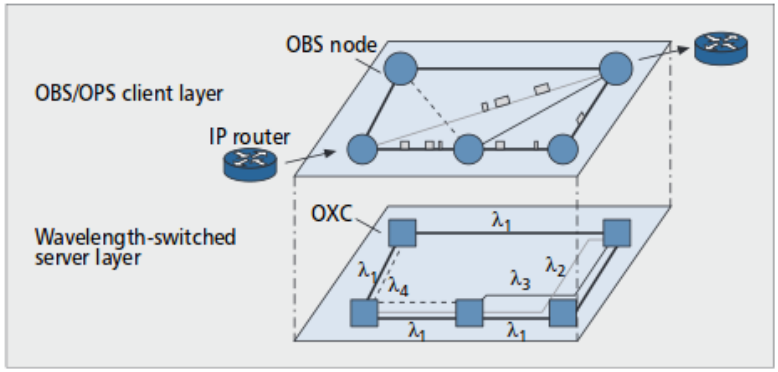

Figure 4.1: Client-server hybrid optical networks [GKB+06].

4.2.2 Parallel Hybrid Optical Network

This class uses two or more optical layer networks side by side, offering different transport services in parallel. Depending on the decision made by an intelligent node, the parallel optical layer networks offers various transport services individually or in combination. Figure 4.2 shows a parallel hybrid optical network in which the service edge node makes the selection for arriving traffic to be transmitted either as bursts or continuous byte stream/ inside the light path. Based on the traffic nature such as QoS requirement, bandwidth, and user request, the service edge selects the arriving traffic transport nature either as optical burst or byte stream.

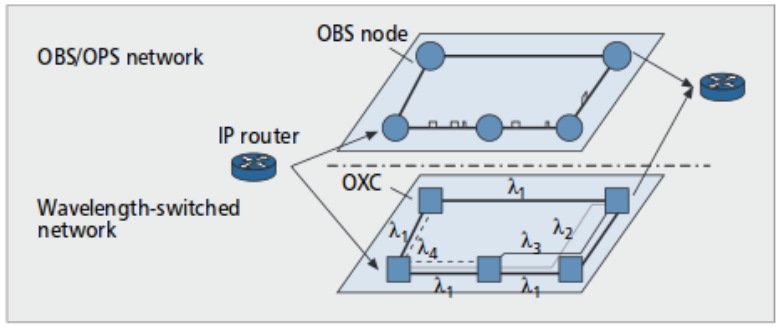

Figure 4.2: Parallel hybrid optical networks [GKB+06].

4.2.3 Integrated Optical Hybrid Optical Network

Unlike both client-server and parallel, integrated hybrid optical networks, integrates two or more network technologies into a single network to share the same bandwidth resources on the same network simultaneously [KOS09]. Hence, the traffic can be transported either in wavelength switched or packet switched mode. Figure 4.3 illus-

trates sharing of wavelength between OCS and OBS/ OPS network technologies(high priority and best effort classes). Each node contains both the wavelength and packet switched devices to transmit the packet based on the QoS differentiation. The packets can either be transmitted over E2E light path or changed to packet switched mode in case of congestion. The intermediate processing by the subsequent nodes is removed when it is transmitted over E2E light paths(high priority class). However, dynamic traffic is handled by using the packet switched mode. From the technological point of view, this method offers an optimal resource utilization, but complex control mechanism.

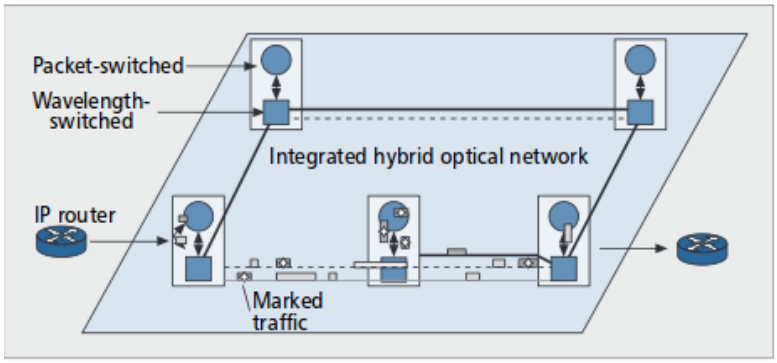

Figure 4.3: Integrated hybrid optical networks [GKB+06].

A couple of IHON variants have been proposed: OpMiGua [BHS06] [KOS09] and Fusion [Tra12]. In both variants, the capacity of the same wavelength is shared between the high priority class and dynamic traffic flows, and the node fully integrated both wavelength and packet switched devices. Detecting the current mode of operation of each packet, inserting, and removing of packets is accomplished by this node.

4.2.4 OpMiGua

OpMiGua [BHS06] networks comprise a Wavelength Routed Optical Network (WRON) enabling constant delay and no packet loss and an SM networks enabling high throughput. With Optical Cross Connect (OXC) and OPS components in a single node, the network operates as both WRON for GST traffic and OPS network for SM traffic. The two service classes: GST and SM, share the wavelength by time division wavelength multiplexing. Using reservation technique the GST class is given absolute priority over the SM class. Hence, the SM class is modeled as the best effort.

As illustrated in Figure 4.4, GST packets follow the defined light paths by the configuration of the OXC, and the SM packets are switched and processed through the optical packet switches according to their header information. In such orientation, the GST packets experiences a fixed delay and are not subject to the packet loss [BNOS05],

while SM packets are dropped if there is congestion. By sending the GST packets through the WRON and SM through the packet switched network on the link not used by the GST traffic, the important features of WRON and OPS network are achieved.

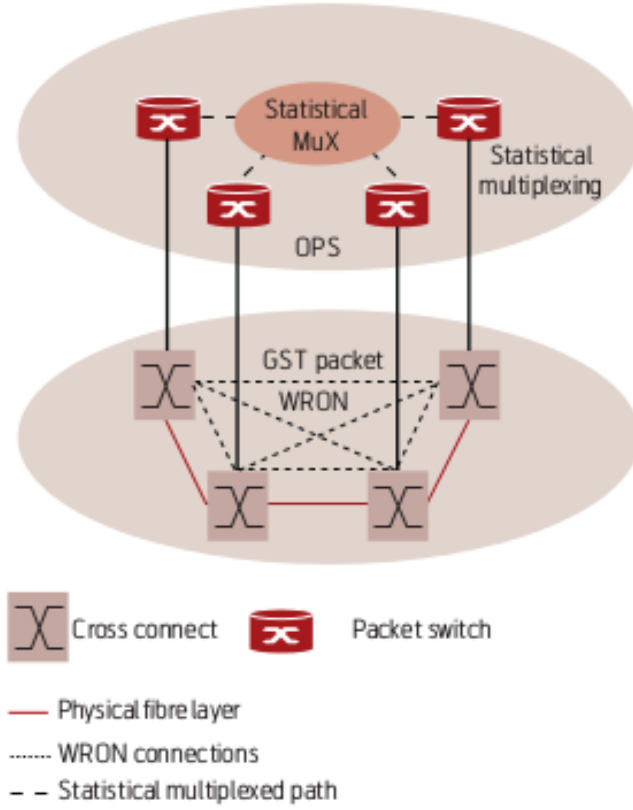

Figure 4.4: A hybrid network model illustrating the sharing of the physical fiber layer. The optical cross connects and optical packet switches are co-located, either as separate units or as one integrated unit. The WRON can be a Static or a Dynamic-WRON [BNOS05].

4.2.5 Fusion Solution/IHON Network

Fusion solution is one variant of IHON that uses a packet switched nodes to transport both GST and SM traffic classes. It combines the best properties of circuit and packet switching in an Ethernet compliant network, as illustrated in Figure 4.5, to obtain high throughput, ultra-low delay, ultra-low PDV, and zero packet loss.

In fusion networking technology, the traffic is divided into two service classes while using the capacity of the same wavelength: namely 1) a GST service class

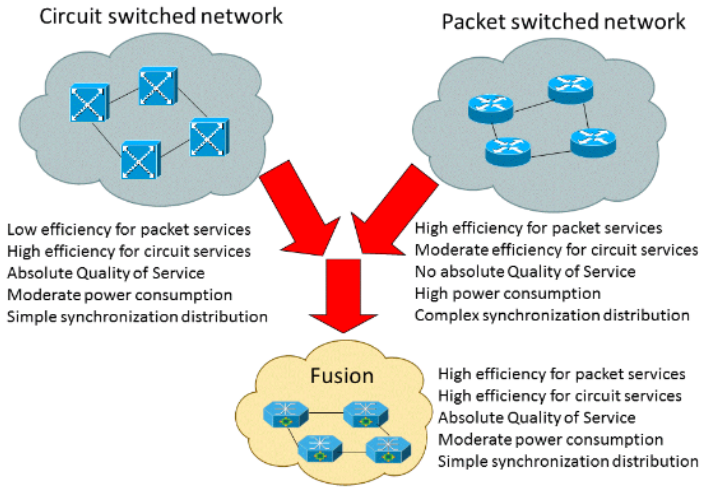

Figure 4.5: Fusion network: created by combining the best properties of packet and circuit switching, extracted from [Tra12].

offering QoS demands such as fixed low delay and no packet loss for the circuit switched traffic, and 2) an SM service class providing high bandwidth efficiency for the Best Effort (BE) packet switched traffic [BHS06].

4.3 IHON Node Design

The basic idea in the IHON network is that the GST packets follow preassigned wavelengths through either static WRON or dynamic WRON from the sender to the receiver while SM packets are inserted in the vacant gaps to enhance link utilization. The link is divided in time without using time slots. When an Ethernet packet arrives at the input port, they are tagged with VLAN-ID in order to distinguish between GST and SM packets. If the arrived packet is GST, they are allowed to pass with absolute priority via the other 10GE interface. However, if the packet is SM, it is first processed and then either buffered until idle time gaps between GST packets is available or dropped to one of the 1GE interfaces according to their VLAN-ID.

Figure 4.6 and Figure 4.7 below shows functional illustration of the IHON node design and the internal operation inside the IHON node respectively. The node consists of SM DMUX, GST gap detector, SM packet scheduler, 2x10 GE line interfaces (Xe0 and Xe1), and 10x1GE client interfaces (ge0-ge1). The line interfaces bring two benefits to the node: it can give 1+1 or 1:1 protection and enable add/drop functionality of transparent Ethernet lines [VBB13]. Each of the GE interfaces is dynamically configurable as either Ethernet lines or SM paths.

The GST and the SM traffic classes are identified and switched at the input port according to VLAN tag used by the nodes. While the GST packet bypasses the packet switch and continues towards the output link, an SM demultiplexer(DMUX) extracts the SM packets from the channel to be processed. The processing is achieved based on the header information.

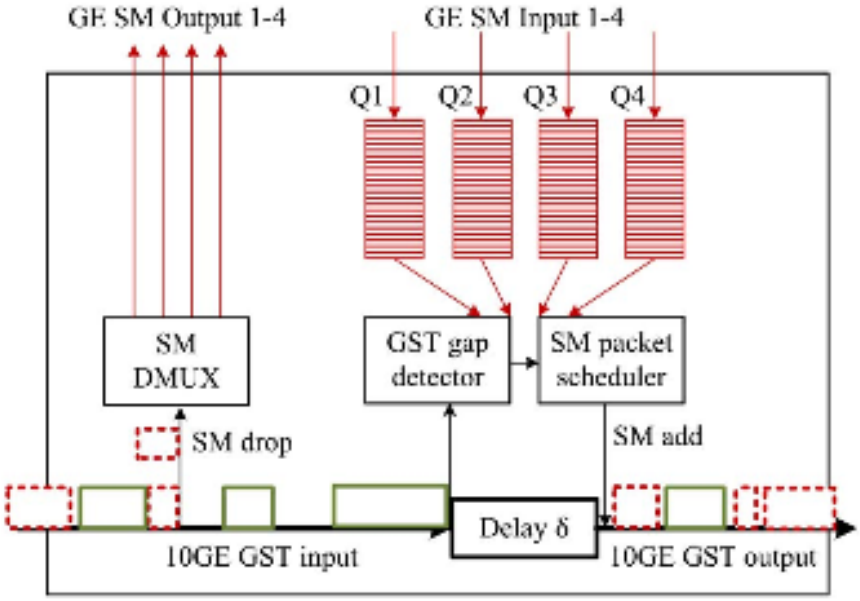

Figure 4.6: Schematic diagram of IHON node design, extracted from [VBB13].

4.3.1 IHON Node Operation

Figure 4.7 illustrates the IHON node internal operation. As depicted, the classifier first classifies the arriving traffic into GST or SM traffic. After classifying, the SM demultiplexer (SM DMUX) drops the SM traffic to the packet switch while GST packets are allowed to bypass the packet switch. The dropped SM packets are placed inside a queue and is processed according to their header information. Depending on the number of input SM streams, the arriving SM packets are assigned a separate queue. This implies that the number of queue in IHON node is the same as the number of input SM streams.

At the input, the GST gap detector senses the incoming and leaving GST traffic. Using the GST gap detector, the inter packet gap between GST packets is measured, and passed the measured value to the SM packet scheduler. It continuously updates information about the vacant gaps and forwards the information to the SM packet

scheduler. The queue is scanned for suitable SM packets that can fit the measured gap, and the SM packet scheduler fills the gap with this packet with the best effort QoS. As a result, using this technique, the efficiency of the link utilization increases.

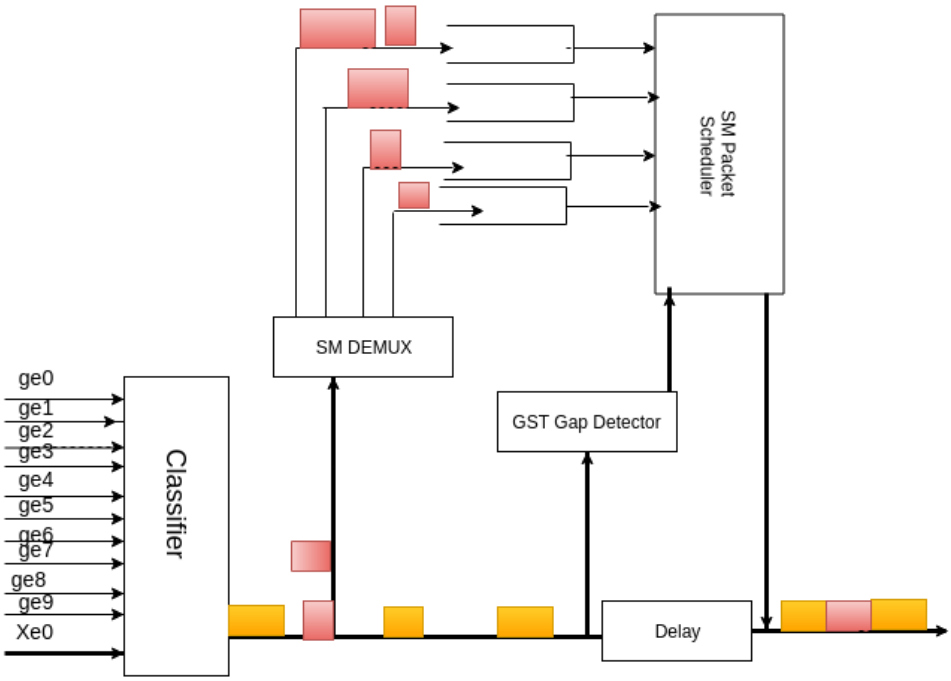

Figure 4.7: Internal operation of IHON node, adopted from [VBB13].

4.3.2 Delay and Packet Delay Variation in IHON Node

A fixed delay, δ, equivalent to the maximum length of SM packet service time, is applied electronically to the GST packets. Within this time, the GST gap detector discovers the length of free time gaps before an SM packet is inserted; hence, prevents the preemption of SM packets by incoming GST packets. Inter-packet time gap, Δ_i, of the GST packet is detected only when the packets enter the delay line. The delay line introduces deterministic E2E GST packet delay and is proportional to the number of hopes the light path traverses.

In order to illustrate the deterministic effect of fixed delay line on the GST traffic, let's consider Figure 4.8(a). The figure shows how the inter GST packet gap remains constant after the GST traffics traverse the delay component. At the input channel, the inter packet gap times of GST packets when the packet enters the delay line are expressed by Equation 4.1 and Equation 4.2 [VBB13]:

$$\Delta_1 = Start(2) - End(1) \tag{4.1}$$

$$\Delta_2 = Start(3) - End(2) \tag{4.2}$$

After the delay component (t+ δ), at the output channel, the gaps of GST packets are given by Equation 4.3 and Equation 4.3 and are kept unchanged [VBB13].

$$\Delta_1^{'} = [Start(2) + \sigma] - [End(1) + \sigma] = \Delta_1 \tag{4.3}$$

$$\Delta_2^{'} = [Start(3) + \sigma] - [End(2) + \sigma] = \Delta_2 \tag{4.4}$$

Since all packets undergo the same fixed delay δ, inter-packet time gaps Δ_i[1] are remained the same at the output channel, $\Delta_i^{'}$=Δ_i. Thus, the IHON network doesn't introduce PDV to the circuit traffic.

4.3.3 Delay and Packet Delay Variation in Ethernet Switch

Figure 4.8(b) and (c) depicts the scheduling techinque used in packet switches with the non-preemptive priority and in IHON node respectively. Unlike non-preemptive GST scheduling in IHON node, electronic packet switches transmit packet with lower priority only if no packets with higher priority is available at the input queue. When a higher priority class arrives (packet 3) while lower class priority packets are being served(packet 2), the packet will be queued till the lower priority packet has finished, as illustrated in Figure 4.8(b). Hence, PDV is introduced in high priority stream.

Figure 4.9 presents the diagram of Ethernet switch, and how the delay of a packet in an Ethernet switch be measured. The delay is measured by starting a timer when the first bit of the packet gets into the Ethernet switch and stopping when the first bit of the packet leaves the switch. The time it takes the switch to transmit a packet depends the speed of the switch. It means that the faster the switch, the quicker the packets can be sent to the destination which in turn the less time the packets needs to say in the queue (lower delay). It is also important to note that the delay accuracy of the packet depends on the traffic rate and pattern.

[1] Δ_i represents the inter packet gap time between GST packets

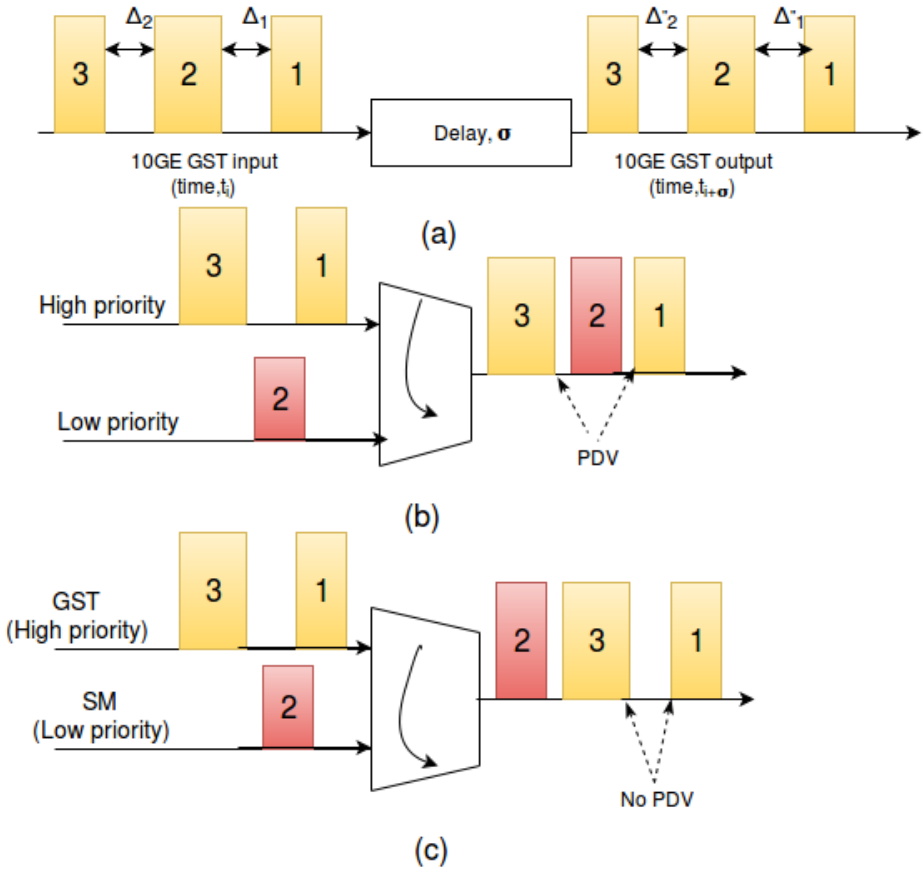

Figure 4.8: a) Inter packet gap and delay experienced by GST packets, b) Scheduling in strict priority QoS in packet switches where packet delay variation (PDV) occurs on high-priority packets, c) Scheduling in fusion node where SM packets are inserted only if there is a suitable gap between the GST packets, extracted from [VBB13].

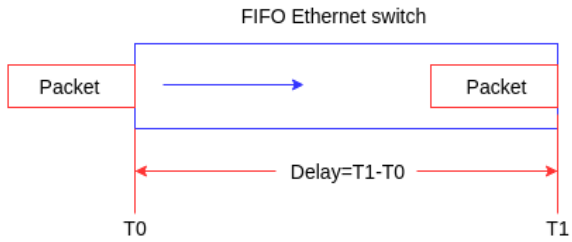

Figure 4.9: FIFO delay on Ethernet switch

It is worth mentioning that IHON doesn't preempt any on-going scheduling of best effort SM packets while it minimizes the processing and energy usage. The reason why it is energy efficient is that the transmission of SM packets is carried out when the transmission of the SM packet will be successful. However, though pre-emptive priority scheduler doesn't introduce PDV, it pre-empts the low priority packets.

4.3.4 Inter-packet Time Gap Computation in IHON Node

An algorithm called round robin gap filling scheduling algorithm [VBB13] is used to compute the inter packet gaps between GST packets on the underutilized wavelength. A monitoring module at the delay line senses the arrival of GST packet at the delay line and the exit time value of the GST time.

Based on the incoming and leaving times of the GST packets and applied fixed time window in IHON system, the inter-packet time gap can be computed. Gaps sensed by the gap detector are saved in a time ordered list according to the corresponding time values. The first gap on each channel of the list is made available to packet scheduler. Afterwards, the SM scheduler knowing the sensed gap, search in round-robin manner the head of SM queues, for SM packet smaller than the sensed gap. The gap computation for one channel according to round-robin gap filling scheduling algorithm is described below, and the notations used to describe the algorithm are presented in Table 4.1.

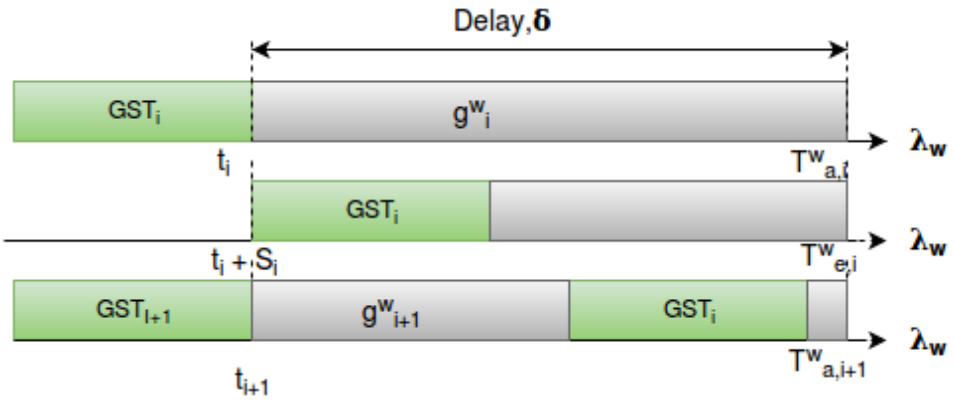

Figure 4.10: Detection of free time gaps with in the time window created by the fixed delay, extracted from [VBB13].

Table 4.1: Definition of parameters used in the gap computation.

Parameters	Definition
$T^{w}_{a,i}$	The incoming time of GST packet i to the delay line of output channel λ_w
$T^{w}_{e,i}$	The leaving time of GST packet i to the delay line of output channel λ_w
δ	Fixed delay
g^{w}_{i}	The gap on the channel w of packet i
S_i	Service time of packet i

In Figure 4.10, two GST packets, GST_i and GST_{i+1}, are considered in order to describe round robin algorithm, where GST_i is the first packet arrived at the delay line and GST_{i+1} is the packet arrived after GST_i.

- When the GST packet i arrives the delay line at time t_i, the arrival time of packet i is updated to the output channel λ_w(busy time starts): $T^{w}_{a,i}=t_i + \sigma$. The inter-packet gap is $g^{w}_{i}=\delta$ if only packet i is available in the delay line and the previous GST packet(i-1) has already left the delay line (i.e. $T^{w}_{a,i} \geq T^{w}_{e,i-1} + \delta$); else the gap is given by $g^{w}_{i}=T^{w}_{a,i}\text{-}T^{w}_{e,i-1}$. Where $T^{w}_{e,i-1}$ is the exit time of previous packet, i-1.
- After the last bit of GST packet i enters the delay line at $t_i + S_i$, the exit time of packet i is updated and the output channel w is released (end of busy time): $T^{w}_{e,i-1}=(t_i + S_i)+ \delta$.
- The current gap value that is given to the scheduler is updated at $T^{w}_{e,i-1}$: For instance, the current gap value is g^{w}_{i+1} computed as illustrated above if the next GST packet exist. Otherwise, it is equals to the maximum packet length, δ.

4.4 IHON Node Aggregation

In optical circuit switching, packet traffic between ingress and egress nodes may have one or more paths with one or more intermediate nodes. Each path has its own wavelength. However, in fusion node by scheduling each GST stream on different time-slots, one or more GST streams can be aggregated on a single wavelength. While the GST streams are transmitted from the source to destination on light path, the SM packets can be added to the intermediate nodes if there is a vacant gap on the wavelength. The quality of service of GST packets is not affected by the insertion of SM packets.

With the help of data containers, one or more GST packets are aggregated together with container control information in fusion node. Figure 4.11 illustrates the aggregation of five GST 1Gb/s Ethernet input streams into one 10 Gb/s Ethernet

output link. The basic idea behind this aggregation scheme is to transfer information regarding the inter-packet gap of GST packets arrived at a port, like GE port assigned to the GST stream. As a result, the aggregator uses this information when reading packets from the buffer and transmitting them in the wavelength channel with the same number of bytes in between packets. The GST packets arrived at the 1Gb/s Ethernet input are tagged and aggregated into their corresponding container while the inter-packet gap is maintained, then SM traffic is dropped at the SM DMUX for processing. Depending on the maximum expected GST packet size and the number of ports being aggregated, the time period reserved for each port varies [VBB$^+$15]. The GST packet bypasses the packet switch, while SM packet is queued and processed in accordance with their header information. With a compression factor of 1Gb/sec to 10Gb/sec, the GST packets will be compressed in time in order to be sent out via 10Gb/sec. Synchronization packets are used to identify the aggregation containers. According to [VBB$^+$15], because of the added overhead, the fusion node is capable of aggregating a maximum of nine 1 GEports where 1 GE port is used for the overheads.

The GST gap detector computes the gap between GST packets and containers to pass it to the SM packet scheduler when GST packet arrives at the delay line. After that, SM packet scheduler scans for the suitable SM packet inside the queue, and insert the SM packets in the computed gaps which greatly optimizes the utilization of the wavelength.

At the egress node, the inverse time compression factor is used to the aggregated GST packets, and the streams are precisely reconstructed using the inter-packet gaps. In every node, the GST stream passes through a fixed delay which depends on the maximum SM length and capacity of the link. This allows preventing of pre-emption SM packets. However, it has a deterministic effect on the end to end delay of the stream.

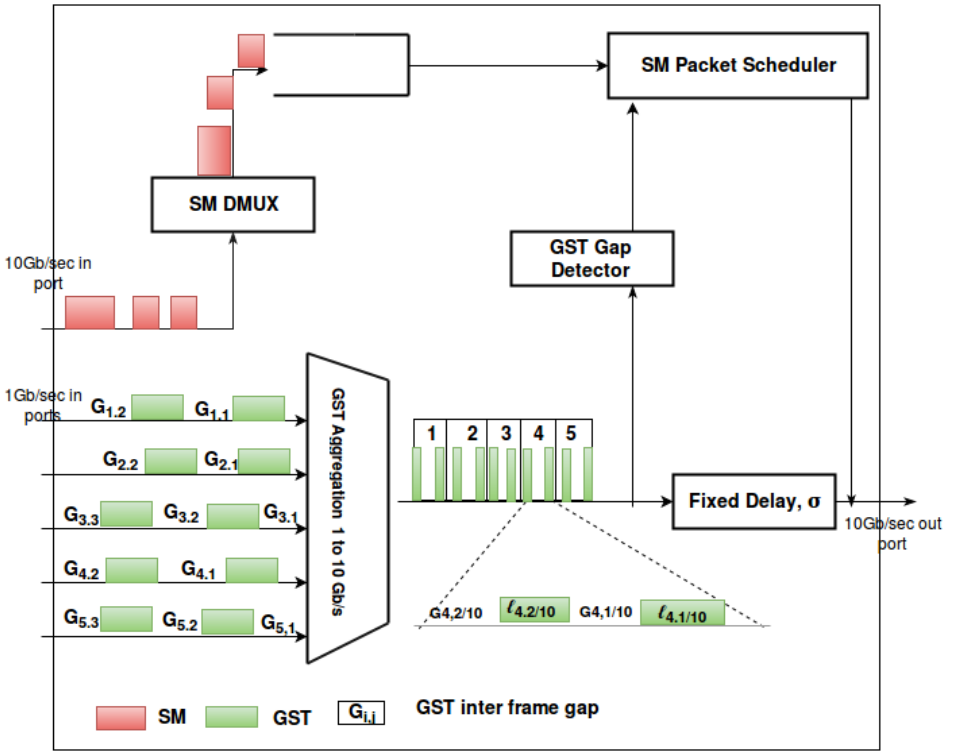

Figure 4.11: Aggregation of five GST streams and SM insertion. The figure explains how GST traffic are aggregated in fusion node, and how the insertion of SM packet is achieved [VBB+15].

In general, the traffic streams; SM and GST, are identified by their VLAN-ID. Each GST stream follows a dedicated path with a light processing in the nodes which in turn reduces processing in the streams.

Chapter 5
Analytical/ Simulation Model

In this chapter, we present the analytical models of the key elements of performance metric, and the simulation model of IHON nodes and Ethernet switches. The end to end latency, maximum separation distance between RRH and BBU, and PDV of several fronthaul solutions with emphasis on Ethernet and IHON networks are discussed.

5.1 Maximum End-to-End Latency

The maximum E2E latency is the maximum time taken for a signal or packet to be transported across a network from source to destination. To illustrate how it is computed in a network, let us consider an LTE Frequency Division Duplexing (FDD) radio interface with C-RAN RAN infrastructure where Hybrid Automatic Retransmit reQuest (HARQ) is processed between UE and BBU at the central office. In such cases, the maximum E2E latency and the maximum separation distance between RRH and BBU are limited due to the timing requirement of the synchronous HARQ protocol used as a retransmission mechanism. Specifically, when the UpLink (UL) data packet is received at the radio frame number i, the BBU or eNB(in LTE network) must send back the corresponding ACK/NACK indication at the radio frame number (i+3) in DownLink (DL) as illustrated in Figure 5.2. This implies that the latency budget for the BBU-RRH[1] is exactly 3ms. Hence, it must hold the following inequality for RTT:

$$RTT_{BBU-RRH} = 2\tau + t_{RRH,UL} + t_{BBU,UL} + t_{BBU,DL} + t_{RRH,DL} \leq 3ms \quad (5.1)$$

Where τ may refers the processioning time fronthaul nodes and any other active components in the fronthaul network.

[1]The time difference between the complete reception of the data frame and the start of transmision of the ACK/NACK indication.

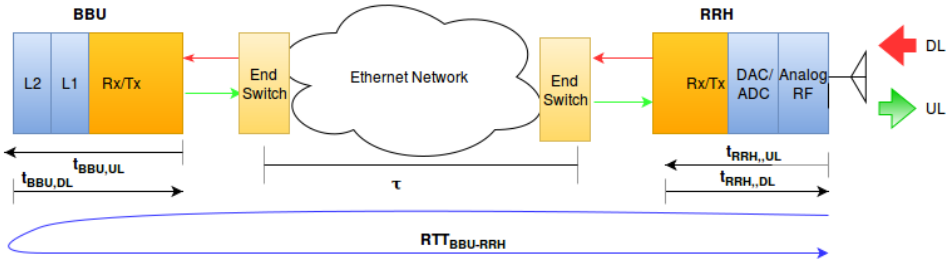

Figure 5.1: The maximum end to end latency in C-RAN network.

RAN standards specify the timing for some physical layer procedures presented between BBU and RRH. The following values are taken from the typical commercial equipment implementing the CPRI interfaces.

$t_{RRH,UL} \simeq 12\ \mu s$, $t_{BBU,UL} \simeq t_{BBU,DL} \simeq 1.3$ ms, $t_{RRH,DL} \simeq 21\mu$ s

BS design largely depend on the vendor implementation, and there are no universal values regardless of internal processing time of BBU and RRH. However, in order to compensate the delay caused by fronthaul network, vendors design BBU to complete the processing and sending ACK/NACK usually with in 2.75ms, instead of 3ms. Thus, about 250μs can be allowed for the fronthaul network.

Since the BBU and RRH are located far apart from each other in C-RAN, there is an additional delay called τ due to transmission delay of the fronthaul network (such as active WDM, Passive Optical Network (PON), Ethernet $\cdots$ etc). All the delay contributions in the Figure 5.1 must be less than 3 ms. In order to maintain this timing, the delay caused by fronthaul network must be compensated.

The delay components of the three parts illustrated in Figure 5.2 and detailed in Table 5.1 are listed in Table 5.2.

5.1.1 Maximum E2E Latency and Separation Distance for Active WDM

Using the above delay budget for the fronthaul network, the maximum separation distance between BBU and RRH and maximum E2E latency can be computed. For instance, let's consider the delay components of fronthaul network with active WDM which contains components provided by both BS vendor and fronthaul vendors illustrated in Table 5.2.

The typical values of the delay components listed in Table 5.2 are RTT values.

Table 5.1: Delay components of each parts of Figure 5.2, extracted from [HJS].

1. RRH to BBU	2. BBU/CPRI processing	3. BBU to RRH
1.1. RRH/RF processing(UL)	2.1. BBU processing	3.1. Transmission delay (RRH to BBU)
1.2. RRH/CPRI / tx/rx processing(UL)	2.2. L1: UL fame decoding	3.2. Active equipment processing(node processing)
1.3. Transmission delay (RRH to BBU)	2.3. L2: ACK/NACK creation	3.3. RRH/CPRI/ tx/rx processing(DL)
1.4. Active equipment processing(node processing)	2.4. L1: DL frame creation	3.4. RRH/RF processing(DL)
	2.5. BBU/ CPRI processing	

Table 5.2: Typical values of delay components in the fronthaul network, extracted from [HJS].

Delay components	Description	Typical values
1. Round trip RRH/RF processing time(RRH)	1.1 + 3.4	∼25-40μsec
2. Round trip RRH/CPRI processing time(RRH, BBU)	1.2 + 2.1 + 2.5 + 3.3	∼10μsec
3. BBU round trip processing	2.2 +2.3 + 2.4	∼2700μsec
4. Fronthaul latency (due to fronthaul equipments)	1.4 + 3.2	∼40μsec(OTN encapsulation, ∼ few μsec(Non OTN encapsulation)

Hence, the minimum RTT for OTN encapsulation can be computed as follows:

$$\text{Min RTT} = 3\text{msec} - (40\mu\text{sec} + 10\mu\text{sec} + 2700\mu\text{sec} + 45\mu\text{sec}) \tag{5.2}$$

$$= 205\mu\text{sec} \tag{5.3}$$

Since the fronthaul standards are specified with the assumption of symmetry, the minimum absolute one way latency is equals to 102.5μsec which in turn leads to the minimum separation fiber distance of 20.5Km given that the one way latency per link is 5μsec/Km:

$$\text{Minimum fiber distance} = 102.5\mu\text{sec}/5\mu\text{sec/Km} \tag{5.4}$$

$$= 20.5\text{Km} \tag{5.5}$$

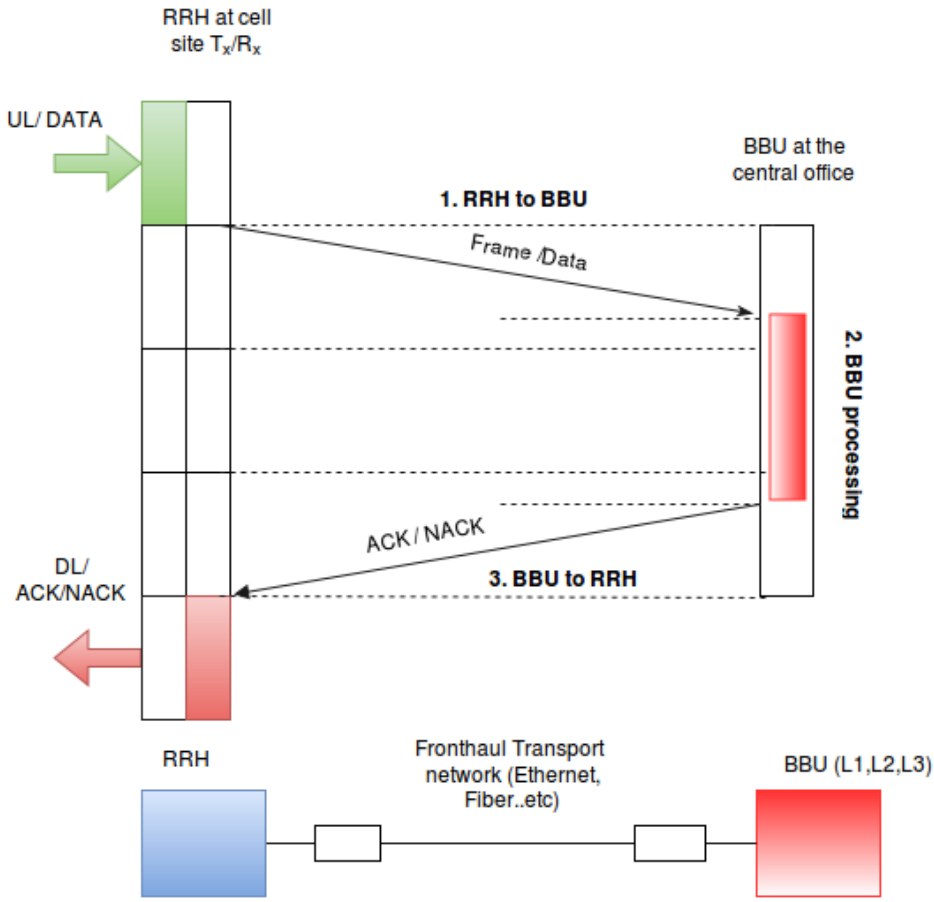

Figure 5.2: Delay contribution of the BBU and RRH along the fronthaul network.

Similarly, the maximum E2E latency that could be supported by active WDM when OTN encapsulation is considered is given by the following expression:

$$\text{Max RTT} = 3\text{msec} - (25\mu\text{sec} + 10\mu\text{sec} + 2700\mu\text{sec} + 45\mu\text{sec}) \tag{5.6}$$

$$= 248\mu\text{sec} \tag{5.7}$$

Therefore, the maximum one way E2E latency is 124μsec, and the maximum separation fiber distance is calculated as:

$$\text{Maximum fiber distance} = 124\mu\text{sec}/5\mu\text{sec/Km} \tag{5.8}$$

$$= 24.8\text{Km} \tag{5.9}$$

According to the above calculations, in OTN transport the value of one-way fronthaul latency is in the range of 102.5 to 124μsec, which correspond to fronthaul link distance of a range 20.5 to 24.8km (assuming the classical value of 5μs/km for one way fiber propagation delay). These calculated values are in accord with the fronthaul requirements, Table 3.2.

5.1.2 Maximum E2E Latency and Separation Distance for Dedicated Fiber

As previously mentioned, the processing time for fronthaul transport (t_{TR}) depends on the specific transport technology. For example, the typical values for OTN encapsulation can be in the range 28 to 41μs ($\sim$40μsec in Table 5.2) and for dedicated links, there is no latency contribution caused by the fronthaul transport over a lower-layer technology($t_{TR} = 0$). The fronthaul is transported "as it is" in dedicated fiber resulting in zero processing time at the nodes. Hence, the maximum RTT for dedicated fiber can be calculated as:

$$\text{Max.RTT} = 3\text{msec} - (40\mu\text{sec} + 10\mu\text{sec} + 2700\mu\text{sec} + 0\mu\text{sec}) \tag{5.10}$$

$$= 250\mu\text{sec} \tag{5.11}$$

Considering the symmetry assumption in fronthaul standard specification, the maximum one way E2E latency is 125μsec, and the maximum separation fiber distance is:

$$\text{Max. fiber distance} = 125\mu\text{sec}/5\mu\text{sec/Km} \tag{5.12}$$

$$= 25\text{Km} \tag{5.13}$$

Hence, the previous numbers lead to a value of maximum one-way fronthaul latency equal to about 125μsec, which is equiva-lent to a maximum fronthaul link distance about 25km(assuming the classical value of 5μs/km for one-way fiber propagation delay).

The values calculated in Section 5.1.1 and Section 5.1.1 are in accord with the typical range of 20 to 25km reported in [STK$^+$15], [HJS], and fronthaul requirements listed in Table 3.2.

5.1.3 Maximum E2E Latency and PDV for Ethernet Networks

The maximum E2E latency calculation in Ethernet network depends on depends on the following parameters [For]:

- **Propagation delay:** Finite amount of time taken by packet to propagate over a link and is constant for a given link length; depends on link length (5usec/km).
- **Packet processing delay:** The delay introduced by typical Ingress/Egress (on passed bridg) processing functions such as decapsulation/encapsulation, route lookup, packet classification for marking/remarking etc; depends on bridge implementation (non-blocking!), For switches/routers the value is constant.
- **Playout buffer delay(store & forward delay for store and forward Ethernet switch):** Delay experienced by packet waiting at an egress queue, waiting for one or more packets to be sent out; depends on configuration the queue and number of packets, which are present in various egress queues. Hence, delay is variable.

Since PDV is variation in the E2E delay experienced by that packet and a nominal or reference delay (ITU Y.1540 6.4.2.1 and RFC 5481 using the minimum delay as a reference), it is important to compute the minimum and maximum delay as follows:

Min.and Max. Delay

Minimum delay in a network is expected when a packet never encounters even a single packet in front of it on egress link when it passes through all the links [Chh13]. Thus,

$$Delay_{min} = \sum_{j} d_{Link\_propagation\_j} + \sum_{j} d_{Packet\_processing} \tag{5.14}$$

As seen from the equation 5.14, the lowest delay is simple addition of link propagation delay & packet processing delay.

Maximum delay in a network is encountered when the packet encounters one or more packets in front of it at egress link of each & every node [Chh13]. Thus,

$$Delay_{max} = \sum_{j} d_{Link\_propagation\_j} + \sum_{j} d_{Packet\_processing} + \sum_{j} d_{store\&fwd} \tag{5.15}$$

Also note that packet delay would vary between lowest & highest delay. So the maximum amplitude of packet delay variation would be:

$$Delay_{max} - Delay_{min} = \sum_{j} d_{store\&fwd} \tag{5.16}$$

5.2 Simulation Model for IHON Node and Standard Ethernet Switch

In this work, we simulate IHON node and Ethernet switch based on non preemptive scheduling using the programming language called simula. Simula/DEMOS is designed and implemented as a full scale general purpose programming. As its name implies, it is an object-oriented simulation language developed at the Norwegian Computing Center in Norway for designing of simulation entities. It has also been used in simulating Very Large-Scale Integration (VLSI) designs, process modeling, and other applications [OJDN70]. In Appendix A, the implementation of IHON node, Ethernet switch, and characterization of the packets used in the simulation are presented.

5.2.1 Traffic Pattern

In the IHON node implementation, the arrival processes of GST and SM traffic are described by negative exponential distributions, where as their packet length's are described by deterministic and uniform distributions respectively. The GST packets are allowed to travel into a network following reserved wavelength available so that they do not experience any packet loss. The rate of GST traffic source is defined using negative exponential distribution with a mean value which is a function of capacity of the output port and the length of GST packet. Hence, it ensures the wanted load from GST traffic on single wavelength. Unlike GST packets, since SM traffic have no pre-established path it may experience a packet loss and is inserted in suitable gaps between GST packets. And its mean value is a function of the channel capacity and length of SM packets drawn from the distribution.

Similarly, negative exponential distributions are used to describe the arrival processes for HP and LP traffic in Ethernet switch implementation. The packet length distribution used to describe the length of HP and LP packet is deterministic distribution. HP traffic are given highest priority, and LP traffic are given low priority. The mean value for HP and LP traffic in Ethernet switch follow the same pattern as GST and SM traffic in IHON node.

Chapter 6
Results and Discussions

In this chapter, the obtained simulation results are presented and analyzed, and the most comprehensive discussion of the results is given. We considered PDV, PLR, and average latency as a performance metrics to evaluate performance of IHON node and Ethernet switch. With analysis of each metrics, an identification of parameter that restricts the overall performance is conducted. The evaluation of IHON and Ethernet network in RoE mobile fronthaul setting is also conducted. From this evaluation, we find how such networks can be dimensioned with respect to: fiber link length, number of nodes, technology $\cdots$ etc.

6.1 Simulation Parameters

Table 6.1 and Table 6.2 presents the set of parameters which have been used during the simulation and the list of notations used for different traffic loads on different interfaces respectively. The value of the total system load used by the GST and SM traffic have been varied throughout the simulation. In this work, system load refers to the sum of SM and GST traffic loads, i.e. L^{T}_{10GE}=n*L^{SM}_{1GE} + L^{GST}_{10GE}, where n is the number of SM input streams. And also, we assume that the wavelength has the same transmission rate of 10 Gbps and the fixed delay is given by the duration of the maximum sized SM packet being scheduled to the output wavelength.

Table 6.1: Simulation parameters used in the analysis of performance metrics of SM and GST packets (for IHON node).

Parameters	**Value**
Seed values	907 234 326 104 711 523 883 113 417 656
Output link capacity	10 Gb/sec
Minimum SM length	40 Bytes

Length of GST packet	1200 Bytes
Maximum SM length	1500 Bytes
Load of GST traffic	varies
Load of SM traffic	varies
Number of SM buffer in a node	4
Maximum number of buffer	4
Buffer size	16 MByte
Number of packets	40000

Table 6.2: Notation of parameters used in the simulation result analysis.

Description	**Notations**
The load of SM traffic on 1 Gb/s interface	L_{1GE}^{SM}
The load of GST traffic on 10 Gb/s interface	L_{10GE}^{GST}
The load of GST and SM traffic on 10 Gb/s interface	L_{10GE}^{T}
The load of LP traffic on 1 Gb/s interface	L_{1GE}^{LP}
The load of HP traffic on 10 Gb/s interface	L_{10GE}^{HP}
The load of HP and LP traffic on 10 Gb/s interface	L_{10GE}^{T}

Note that in the descriptions below, L_{1GE}^{SM} is equivalent to the total load contributed from the four 1GE SM traffic on 10 GE traffic.

6.2 IHON Node Performance

To study the performance of IHON node while transporting GST and SM traffic, the traffic has been transported and analyzed on a 10GE output wavelength. Figure 6.1 illustrates how these traffic has been generated, and utilize the output link. Firstly, the GST and SM traffic were generated. After generating, the GST traffic was sent to the 10 GE port of the IHON node while the SM traffic was queued in a buffer until a suitable gap was detected. Secondly, both the GST and SM traffic was processed and sent out through the same output port.

For IHON node, the average latency, PLR, and PDV of SM and GST traffic with respect to GST load are shown in Table 6.3. The values are obtained by holding SM load fixed, L_{1GE}^{SM}=0.3.

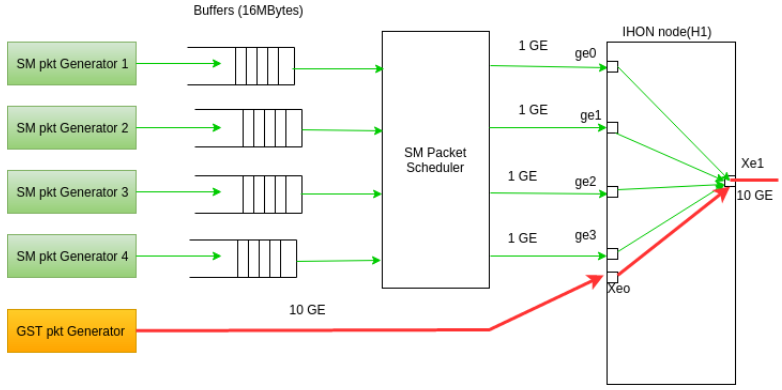

Figure 6.1: Diagram illustrating how the IHON node is connected to Packet generators for measuring the performance metrics.

Table 6.3: Average latency, PLR, and PDV of SM and GST traffic as function of GST load for SM load=0.3 (IHON node).

SN.	**Total L_{1GE}^{SM}**	**L_{10GE}^{GST}**	Average GST latency (μsec)	Average SM latency(sec)	PDV of GST(msec)	PDV of SM(μsec)	PLR of SM
1	0.3	0.1	1.2	$0.014 \pm 1.37 \times 10^{-4}$	0.0	0.35	0.0
2	0.3	0.2	1.2	$0.021 \pm 1.69 \times 10^{-4}$	0.0	0.37	0.0
3	0.3	0.3	1.2	$0.027 \pm 1.70 \times 10^{-4}$	0.0	0.372	0.0
4	0.3	0.4	1.2	$0.034 \pm 1.77 \times 10^{-4}$	0.0	0.281	0.0
5	0.3	0.5	1.2	$0.039 \pm 1.70 \times 10^{-4}$	0.0	0.55	0.0
6	0.3	0.6	1.2	$0.0417 \pm 1.41 \times 10^{-4}$	0.0	0.76	0.0005
7	0.3	0.63	1.2	$0.0422 \pm 1.14 \times 10^{-4}$	0.0	1.62	0.0026
8	0.3	0.64	1.2	$0.0424 \pm 1.20 \times 10^{-4}$	0.0	1.96	0.0033
9	0.3	0.65	1.2	$0.043 \pm 1.28 \times 10^{-4}$	0.0	3.9	0.00398
10	0.3	0.67	1.2	$0.048 \pm 1.01 \times 10^{-4}$	0.0	2.89	0.0053

6.2.1 GST Traffic Performance

The following results have been obtained by using Table 6.1 as a simulation parameter, and loading the output wavelength with packet length distribution and with the inter-packet gap between GST packets as described in Chapter 5.

The average latency, PLR, and PDV of GST traffic are discussed in the following subsections.

Average Latency

In IHON node, latency refers to the delay when the first bit of the packet gets into the IHON node until the first bit of the packet leaves the FDL. This parameter greatly affects how usable the nodes as well as communication are.

Every sub-simulation returns an average value for latency of GST packet, obtained by averaging all the delays experienced by every single GST packet during the sub-simulation. By varying the system load (n*L_{1GE}^{SM} + L_{10GE}^{GST}), we observed the average latency of GST traffic. The simulated average latency of GST traffic was constant with a value of 1.2μsec, which equals to the FDL time. It shows that the 10GE GST traffic was shown to be independent of the added SM traffic and its load. This is due to the fact that the GST traffic is transmitted with absolute priority. Note that the FDL time was set to the service time of maximum packet length of SM packet, δ=1.2μsec.

The average latency of GST traffic isn't affected by the system load and insertion of SM traffic. Thus, the result reveals that its average latency is constant regardless of the node congestion.

Packet Delay Variation

As per ITU Y.1540, "PDV is the variation in packet delay with respect to some reference metrics (minimum delay in this work)". The service quality and PDV tolerability of an application are highly influenced by PDV.

By recording the time when the first bit of GST packets arrived at the delay line, and when the last bit of the packet left the start of the FDL, the maximum and minimum delay of GST packet is computed. Using this concept, the result of the simulator showed that the packet delay variation of GST packets was zero. This is because the traffic aggregation of SM traffic on the top a 10 Gb/s wavelength is done without introducing PDV to the GST traffic of following the wavelength. Furthermore, the inter-packet gap between the GST stream is preserved, and the GST streams are sent out precisely as it arrived. Consequently, it results in zero

packet delay variation. Like the average latency, the PDV of the GST traffic isn't affected by the system load and insertion of SM traffic.

And also, GST packets in IHON node undergo a fixed delay of 1.2μsec, corresponding to the service time of a maximum length SM packet. At the output wavelength, all GST packets experience this fixed delay. Hence, it doesn't introduce PDV to GST traffic.

Packet Loss Rate

When one or more transmitted packets fail to arrive at their destination, packet loss occurs. In IHON node, it is typically caused by blocking and congestion. Since different applications have different PLR tolerability, it has noticeable effects in all types of communications. Packet loss is measured as a percentage of the number of lost packets with respect to the total transmitted packets.

The simulation result showed that the PLR of GST traffic was zero, i.e. all GST traffic generated by the source were received at the output port of the IHON node. This is because GST packets pass through FDL, which gives time to the monitoring module to calculate the gap length between GST packets. SM packets are scheduled only if the gap is sufficient to transmit the packet. Hence, IHON nodes avoid losing of GST packets.

6.2.2 SM Traffic Performance

By varying the load of GST traffic, we observed the performance of SM traffic for a fixed SM load.

Average Latency

For low SM load, Figure 6.2a, the average latency increases from 1.2μsec to 18μsec when the GST load, L_{10GE}^{GST} was increased from 0.1 to 0.89 with an increasing interval of 0.1. However, when we increase L_{1GE}^{SM} from 0.1 to 0.3, Figure 6.2b, the average latency was further increased. Increasing more SM traffic, after the system load 0.8, will cause a buffer overflow; this leads the average latency to increase exponentially and causes a packet loss as shown in Figure 6.4.

As can be seen from Figure 6.2, the average latency of SM traffic is increased for increasing the GST load. The increment of GST load adds more traffic to the output wavelength which in turn increases the waiting time of SM packet at the node. This means that increasing GST load will decrease the chance of SM traffic to be inserted. Generally, the higher the GST traffic load, the longer the average latency of SM traffic.

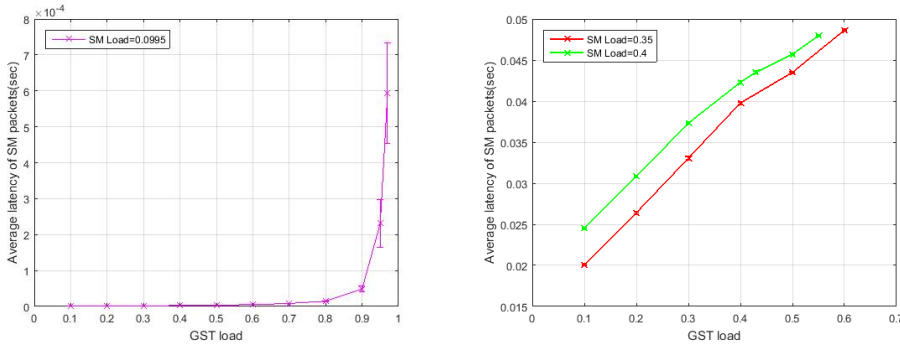

(a) SM load=0.1

(b) SM load=0.35 and 0.4

Figure 6.2: Average latency of SM traffic as function of GST load for SM load=0.1, 0.35 and 0.4(IHON node).

When the system load is low, then the buffers inside the node will never be full. In this simulation, since we are using variable SM packet length (40 to 1500 bytes), the average latency depends on the packet length. It means that the latency of sending a 40-byte packet and a 1500 byte is different depending on the packet length.

Packet Delay Variation

As has been mentioned in Section 6.2.1, PDV influents service quality of an application. Thus, the average PDV of SM packets were acquired from the simulation for analysis. The PDV data on Table 6.3 of SM traffic and the resulting Figure 6.3 shows that when the GST load of the system load traffic increased, the PDV has increased from 20.1μsec to 411.232μsec. This indicates that the PDV of SM packet is influenced because of the service classification, i.e. traffic load and SM traffic scheduling algorithm [VBB13].

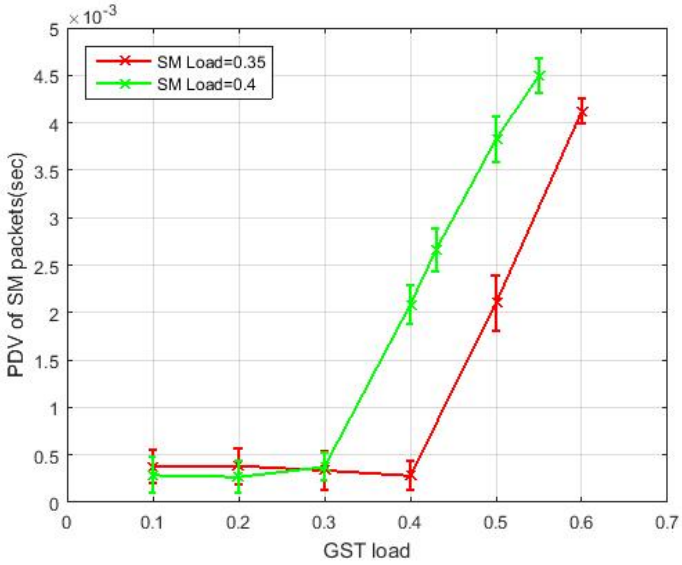

Figure 6.3: Packet delay variation of SM traffic as function of GST load (IHON node).

Packet Loss Ratio

One of the most important factors in the analysis of IHON node performance for SM traffic is illustrated in Figure 6.4. Based on the figure, no PLR was observed within system load interval [0,0.89]. When the system load reaches 0.89, SM packets start getting dropped. From that point onward buffer overflow causes the loss to increase exponentially.

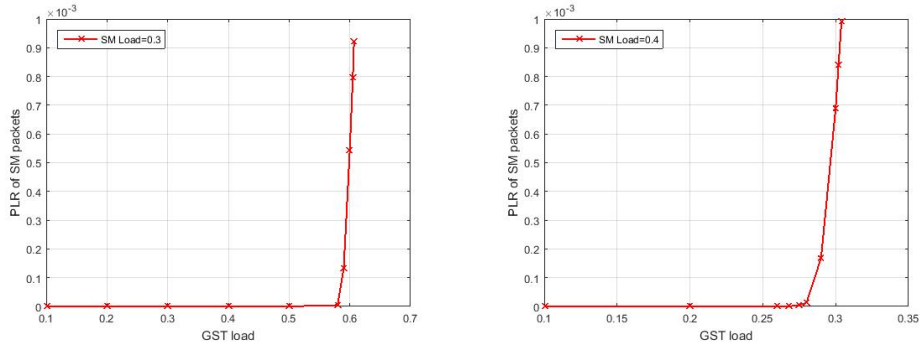

(a) SM load=0.3 (b) SM load=0.4

Figure 6.4: PLR of SM traffic as function of GST load (IHON node).

For L_{1GE}^{SM}=0.3, the added SM traffic increases the 10GE wavelength utilization up to 89% without any losses and with SM PLR=$1E^{-03}$ up to 92% utilization.

6.2.3 Comparison Between GST and SM Traffic Performance in IHON Node

Based on the results, Table 6.3, the average latency, PLR, and PDV of GST and SM traffic were analyzed and compared. The exploration of these parameters helped us to deeply understand the performance of IHON node towards traffic of different priority.

Average Latency

Figure 6.5 shows the average latency of GST and SM traffic for SM load=0.1. From the figure, it is observed that the average latency of SM traffic increases when the GST load is increased from 0.1 to 0.89. This is because IHON node has a buffer to store SM traffic when suitable gap between GST packets is not found, which results in longer delay. When the GST load is low, the buffer's queue length will be short and SM packets will pass through IHON node with a shorter delay. On the other hand, when the GST load is increased, the chance of getting suitable gap is low and the SM packet will stay a longer time in the buffer.

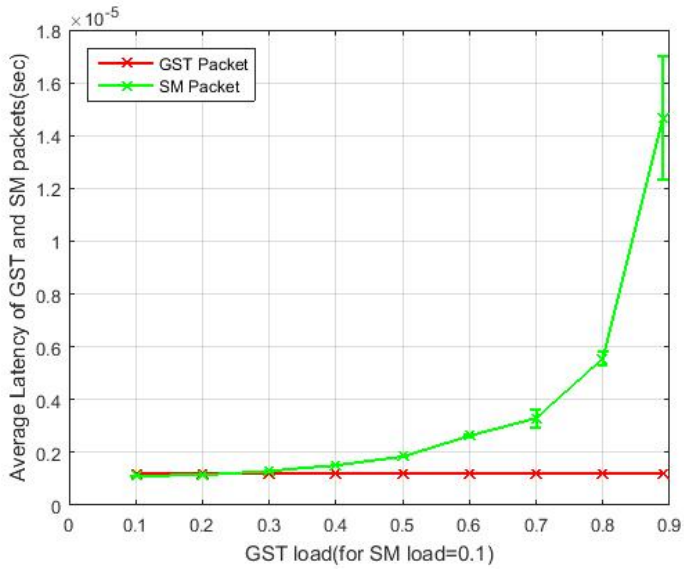

Figure 6.5: Average latency of SM and GST traffics as function of GST load for SM load=0.1 (IHON node)

The average latency of GST traffic is kept constant regardless of the added traffic on the wavelength. Thus, the simulation result proved that GST traffic wasn't affected by the system load with both increased GST load and inserted SM traffic. It implies that GST traffic is transported with absolute priority.

Packet Delay Variation

Another important parameter for analyzing the IHONs node performance of delivering service with continuity and stability is PDV. Figure 6.6 illustrates the result of PDV of SM and GST traffic. For SM traffic, the PDV has increased when the load of GST traffic is increased from 0.1 to 0.9. This proved that because of the service classification in IHON node, the PDV of SM packet is influenced by the system load and SM traffic scheduling algorithm [VBB13].

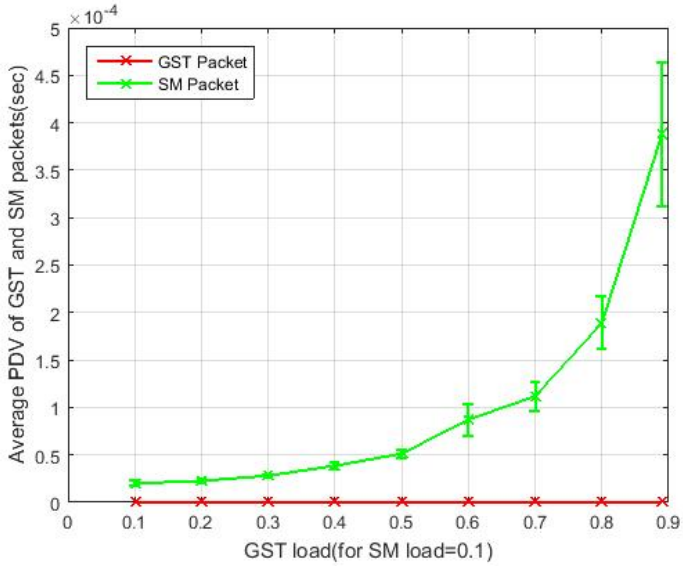

Figure 6.6: Packet delay variation of SM and GST traffics as function of GST load for SM load=0.1(IHON node).

PDV of GST traffic is kept constant at 0 level while the system load is increasing. This implies that the PDV of the GST traffic isn't affected by the system load and insertion of SM traffic.

Packet Loss Ratio

As described in Section 6.2.1, IHON node causes no packet loss for GST packets, and Figure 6.4 shows that SM packets start dropping when the system load reaches 0.89. An obvious difference occurred at the system load 0.89, where the PLR of

SM packet began to increase sharply because of buffer overflow. However, the GST packets experience no packet loss and are independent of system load. This is because the traffic aggregation of SM traffic on the top a 10 Gb/s wavelength is done without packet loss to the GST traffic of following the wavelength.

6.3 Ethernet Switch Performance

To study the performance of non-preemptive Ethernet switch while transporting HP and LP traffic, the diagram shown in Figure 6.7 were implemented in the simulation program. In this scenario, the Ethernet switch transmits LP packet only if no packets with higher priority (HP packets) is available at the input queue. When HP packet arrives while LP packets are being served, the packet will be queued till the lower priority packet has finished.

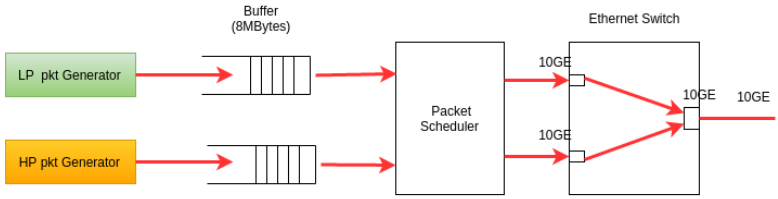

Figure 6.7: Illustration of Ethernet Switch for measuring the performance of HP and LP traffic.

For Ethernet switch, average latency, PLR, and PDV of LP and HP traffic with respect to HP load are illustrated in Table 6.4. The values are obtained by keeping LP load fixed, L_{1GE}^{SM}=0.4.

Table 6.4: Average latency and PDV of LP and HP traffics as function of HP load for HP load=0.4 (Ethernet switch).

SN.	$\mathbf{L_{1GE}^{LP}}$	$\mathbf{L_{10GE}^{HP}}$	Average HP latency (μsec)	Average LP latency(μsec)	PDV of HP(μsec)	PDV of LP(μsec)
1	0.4	0.1	$0.076 \pm 7.16 \times 10^{-9}$	4.33	1.19977	35.16
2	0.4	0.2	$0.15 \pm 1.67 \times 10^{-8}$	11.67	1.19988	66.16
3	0.4	0.3	$0.22 \pm 1.43 \times 10^{-8}$	505.9	1.19991	10.49
4	0.4	0.4	$0.30 \pm 1.41 \times 10^{-8}$	2857.33	1.19990	993.04
5	0.4	0.50	$0.37 \pm 2.21 \times 10^{-8}$	5002.6	1.19995	10097.2
6	0.4	0.57	$0.47 \pm 2.76 \times 10^{-8}$	63529	1.19997	10608.52

6.3.1 HP Traffic Performance

In this part, the performance of HP traffic is presented with respect to: average latency, PLR, and PDV.

Average Latency

Figure 6.8 presents the average latency of HP traffic with respect to HP load for L_{IGE}^{LP}=0.4 and 0.45. Form the figure, we see that the average latency is increasing with increasing value of HP load. This is because HP packets have to wait in a queue when they arrive while the LP packets are serving. When the system load increases, the probability of getting the output wavelength free is low. As a result, the latency of HP packet increases. The maximum latency experienced by HP packet was 1.2μsec.

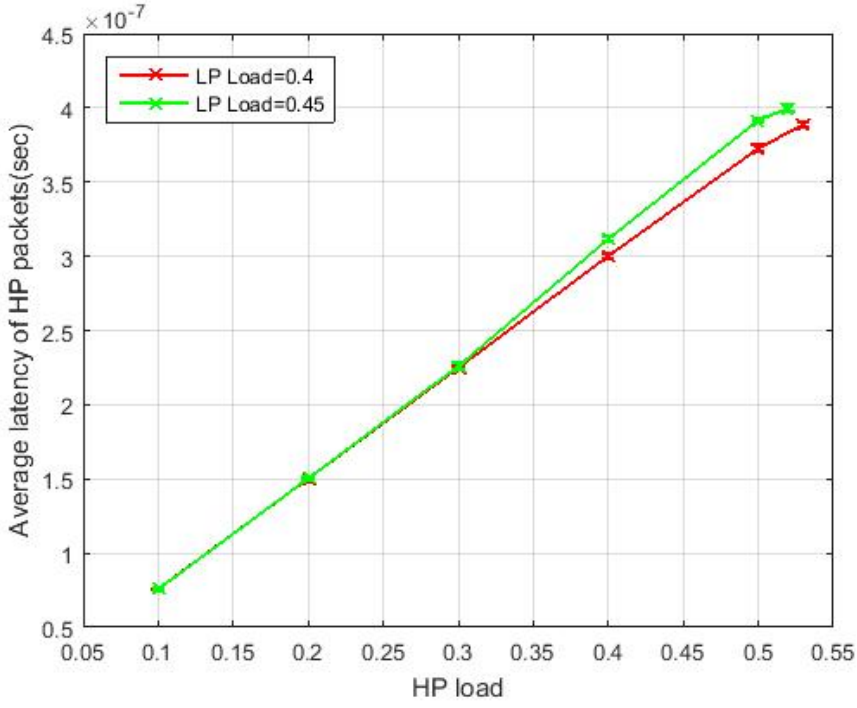

Figure 6.8: Average latency of HP traffic as function of HP load for LP load 0.4 and 0.45(Ethernet switch).

From Section 6.2.1 and Figure 6.8 we see that the average latency of GST traffic in IHON node is higher than the average latency of LP traffic in Ethernet switch. The average latency of GST packet is constant with a value of 1.2μsec, whereas the

average latency of HP packet is increasing with increased system load but it has lower latency value. This is because HP packets are not delayed by FDL and they access the output wavelength as soon as they arrive unless the lower priority packet is serving.

Packet Delay Variation

Figure 6.9 presents the packet delay variation of LP traffic as a function of HP load for different values of LP load. As we can see from the figures, the PDV is increased for increasing HP load. However, the increment interval is not noticeable. It varies between 1.1997μsec and 1.1999μsec. This is due to the fact that the inter-packet gap for both high priority (HP traffic) and low priority (LP traffic) is not preserved which leads to the observation of this measured value. And also, the non-preemptive scheduling algorithm in Ethernet switch introduces synchronization problem, jitter [GCT+15].

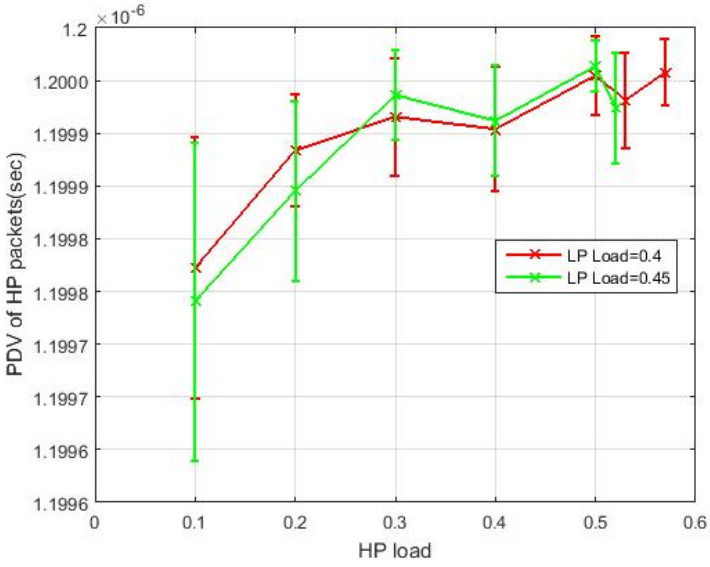

Figure 6.9: PDV of HP traffic as function of HP load for HP load=0.4 and 0.45 (Ethernet switch).

As discussed in Section 6.3, in Ethernet switch, packets from higher priority class are always scheduled first. If the queue of this class is empty, packets from the lower priority class are transmitted. The higher priority packet experiences delay equal to the service time of the maximum length of LP packet when it arrives while the maximum LP packet is serving. And also, the minimum delay experienced by HP packet is zero when the HP packets are served freely. Consequently, Ethernet switch

introduces PDV equals to the duration of maximum length of LP packet to HP traffic. The measured PDV value was approximately 1.2μsec.

Packet Loss Ratio

Like the PLR of GST traffic in IHON node, the PLR of HP traffic was zero, i.e. all HP packet generated in the source were received at the output port of the Ethernet switch. This shows that the HP traffic is given higher priority.

6.3.2 LP Traffic Performance

The performance of LP traffics in Ethernet switch is described below.

Average Latency

As shown in Figure 6.10, the LP packet latency increases slowly as the 10GE HP load increases. The average Latency increases exponentially from 1msec to 8msec for L_{IGE}^{LP}=0.4 and 0.45. This is because packets with low priority are transmitted only if the higher priority input queue has no available packet to transmit. As the HP load increases, the low priority queue begins to fill up due to the arriving LP traffic while the output wavelength is not free. As a result, the amount of latency the LP packet experiences going through the queue increases.

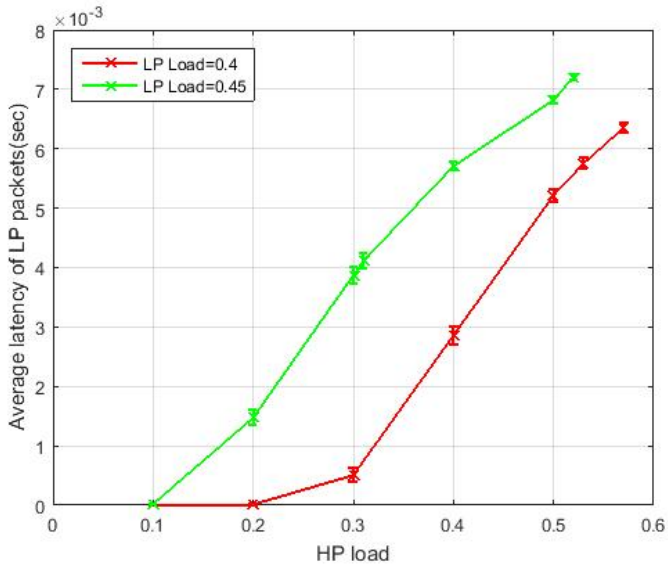

Figure 6.10: Average latency of LP traffic as function of HP load for LP load=0.4 and 0.45 (Ethernet switch).

The maximum latency the LP packets experience in queue is proportional to buffer size. The longer the line of LP packets in a queue waiting to be transmitted, the longer the average waiting time is.

Packet Delay Variation

Figure 6.11 presents the PDV of LP traffic as function of HP load for L^{LP}_{1GE}=0.4 and 0.45. Form the figure we see that the PDV increases for increasing values of L^{HP}_{10GE}. An important observation when comparing the PDV of LP traffic for L^{LP}_{1GE}=0.4 and 0.45 is that the PDV for LP load L^{LP}_{1GE}=0.45 is higher than the PDV for LP load L^{LP}_{1GE}=0.4. Since LP traffic is treated as a best effort traffic, the minimum and maximum latency value of LP packet is higher than the min. and max. latency value of HP packet.

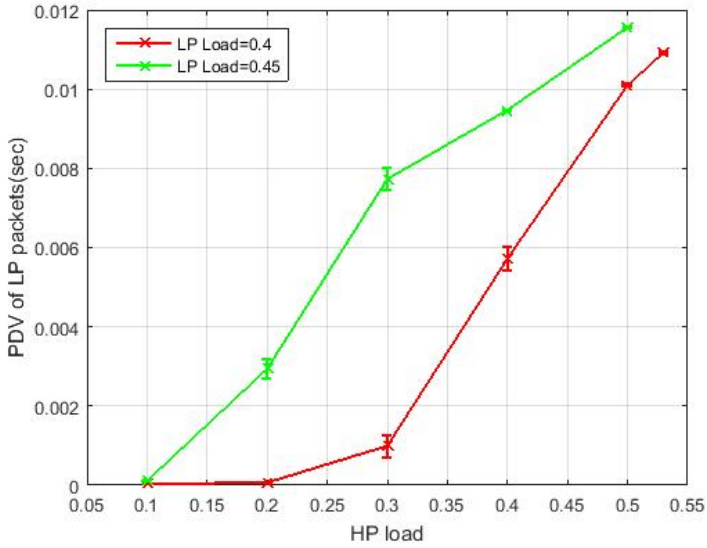

Figure 6.11: Packet delay variation of LP traffic as function of HP load for LP load=0.4 and 0.45 (Ethernet switch).

Packet Loss Ratio

Figure 6.12a shows from L^{HP}_{10GE}=0.1 to L^{HP}_{10GE}=0.45 there wasn't packet losses i.e. every single LP packet sent was transmitted via the output wavelength. However, when L^{HP}_{10GE} is 0.45, there was a PLR of 0.0001. Afterwards, the PLR has sharply increased when the system load is increased. Since the low priority queue has a finite buffer size, at high system load the LP queue receives packets while HP traffic is serving. The increasing HP load causes the LP traffic to stay longer time at the

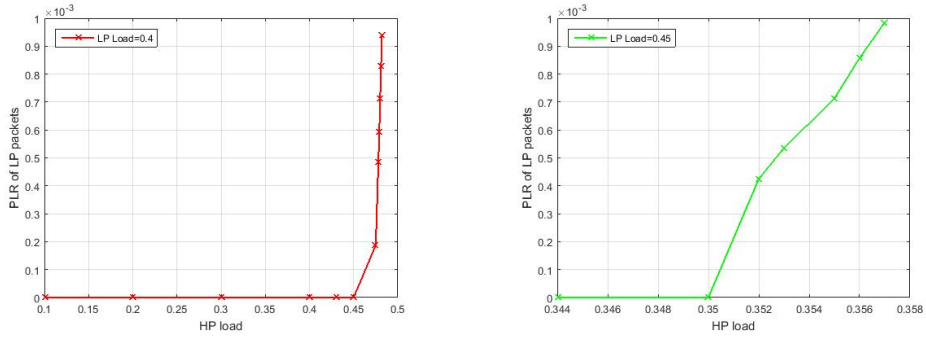

(a) LP load=0.4 (b) LP load=0.45

Figure 6.12: PLR of LP traffic as function of HP load for LP load=0.4 and 0.45 (Ethernet switch).

queue. As a result, the queue of LP becomes full in short time. In this case, the LP packets arriving after the queue is full are discarded and the number of discarded LP packet increases for increasing HP load. The results for L_{1GE}^{LP}=0.4 and 0.45 are presented in Figure 6.12, Figure 6.12a and Figure 6.12b.

It is worth mentioning that increasing more traffic while the buffer size of HP and LP packets is fixed, will cause a buffer overflow, which in turn increases the number of packets lost exponentially. The observed result proved that packets getting dropped after the buffer of the packet is full.

6.4 Mobile Fronthaul Networks

We have gone through the fronthaul network requirement given by IEEE 802.1CM and the RoE standards for transporting radio signals over a packet switched network given by IEEE 1904.3 to evaluate IHON and Ethernet network for fronthaul C-RAN network. To evaluate the performance of these networks, let us consider a scenario when there are more than two nodes in a network shown in Figure 6.13. The reason why we didn't start evaluating with one node is that two or more nodes are needed for mixing different traffic service classes.

Figure 6.13: Mobile fronthaul network under study. The nodes can be either IHON node or Ethernet switch depending on the network under evaluation.

In the following sections, we evaluate the different parameters of the IHON nodes in a RoE mobile fronthaul setting. Our aim is to find how such a network can be dimensioned with respect to: technology, fiber length, and number of nodes. It is important to note that the latency results described below represent only the queuing and transmission delays; but the nodal delay, which depends entirely on the implementation of the node, has not been taken into account.

6.4.1 Evaluation of IHON Network for Mobile Fronthaul Network

The overall fronthaul requirements are listed in Table 3.1, Table 3.2, and Table 3.3. They are mainly focused on performance metrics: PLR, average latency, and PDV. In Section 6.2, we have measured the result of these performance metrics in IHON node when transporting one 10GE GST traffic and four 1GE SM traffics aggregated on a single 10 Gb/s wavelength. The results were measured by changing the total load of aggregated SM traffic, total L_{1GE}^{SM} on 10 GE, from 0.1 – 0.4, and the number of SM streams (n) used to supply the total load were four; for each load size, each SM stream contributes an equal amount of load. The measured values are used to evaluate the performance of IHON network for mobile fronthaul network.

Average Latency

The first performance metric used for evaluation of IHON network for fronthual C-RAN is average latency. According to IEEE 802.1CM and Table 3.2, the maximum E2E latency between BBU and RRH required for mobile fronthaul is specified as 50μsec(including fiber length and PDV), and the latency budget is 5μsec when cable propagation is excluded. Within this 50μsec latency, the maximum separation distance between BBU and RRH (link length) is limited and depends on the number of nodes in the network. To calculate the link length as function of number of nodes (N), the following equation has been used:

Maximum E2E latency (L_{total}):

$$L_{total} = N \times D_{node} + D_T \times Link_{length} \tag{6.1}$$

where,
N = Number of nodes.
D_{node}= Latency in a single node, 1.2μsec (obtained from our simulation).
$Delay\_PDV_{node}$=PDV in a single node, 0μsec (obtained from our simulation).
D_T=Transmission latency, 5μsec/km.

L_{total}= Maximum E2E latency, 50μsec.
$Link_{length}$= Maximum link length.

Table 6.5: Maximum link length and number of nodes in IHON network to meet the fronthaul requirements for GST traffic where L_{total}=50μsec, D_T=5μsec/km, and D_{node}=1.2μsec.

N	Total D_{node}(μsec)	$Link_{length}$(Km)
2	2.4	9.52
3	3.6	9.28
4	4.8	9.04
5	6	8.8
6	7.2	8.56

Table 6.5 presents the relationship between the number of nodes in IHON fronthaul network and the maximum separation distance between BBU and RRH for GST traffic. In the table, the second column indicates the overall delay in the nodes, whereas the third column is the link length between BBU and RRH in the network. The table shows that for increasing the number of nodes in the network, the link length decreases. For instance, for IHON network with 3 nodes require 9.28 Km fiber link length. Similarly, for IHON network with 4 nodes require 9.04 Km fiber link length.

The simulation results and Table 6.5 proved that IHON networks are capable of carrying radio signals over packet-based fronthaul network provided that the number of nodes in the table corresponds to its respective link length. Unfortunately, obtaining the average latency of BE or SM traffic that meets fronthaul requirement is not so straightforward, since this traffic depends on a load of GST traffic.

Packet Delay Variation

Another performance used for evaluation of IHON network for a fronthaul network is PDV. In Table 3.2, the maximum PDV specified is 5μsec or 10% of E2E latency. The simulated result of PDV for GST traffic was zero. Thus, the GST traffic class meets the fronthaul requirement in PDV comparison.

The fronthaul requirement is higher than peak PDV of GST traffic for any system load in the interval [0,0.99]. Consequently, of the three performance metrics (average latency, PDV, PLR), the IHON network performs best in PDV for GST traffic. It has no restriction in wavelength utilization of IHON network.

Packet Loss Ratio

At last, the performance evaluated is PLR. Fronthaul networks have a very strict PLR requirement which is in the interval [10^{-6},10^{-9}]. As described in Section 6.2, GST packets experience no packet loss regardless of the network congestion. So, the GST traffic is transported through the IHON fronthaul network with absolute priority.

In our simulation, GST packet loss wasn't observed at any system load, while SM packets getting dropped for system load beyond L_{10GE}^{T}=0.89 for SM load=0.3. With system load in the interval [0,0.99], GST traffic class meets the fronthaul requirement, and can be served properly in IHON network.

6.4.2 Evaluation of Ethernet Network for Mobile Fronthaul Network

This section evaluates the performance of Ethernet network for mobile fronthaul network in terms the above mentioned performance metrics.

Based on the observations from Figure 6.8, Figure 6.9, Figure 6.10, and Figure 6.12 and data from Table 6.6 the average latency, PDV, and PLR required for transporting the HP and LP over Ethernet fronthaul network have been studied. To evaluate the performance of Ethernet network for fronthaul network, let us consider a scenario when LP load is 0.4 (assumed threshold value) and the HP load varies in the interval [0.1,0.59].

Average Latency

As previously described, the maximum E2E latency between BBU and RRH in mobile fronthaul network is 50μsec (including fiber length, PDV, bridged delays). And, the latency requirement when cable propagation excluded is 5μsec.

Table 6.6 presents the average latency of HP and LP packets with respect to the HP loads for values of LP load, L_{1GE}^{LP}=0.4. From the table, we see that the average latency of HP traffic is lower than the latency fronthaul requirement in MFH. It also shows that the average latency of both HP and LP traffic varies with the system load.

Since the average latency of HP packets in Ethernet switch varies with system load, its maximum latency was used for evaluating the Ethernet network. From our simulation, we found that the maximum latency of HP packets in an Ethernet switch is 1.2μsec. Using this value, the maximum link length as a function of number of nodes is calculated using Equation 6.2:

Maximum E2E latency (L_{total}):

$$L_{total} = N \times (D_{node} + Delay\_PDV_{node}) + D_T \times Link_{length} \quad (6.2)$$

where, N = Number of nodes.
D_{node}= Latency in a single node, 1.2μsec (obtained from our simulation).
$Delay\_PDV_{node}$=PDV in a single node, 1.2μsec (obtained from our simulation).
D_T=Transmission latency, 5μsec/km.
L_{total}= Maximum E2E latency, 50μsec.
$Link_{length}$= Maximum link length.

Table 6.6: Average latency comparison between LP and HP traffics of Ethernet switch and fronthaul requirements for LP load=0.4.

SN.	**Average Latency**				
	$\mathbf{L_{1GE}^{LP}}$	$\mathbf{L_{10GE}^{HP}}$	HP_latency(μsec)	LP_latency (sec)	Fronthaul requirement
1	0.4	0.1	$0.07 \pm 7.1 \times 10^{-10}$	$4.33\times10^{-6}\pm1.44\times10^{-7}$	5μsec (excluding cable length)
2		0.2	$0.15 \pm 1.7 \times 10^{-9}$	$11.6\times10^{-6}\pm1.13\times10^{-6}$	
3		0.3	$0.22 \pm 1.4 \times 10^{-9}$	$0.51\times10^{-3}\pm0.12\times10^{-3}$	
4		0.4	$0.30 \pm 1.4 \times 10^{-9}$	$2.85\times10^{-3}\pm0.14\times10^{-3}$	
5		0.5	$0.37 \pm 2.2 \times 10^{-9}$	$5.32\times10^{-3}\pm0.11\times10^{-3}$	

Table 6.7: Maximum link length and number of nodes in Ethernet network to meet the fronthaul requirements for HP traffic where L_{total}=50μsec, D_T=5μsec/km, and D_{node}=1.2μsec.

N	Total (D_{node} + $Delay\_PDV_{node}$)(μsec)	$Link_{length}$(Km)
2	4.8μsec	9.04
3	7.2μsec	8.56
4	9.6μsec	8.08
5	12μsec	7.6
6	14.4μsec	7.12

In this work, the Ethernet switch implemented was a cut-through switch in which a packet is forwarded as soon as it arrives. As a result, the HP packet's latency is very low. HP packets can be transmitted via Ethernet fronthual network provided that the relationship between maximum separation distance and a number of node in the network is as presented in Table 6.7. For instance, for Ethernet network with 3 nodes require 8.56 Km fiber link length. Similarly, for Ethernet network with 2 nodes require 9.04 Km fiber link length.

Packet Delay Variation

In Table 3.2, the maximum PDV specified for fronthaul network is 5μsec or 10% of E2E latency. For HP traffic, the PDV of a single node was approximately 1.2μsec regardless of the system load. To evaluate Ethernet network for fronthaul with regard to PDV, the following equation has been used:
Maximum PDV (PDV_{total}):

$$PDV_{total} = N \times PDV_{node} \tag{6.3}$$

where,
N = Number of nodes.
PDV_{node}=PDV in a single node, 1.2μsec (obtained from our simulation).
PDV_{total}= Maximum PDV, 5μsec.

Table 6.8: The Number of nodes in Ethernet network to meet the PDV fronthaul requirements for HP traffic where PDV_{total}=5μsec and PDV_{node}=1.2μsec.

N	PDV_{node}(μsec)	PDV_{total}(μsec)
2	1.2	2.4
3		3.6
4		4.8

As shown in Table 6.8, the HP traffic in Ethernet network meets the PDV fronthaul requirement as long as the number of nodes in the Ethernet network is at most 4. This implies that HP packets can be transmitted via Ethernet fronthual network when the number of nodes in the network is at most 4.

Packet Loss Ratio

Like GST traffic, HP packet loss wasn't observed at any system load. Table 6.9 depicts that the PLR of HP and LP packets with respect to the HP loads for LP load=0.4. The table shows that the observed PLR of HP is lower than the PLR requirement in mobile fronthaul requirements.

Table 6.9: PLR comparison between LP and HP traffics of Ethernet switch and Fronthaul requirements for LP load=0.4.

SN.	**Packet Loss Ratio**				
	$\mathbf{L_{1GE}^{LP}}$	$\mathbf{L_{10GE}^{HP}}$	HP_PLR(μsec)	LP_PLR (μsec)	Fronthaul requirement
1	0.4	0.1	0.0	0.0	10^{-6}-10^{-9}
2		0.2	0.0	0.0	
3		0.3	0.0	0.0	
4		0.4	0.0	0.0	
5		0.5	0.0	0.0061	

The results for HP traffic shown in Table 6.9 confirms that the Ethernet network meets the PLR requirement for fornthaul C-RAN requirements; the PLR of HP traffic was zero. This implies that HP packets can be transmitted via Ethernet fronthual network without any packet loss.

6.5 Application of Ethernet streams in Fronthaul Network

As explained in the previous discussions the use of Ethernet or IHON network for fronthaul provides differentiated service using the high priority and low priority traffic classes. In this section, we present the light of our results with regard to the type of application/service the SM and LP classes are suitable for, given that the GST and HP classes are loaded with RoE traffic.

The simulation results and numerical analysis confirm that the Ethernet and IHON network are suitable for deployment in the mobile fronthaul network with differentiated service. Since high priority classes (GST or HP class) require very low latency, they are used to transport RoE traffic in RoE fronthaul network. These classes should be used for transporting time-sensitive information and receive the priority and QoS only GST or HP traffic can provide. A typical example of this class would be online gaming, online banking, video conferencing, telemedicine and e-health, and synchronization information.

Throughout the thesis SM and LP traffic were described as traffic type with a low priority. In the same fronthaul network as HP classes, the low priority service classes are used to transport the non-critical data traffic. General data such as E-mail, web traffic, and file transfer have very variable bandwidth demand and are sensitive to PLR, but they have very low latency demands because of which retransmission mechanism is possible. Thus, these service classes fit well into the SM transport. These traffic aren't sensitive to QoS metrics: latency, PDV, and jitter, and such

traffic class get what is left after high priority traffic. Within the low priority classes, they might be further differentiated across a range of applications with different QoS; different QoS differentiation mechanism is possible to implement.

To illustrate the share of HP class traffic with the lower priority traffic, let us consider an IHON node loaded with SM load=0.3 and GST load that varies within the interval [0,0.69] shown in Figure 6.4. As discussed above, the results have proven that the GST class can be loaded with RoE traffic to transport it with absolute transfer guarantees and circuit switched QoS. While achieving a high throughput efficiency of 89.0%, the SM classes can transport the rest data with no packet loss. However, SM packets start getting dropped at L_{10GE}^{GST}=0.59. Thus, we can conclude that inserting SM in the gap increases the 10GE wavelength utilization up to 89.0% without any packet losses, and with SM PLR=$1E^{-03}$ up to L_{10GE}^{T}=0.92 or 92% utilization. The IHON node enables transport of SM packet network with high utilization up to 92%.

Chapter 7
Summary and Conclusion

7.1 Summary

Due to the ever-increasing demand for network traffic and application, the network capacity has to grow to match this demand. Newer technologies both in the optical and electrical fields allow greater capacity to cope with the huge data, but this is at the expense of the cost of the new equipment. Power consumption in cell sites and the switching devices to offer greater speed are becoming a greater and greater portion of the overall network cost. To increase the performance of the switch and reduce the power consumption in the cell sites (in mobile networks), the resources have to be used efficiently. Thus, the operators have been looking for methods to address this growing cost. As a result, a C-RAN featuring a fronthaul network is proposed by [Ins11]. This work basically connects the performance of IHON and Ethernet network to the fronthaul network requirements of C-RAN.

Firstly, we studied the background and motivation of the mobile fronthaul network and deeply exploited the need of packed based fronthaul networks. The evolution of these networks from the first stage up to the current stage have been studied. Moreover, several mobile fronthaul solution for the transportation of traffic were concretely studied. Ethernet frame format for transporting radio signals with the help of RoE header was also discussed.

Secondly, the fronthaul requirements from the IEEE 802.1CM standard and other references (listed in Chapter 3) were deeply studied. For mobile fronthaul network, the PLR, PDV, average latency, and synchronization requirements have been discussed. Furthermore, the maximum distance between BBU and RRH that can be supported by a specific latency value has also been discussed.

Thirdly, numerical and simulation method of our scenarios were discussed. Numerical analysis for the different fronthaul transport options has been discussed and compared with the fronthaul requirements described in Chapter 3. The implementa-

tion of IHON nodes with one 10GE GST port and four 1GE SM port and standard Ethernet switches is explained in Appendix A.

Finally, we have evaluated the different performance parameters of the switches in a RoE mobile frontal setting and dimensioned with respect to: technology, fiber length, and number of nodes. We presented the light of our results with regard to the type of application/service the SM and LP classes are suitable for, given that the GST and HP classes are loaded with RoE traffic.

Demos programming was used to achieve the objective of this work. Two generators, one GST packet generator, and SM packet generator have been used to generate the two traffics of IHON network. In order to get an accurate result, several validation techniques, starting from a trace up to analytical analysis, have been used. Moreover, results such as the PDV, PLR, average latency, and other related metrics were obtained from the simulator. All the necessary results have been presented with 95% confidence interval.

7.2 Conclusion

In this thesis work, the overall performance of IHON node and standard Ethernet switch were analyzed. We measured average latency, PDV, and PLR for both GST and SM traffic in IHON node, and for both HP and LP traffic in Ethernet switch. With regard to IHON node, the performance of delivering high quality of service was approved and reflected on GST and fits the technical specification of fusion node. Similarly, the high quality of service was reflected on HP traffic in Ethernet switch. Both SM and LP traffic are suitable for transporting time insensitive information.

The recommendation from the IEEE 802.1CM standard and other articles were considered for examining and investigating how IHON and Ethernet fronthaul networks should provide the required quality of service. The results obtained from the simulator was compared with these recommendation standards and are presented as follows:

Scenario I: In this scenario, one 10GE GST stream and four 1GE sub-wavelength SM injected on the leftover capacity, was considered. The measured average latency for GST packet in a single node was approximately 1.2μsec. Using this value, the maximum separation distance between BBU and RRH (link length) is limited and depends on the number of nodes given that the maximum E2E fronthaul latency is as presented in Table 3.2. The results in Table 6.5 show that for increasing the number of nodes in the network, the link length decreases.

Maximum PDV of GST traffic was measured as zero, and no GST packet loss was registered, which shows us a better performance than the recommended fronthaul

requirement. Hence, we conclude that fusion network performs better than what is recommended in IEEE 802.1CM standard in PDV and PLR comparison. Since the GST traffic met the fronthaul requirement, they can be used for transporting RoE traffic while SM traffic can used for transporting time insensitive application.

Scenario II: For a scenario where there is high priority class traffic (HP traffic) and lower priority class traffic (LP) on 10GE wavelength, the measured average latency for the higher priority class was approximately between 0.01μsec and 0.55μsec for LP load=0.3, and the measured maximum latency was 1.2μsec. However, we took the maximum latency value for evaluating the performance of Ethernet network for fronthaul network. Like GST traffic in IHON network,the maximum separation distance between BBU and RRH (link length) is limited and depends on the number of nodes. The relation between the number of nodes and link length is tabulated in Table 6.7. However, the measured PDV of HP traffic in Ethernet switch limits the Ethernet fronthaul network to have a maximum of four nodes in order to the PDV fronthaul requirement.

The measured PLR of HP traffic in Ethernet switch was zero. Comparing this value with fronthaul requirement, Ethernet network performs better than what is recommended in IEEE 802.1CM standard. Hence, the performance of Ethernet switch fits into C-RAN fronthaul requirement in PLR comparison. As a result, the HP classes can be used for transporting RoE traffic.

Additionally, the measured performance metrics of HP and GST classes are much lower than what is recommended in ITU-T recommendation for the most sensitive applications, see Appendix B.

Other important points that this thesis work has measured and evaluated:

1. The important design concepts of fusion node have been confirmed.
2. The fusion node aggregation of multiple 1GE SM traffic and 10GE on a single wavelength has been achieved without affecting the deterministic nature of circuit switching.
3. The simulation result confirms that the average latency of GST packet is independent of the system load and experiences a zero packet delay variation in a node.
4. The efficient utilization of bandwidth has been achieved by inserting suitable SM traffic in the computed gap between GST packets.
5. HP traffic experiences a PDV equals to the duration of maximum sized LP traffic in Ethernet switch.

Chapter 8
Future Work

8.1 Future Work

This chapter presents some suggestions to consider and further investigate in future work. The following points are suggested for improved performance and accurate evaluation of packet switched mobile fronthaul network:

- As previously mentioned in Chapter 3 and Chapter 6, the evaluation of IHON and Ethernet network was made based on the maximum absolute one way latency, 50μsec (including PDV, cable length$\cdots$ etc), and maximum latency per link, 5μsec (excluding cable propagation). However, the 5μsec delay may no longer dominate the total link latency as the distance and network complexity increases. Multimedia traffic services in mobile network occupy asymmetric bandwidth in uplink and downlink. Thus, the specifications and the fronthaul standards may need to be revisited as they were specified with the assumption of symmetry.

- In this work, we have evaluated the performance of Ethernet network without considering synchronization effect. The thesis can further be extended to include this important feature of mobile networks. Furthermore, we considered packet loss only when the buffer is full. In a large packet-switched network, packets can be lost because of a node failure, contention between two packets arriving at the same time at the same port and synchronization problem. Therefore, for the accurate evaluation Ethernet network, the above points would be necessary to take them into consideration.

- The simulation model for Ethernet switch was based on the cut-through mode in which the Ethernet frame is forwarded as soon as the destination address has been read. The thesis can then be extended to evaluate the store-and-forward switch in which the entire Ethernet frame is stored and checked before forwarding on the appropriate output port.

- We focused on the latency, PLR, and PDV requirements of fronthual transport options. However, they are not the only time-related performance metrics of fronthaul networks. A complete fronthaul network must provide phase, time, and frequency synchronization between the BBU unit and one or more RRH units. These synchronizations can be quantified using fractional frequency offset, jitter/wander, and phase/time error parameters.
- The simulation presented in this work is asynchronous. It is important to include synchronization feature in the simulation. In synchronous Ethernet, a reference clock is extracted from the received data in each node. In order to gain precise frequency, time, and phase synchronization, mechanisms such as IEEE 1588 or Precision Time Protocol (PTP) is required to achieve synchronsim through the exchange of time-stamped packet [IS].

References

[ABC+14] J.G. Andrews, S. Buzzi, Wan Choi, S.V. Hanly, A. Lozano, A.C.K. Soong, and J.C. Zhang. What will 5g be? *Selected Areas in Communications, IEEE Journal on*, 32(6):1065–1082, June 2014.

[AWP15] N. P. Anthapadmanabhan, A. Walid, and T. Pfeiffer. Mobile fronthaul over latency-optimized time division multiplexed passive optical networks. In *2015 IEEE International Conference on Communication Workshop (ICCW)*, pages 62–67, June 2015.

[Bay01] P. Bayvel. Wavelength routing and optical burst switching in the design of future optical network architectures. In *Optical Communication, 2001. ECOC '01. 27th European Conference on*, volume 4, pages 616–619 vol.4, 2001.

[BHS06] S. Bjornstad, D. R. Hjelme, and N. Stol. A packet-switched hybrid optical network with service guarantees. *IEEE Journal on Selected Areas in Communications*, 24(8):107, Aug 2006.

[BNOS05] Steinar Bjørnstad, Martin Nord, Torodd Olsen, and Norvald Stol. Burst, packet and hybrid switching in the optical core network, 2005.

[CCY+15] A. Checko, H.L. Christiansen, Ying Yan, L. Scolari, G. Kardaras, M.S. Berger, and L. Dittmann. Cloud ran for mobile networks #x2014;a technology overview. *Communications Surveys Tutorials, IEEE*, 17(1):405–426, Firstquarter 2015.

[Chh13] J. Chhapekar. Mathematical analysis amp; model of packet delay variation experienced by ieee 1588 packets. In *Advance Computing Conference (IACC), 2013 IEEE 3rd International*, pages 347–350, Feb 2013.

[CJCB15] A. Checko, A. C. Juul, H. L. Christiansen, and M. S. Berger. Synchronization challenges in packet-based cloud-ran fronthaul for mobile networks. In *Communication Workshop (ICCW), 2015 IEEE International Conference on*, pages 2721–2726, June 2015.

[CPLC+13] P. Chanclou, A. Pizzinat, F. Le Clech, T.-L. Reedeker, Y. Lagadec, F. Saliou, B. Le Guyader, L. Guillo, Q. Deniel, S. Gosselin, S.D. Le, T. Diallo, R. Brenot, F. Lelarge, L. Marazzi, P. Parolari, M. Martinelli, S. O'Dull, S.A. Gebrewold, D. Hillerkuss, J. Leuthold, G. Gavioli, and P. Galli. Optical fiber solution for

mobile fronthaul to achieve cloud radio access network. In *Future Network and Mobile Summit (FutureNetworkSummit), 2013*, pages 1–11, July 2013.

[CTH+12] N. Cvijetic, A. Tanaka, Yue-Kai Huang, M. Cvijetic, E. Ip, Yin Shao, and Ting Wang. 4 #x002b;g mobile backhaul over ofdma/tdma-pon to 200 cell sites per fiber with 10gb/s upstream burst-mode operation enabling #x003c; 1ms transmission latency. In *Optical Fiber Communication Conference and Exposition (OFC/NFOEC), 2012 and the National Fiber Optic Engineers Conference*, pages 1–3, March 2012.

[Dav14] John Davies. Mobile fronthaul optimized for cloud ran. https://techzine.alcatel-lucent.com/mobile-fronthaul-optimized-cloud-ran, April 2014. [Online; accessed 13-February-2016].

[EA] NEC Corporation Nokia Networks Alcatel-Lucent CPRI Specification Ericsson AB, Huawei Technologies Co. Ltd. Common public radio interface (cpri); interface specification. http://www.cpri.info. [Online; accessed 07-March-2016].

[EHHP14] Emstad, Heegaard, Helvik, and Paruereau. *TTM4110-Dependability and performance with discrete event simulation.* 2014.

[Eri15] Ericsson. Cloud ran: the benefits of virtualization, centralization and coordination. http://www.ericsson.com/news?categoryFilter=white_papers_1270673222_c, September 2015. [Online; accessed 08-February-2016].

[ETS] ETSI. Open radio equipment interface. https://www.etsi.org/technologies-clusters/technologies/ori. [Online; accessed 05-March-2016].

[For] IEEE 1904.3 Task Force. Radio over ethernet. http://www.ieee1904.org/3/meeting_archive/2015/02/tf3_mtg_files.shtml. [Online; accessed 05-March-2016].

[GCT+15] Nathan J. Gomes, Philippe Chanclou, Peter Turnbull, Anthony Magee, and Volker Jungnickel. Fronthaul evolution: From {CPRI} to ethernet. *Optical Fiber Technology*, 26, Part A:50 – 58, 2015. Next Generation Access Networks.

[GKB+06] C.M. Gauger, P.J. Kuhn, E.V. Breusegem, M. Pickavet, and P. Demeester. Hybrid optical network architectures: bringing packets and circuits together. *Communications Magazine, IEEE*, 44(8):36–42, Aug 2006.

[Gro] TSN Group. Time-sensitive networking for fronthaul:ieee802.1cm. http://www.ieee802.org/1/pages/802.1cm.html. [Online; accessed 12-February-2016].

[HDCCL14] Jinri Huang, Ran Duan, Chunfeng Cui, and I. Chih-Lin. Overview of cloud ran. In *General Assembly and Scientific Symposium (URSI GASS), 2014 XXXIth URSI*, pages 1–4, Aug 2014.

[HDDM13] M. Hadzialic, B. Dosenovic, M. Dzaferagic, and J. Musovic. Cloud-ran: Innovative radio access network architecture. In *ELMAR, 2013 55th International Symposium*, pages 115–120, Sept 2013.

[HJS] S M Shin H J Son. Fronthaul size: calculation of maximum distance between rrh and bbu. http://www.netmanias.com/en/?m=view&id=blog&lm=simple&page=4&no=6276. [Online; accessed 01-March-2016].

[IEA] Mobile Networks Irvine (Ericson AB). Transport impacts. http://www.ieee802.org/1/files/public/docs2014/new-irvine-mobile-networks-fronthaul-0914.pdf. [Online; accessed 05-March-2016].

[Ins11] China Mobile Research Institute. C-ran: The road towards green ran. *White paper*, pages 1–48, October 2011. [Online; accessed 08-February-2016].

[Int16] Common Public Radio Interface(CPRI). Interface specification. http://www.cpri.info/, 2016. [Online; accessed 27-January-2016].

[IS] IEEE-SA. 1588-2002 - ieee standard for a precision clock synchronization protocol for networked measurement and control systems. https://standards.ieee.org/findstds/standard/1588-2002.html. [Online; accessed 17-May-2016].

[KOS09] A. Kimsas, H. Overby, and N. Stol. Analysis of a bufferless opmigua node. In *Telecommunications, 2009. AICT '09. Fifth Advanced International Conference on*, pages 381–388, May 2009.

[Ler14] Frédéric Leroudier. Fronthaul: Small cells' new best friend. http://www.ospmag.com/issue/article/Fronthaul-Small-Cells-New-Best-Friend-Part-2, April 2014. [Online; accessed 29-February-2016].

[LKB09] Christian Lanzani, Georgios Kardaras, and Deepak Boppana. Remote radio heads and the evolution towards 4g networks, 2009.

[LPHL14] Bin Lin, Xiaoying Pan, Rongxi He, and Sen Li. Joint wireless-optical infrastructure deployment and layout planning for cloud-radio access networks. In *Wireless Communications and Mobile Computing Conference (IWCMC), 2014 International*, pages 1027–1032, Aug 2014.

[MS12] P. McClusky and J.L. Schroeder. Fiber-to-the-antenna: Benefits and protection requirements. In *Telecommunications Energy Conference (INTELEC), 2012 IEEE 34th International*, pages 1–6, Sept 2012.

[Msh12] T. Mshvidobadze. Evolution mobile wireless communication and lte networks. In *Application of Information and Communication Technologies (AICT), 2012 6th International Conference on*, pages 1–7, Oct 2012.

[NMW+12] S. Namba, T. Matsunaka, T. Warabino, S. Kaneko, and Y. Kishi. Colony-ran architecture for future cellular network. In *Future Network Mobile Summit (FutureNetw), 2012*, pages 1–8, July 2012.

[OBS16] OBSAI. Open base station architecture. http://www.obsai.com/, 2016. [Online; accessed 27-January-2016].

[OJDN70] Bjørn Myhrhaug Ole-Johan Dahl and Kristen Nygaard. Common base language, norwegian computing center. http://www.edelweb.fr/Simula/#7, 1970. [Online; accessed 28-May-2016].

[OSHT01] M. J. O'Mahony, D. Simeonidou, D. K. Hunter, and A. Tzanakaki. The application of optical packet switching in future communication networks. *IEEE Communications Magazine*, 39(3):128–135, Mar 2001.

[PCDS14] A. Pizzinat, P. Chanclou, T. Diallo, and F. Saliou. Things you should know about fronthaul. In *Optical Communication (ECOC), 2014 European Conference on*, pages 1–3, Sept 2014.

[PLJ+14] Mugen Peng, Yuan Li, Jiamo Jiang, Jian Li, and Chonggang Wang. Heterogeneous cloud radio access networks: a new perspective for enhancing spectral and energy efficiencies. *Wireless Communications, IEEE*, 21(6):126–135, December 2014.

[PMC15] PMC. Enabling c-ran: The case for otn mobile fronthaul, 2015. [Online; accessed 05-March-2016].

[PWLP15] Mugen Peng, Chonggang Wang, V. Lau, and H.V. Poor. Fronthaul-constrained cloud radio access networks: insights and challenges. *Wireless Communications, IEEE*, 22(2):152–160, April 2015.

[QY99] Chunming Qiao and Myungsik Yoo. Optical burst switching (obs) - a new paradigm for an optical internet. *J. High Speed Netw.*, 8(1):69–84, March 1999.

[SGR+11] S. Smolorz, E. Gottwald, H. Rohde, D. Smith, and A. Poustie. Demonstration of a coherent udwdm-pon with real-time processing. In *Optical Fiber Communication Conference and Exposition (OFC/NFOEC), 2011 and the National Fiber Optic Engineers Conference*, pages 1–3, March 2011.

[SRV08] R. Sanchez, L. Raptis, and K. Vaxevanakis. Ethernet as a carrier grade technology: developments and innovations. *Communications Magazine, IEEE*, 46(9):88–94, September 2008.

[SSR11] N. Stol, M. Savi, and C. Raffaelli. 3-level integrated hybrid optical network (3lihon) to meet future qos requirements. In *Global Telecommunications Conference (GLOBECOM 2011), 2011 IEEE*, pages 1–6, Dec 2011.

[STK+15] N. Shibata, T. Tashiro, S. Kuwano, N. Yuki, Y. Fukada, J. Terada, and A. Otaka. Performance evaluation of mobile front-haul employing ethernet- based tdm-pon with iq data compression [invited]. *IEEE/OSA Journal of Optical Communications and Networking*, 7(11):B16–B22, November 2015.

[TMC14] TMCnet. Mobile fronthaul for cloud-ran deployment. http://www.tmcnet.com/tmc/whitepapers/documents/whitepapers/2014/10051-mobile-fronthaul-cloud-ran-deployment.pdf, April 2014. [Online; accessed 14-February-2016].

[Tra12] TransPacket. Fusion networking explained: Bringing true circuit and packet properties to the packet network. http://www.transpacket.com/wp-content/uploads/2012/06/White_paper_fusion_intro_12062012.pdf, July 2012. [Online; accessed 08-February-2016].

[Tra13] TransPacket. a fusion networking add-drop muxponder. http://www.transpacket.com/wp-content/uploads/2011/12/TransPacket-H1-Product-overview-v1.pdf, April 2013. [Online; accessed 08-February-2016].

[TZJ11] O. Tipmongkolsilp, S. Zaghloul, and A. Jukan. The evolution of cellular backhaul technologies: Current issues and future trends. *Communications Surveys Tutorials, IEEE*, 13(1):97–113, First 2011.

[VBB13] R. Veisllari, S. Bjornstad, and K. Bozorgebrahimi. Integrated packet/circuit hybrid network field trial with production traffic [invited]. *IEEE/OSA Journal of Optical Communications and Networking*, 5(10):A257–A266, Oct 2013.

[VBB+15] R. Veisllari, S. Bjornstad, J. P. Braute, K. Bozorgebrahimi, and C. Raffaelli. Field-trial demonstration of cost efficient sub-wavelength service through integrated packet/circuit hybrid network[invited]. *IEEE/OSA Journal of Optical Communications and Networking*, 7(3):A379–A387, March 2015.

[WAS15] T. Wan and P. Ashwood-Smith. A performance study of cpri over ethernet with ieee 802.1qbu and 802.1qbv enhancements. In *2015 IEEE Global Communications Conference (GLOBECOM)*, pages 1–6, Dec 2015.

[WZZ14] Kaiwei Wang, Ming Zhao, and Wuyang Zhou. Traffic-aware graph-based dynamic frequency reuse for heterogeneous cloud-ran. In *Global Communications Conference (GLOBECOM), 2014 IEEE*, pages 2308–2313, Dec 2014.

[ZBJ08] S. Zaghloul, W. Bziuk, and A. Jukan. A scalable billing architecture for future wireless mesh backhauls. In *Communications, 2008. ICC '08. IEEE International Conference on*, pages 2974–2978, May 2008.

Appendix A

IHON Node and Ethernet Switch Implementation

A.1 IHON Node Implementation

The simulation model for IHON node consists of two different kind of generator entities in order to simulate the arrival of GST and SM traffic. These entities are called GST_Generator and SMGenerator. Moreover, the simulation model consists of three additional entities: GSTPacket, SMPacket, and SM_packet_scheduler, and three queues: SM_Waiting, SM_pkt_check, and GST_pkt_check.

All entities are modeled based on the entity-entity synchronization with waitq's. The waitq's queues doesn't introduce any delay to the node, but it is used for synchronizing purpose.

A.1.1 GST_Generator Entity

The "GST_Generator" entity generates "GSTPacket" entities in a loop with mean arrivals per second defined by the poisson "GST_pkt_". Since GST packets have the absolute priority, they are not interrupted by SM packets. As soon as a GST packet is generated, it is scheduled immediately, and the output wavelength is acquired until the packet is completely transmitted.

Packets generated per simulation time from this source are fixed using a FOR-loop.

A.1.2 SMGenerator

The "SMGenerator" entity generates "SMPacket" entities in a loop with mean arrivals per second defined by the poisson "SM_pkt_". This entity check a queue called "SM_pkt_check" for the number of SM objects before scheduling a new SM packet. If the number of SM packet object exceeds 0, the SM packets from SM_pkt_check queues are scheduled before scheduling a new SM packet.

The number of packets generated by this type of source is fixed per simulation time. It operates in looped-manner with For-loop to generate fixed number of SM packets.

A.1.3 GSTPacket Entity

Every time a GST packet is generated and scheduled, the corresponding output wavelength is marked as busy(acquired) and fixed delay line as not empty to guarantee that it is being used to carry a GST packet. Hence, the GST source is directly linked to the output wavelength. Inside this entity, a bin called "Fixed_delay_line" is used to check if there is already a GST packet inline to find out when to change the pointer of the current GST packet. When the last bit of the GST packet arrives at FDL, it will be delayed for an FDL time. Until the last bit of the GST packet has left the start of the FDL, it is busy and release it for further use. After holding for the FDL length(in time), the GST packet take the resource and hold it for service time of GST, then release both the fixed delay line and output wavelength.

When GST packets arrives at the output link, the arrival, service and exit time of this packet is registered. And, after traversing the FDL, the arrival, service and exit times are reset again for another new packet. The booking for each GST packets such as average latency, PDV, the minimum and maximum latency is collected inside this entity.

A.1.4 SMPacket Entity

SMPacket entity has one parameter called "input" to itself. This parameter defines the number of SM input stream to the IHON node, and each input channel has a dedicated queue on the output wavelength. When a SM packet is generated from its respective source, the queue associated to this source is checked whether it exceeded the maximum buffer size or not. SM packets scheduled at the SM generator are stored in their respective buffer index upon their arrival if the buffer size at the index is less than the maximum buffer size. SM packet arrived when the buffer is full are marked as dropped. In side this entity, latency and packet delay variation of the SM traffic statistics are measured and collected. Moreover, the dropped SM traffic are measured for calculating the PLR.

A.1.5 SM_packet_scheduler Entity

The SM_packet_scheduler entity takes SM packets from the "SM_Waiting" queues. At the beginning, the buffer length of each input SM packets are checked. When a buffer with SM packets are found, the packets are taken with service time equivalent to service time of their length.

Inside this entity, the status of output wavelength and FDL is checked. If both the output wavelength and FDL are free, the SM packet taken from any of the buffer is served freely. However, if the delay line is not available, and there is an available gap, the length of the gap is computed according to the round robin filling gap discussed in Chapter 4 of Section 4.3.4.

If the computed gap is less than the minimum length of SM packet, hold this entity for the gap and recheck after GST has been scheduled.

A.1.6 SM_Waiting bin

This bin is used to inform "SM_packet_scheduler" entity that there is a packet in "SMPacket" entity for serving if it is arrived.

A.1.7 SM_pkt_check and GST_pkt_check queues

The use of these two queues avoids the excessive number of unprocessed SM packet and GST packet objects so that the processing time of the simula programming is greatly reduced.

A.2 Ethernet Switch Implementation

Like IHON node, the simulation model for Ethernet switch consists of two different kind of generator entities in order to simulate the arrival of HP and LP packets. These entities are called HP_Generator and LPGenerator. Moreover, the simulation model consists of four additional entities: HPPacket, LPPacket, HP_packet_scheduler, and LP_packet_scheduler and four queues: LP_Waiting, HP_Waiting, HP_pkt_check, and LP_pkt_check.

A.2.1 HP_Generator Entity

A single "HP_Generator" entity generates "HPPacket" in a loop with mean arrivals per second defined by the poisson "HP_pkt_". The packet length distribution is presented in Section 5.2.1.

A.2.2 LP_Generator Entity

The "LPGenerator" entity generates "LPPacket" entities in a loop with mean arrivals per second defined by the poisson "LP_pkt_". The distribution that governs the arrival of the next packet is presented in Section 5.2.1. As soon as a LP packet is generated, it is scheduled immediately.

The number of packets generated by this entity is fixed per simulation time. It operates in looped-manner to generate fixed number of SM packets.

A.2.3 HPPacket Entity

This entity class works with the entity class "HP_packet_scheduler" to transmit the HP packets in the system. All HP packets generated by the "HP_Generator" entity go to a buffer, called "Buffer_HP". After that, the packets are served one by one in FIFO basis. This entity always acquire the output wavelength if HP buffer is not empty.

A.2.4 LPPacket Entity

The "LPPacket" entity behaves close to the behaviour of "HPPacket" entity. It is one of the entities that has entity-entity cooperation with "LP_packet_scheduler". The entity waits for cooperation to to this scheduler and operates in a looped-manner. When LP packets are generated, they are queued in buffer upon their arrival if the buffer size at the index is less than the maximum buffer size. LP packet arrived when the buffer is full are marked as dropped. It is important to note that LP packets will never be served unless the HP buffer is empty. Once the HP buffer is empty. the system allows this entity to be served by the output wavelength. HP packets arriving when the LP packets are being served will wait for the time equivalent to the length of LP packet.

All the necessary computations such as the number of dropped packets, latency, and PDV of the LP traffic are done inside this entity.

A.2.5 HP_packet_scheduler Entity

The HP_packet_scheduler entity coops "HPPacket" entity from the "Buffer_HP" queues. Before serving the LP packets, the buffer length of HP packets is checked. When the buffer is not empty,then HP packets are served with time equivalent to the service time of the HP packet length to be served by the output wavelength.

A.2.6 LP_packet_scheduler Entity

The behaviour of this entity is almost exact to the behaviour of "HP_packet_scheduler" entity. This entity schedules the "LPPacket" entity only if the buffer of HP packets is empty; this is the only difference between the "HP_packet_scheduler" and "LP_packet_scheduler " entity. When the HP buffer is empty and LP buffer is not, then packets from the LP buffer are served by the output wavelength for a time equivalent to the service time of the LP packet.

However, if a LP packet is generated when the buffer is full and the output wavelength is occupied, the LP packet will be dropped. HP packets will not be dropped because they are given highest priority.

A.2.7 HP_Waiting Bin

"HP_Waiting" object is introduced to synchronize and inform all the system class's that the "Buffer_HP" is empty or the output wavelength is busy. This specific bin object is used to realize the cooperation between "HP_packet_scheduler" and "HPPacket" entity.

A.2.8 LP_Waiting Bin

Like "HP_Waiting", "LP_Waiting" object is introduced to synchronized and inform all the system class's the status of the "Buffer_LP" or output wavelength. And, it realizes realizes the cooperation between "LP_packet_scheduler" and "LPPacket" entity.

A.3 IHON and Ethernet Source Codes

Both IHON and Ethernet source codes are provided in the attached Zip file.

A.4 Input File and Output File

All input parameters required for the simulator are inserted through an input file, which allows us to run the simulation code by simply changing only the necessary information. Thus, it possible to perform different simulations without changing the body of simulation code. For instance, the input file for IHON code contains the following parametrs:

- Capacity of the wavelength;
- Length of the GST packet;
- The number of SM buffers in a single node;
- The minimum and maximum length of SM packets.

A typical example of an input file is found in the appendix Chapter C, Section C.1 and Section C.2.

After the required processing in the IHON node, ten output files are generated to keep track easily of the results:

- Input.txt, which has all the parameters required for this simulation, such as capacity, minimum SM packet length and so on.
- Average_latency_GST_plot.txt, which has GST latency results of the simulator of different GST loads.
- PDV_GST_plot.txt, which has GST PDV results of the simulator for different GST loads.
- ConfInte95_latency_gst.txt, which has the 95% confidence interval of GST latency results of the simulator for different GST loads.
- ConfInte95_PDV_gst.txt, which has the 95% confidence interval of GST PDV results of the simulator for different GST loads.
- Average_latency_SM_plot.txt, which has SM latency results of the simulator of different GST loads.
- PDV_SM_plot.txt, which has SM PDV results of the simulator for different GST loads.
- ConfInte95_latency_sm.txt, which has the 95% confidence interval of SM latency results of the simulator for different GST loads.
- ConfInte95_PDV_sm.txt, which has the 95% confidence interval of SM PDV results of the simulator for different GST loads.
- ConfInte95_PLR_sm.txt, which has the 95% confidence interval of SM PLR results of the simulator for different GST loads.
- PLR_SM_plot.txt, which has SM PLR results of the simulator of different GST loads.

At the end of the simulation, all the above output files are generated to present results of the implemented algorithm.

Similarly, the Ethernet code generates ten output files for the sake of analysis:

- Input_Ethernet.txt, which has all the parameters required for this simulation, such as buffer size, capacity, minimum LP packet length and so on.
- Average_latency_HP_plot.txt, which has HP latency results of the simulator of different HP loads.
- PDV_HP_plot.txt, which has HP PDV results of the simulator for different HP loads.
- ConfInte95_latency_HP.txt, which has the 95% confidence interval of HP latency results of the simulator for different HP loads.

- ConfInte95_PDV_HP.txt, which has the 95% confidence interval of HP PDV results of the simulator for different HP loads.
- Average_latency_LP_plot.txt, which has LP latency results of the simulator of different HP loads.
- PDV_LP_plot.txt, which has LP PDV results of the simulator for different HP loads.
- ConfInte95_latency_LP.txt, which has the 95% confidence interval of LP latency results of the simulator for different HP loads.
- ConfInte95_PDV_LP.txt, which has the 95% confidence interval of LP PDV results of the simulator for different HP loads.
- ConfInte95_PLR_LP.txt, which has the 95% confidence interval of LP PLR results of the simulator for different HP loads.
- PLR_LP_plot.txt, which has LP PLR results of the simulator of different HP loads.

A.5 Simulator Validation

The developed simulator is validated using two different approaches. The first approach is to trace the output of simulation for each event with the use of built-in DEMOS library function called trace. In this way, the report generated by Demos after the simulation testing ensures that the entities in the simulator behaves as intended at the right instance of time and/or in response to the events they are meant to. By doing so, the simulator is found to be working as intended.

The other approach used for validating the simulator is to compare the results of the simulator with the fronthaul requirement and ITU-T recommendation.

Appendix B
QoS Targets for Reference Service Classes

Table B.1: Requirements of demanding services and applications based on ITU-T recommendation Y.1541 [SSR11]

Service Classes	**Y.1541 QoS Class**	**Upper bound PLR**	**Upper bound Delay**	**Upper bound jitter**	**Bandwidth needed**
i. Video streaming	6 or 7	10^{-5}	100ms or 400ms	50ms	High
ii. Video Conversational	0 or 1	10^{-3}	100ms or 400ms	50ms	High
iii. Music streaming	6 or 7	10^{-5}	100ms or 400ms	50ms	Low to medium
iv. Voice conversational	0 or 1	10^{-3}	100ms or 400ms	50ms	Low
v. Interative messaging	3 (or2)	10^{-3}	400ms or 100ms	undef.	Low
vi. Control traffic	2	10^{-3}	100ms	undef.	Low
vii. General data transfer	4 or 5	10^{-3} *or undef.*	undef. or undef.	undef.	Low to High

Appendix C
Example of Input File

Note that since our simulation code uses a lot of wait queues, the simulation is slower and cim -m<tall> filename must be used to compile with increased memory. For example: cim -m100 IHON.sim will allow the simulator to use 100 Mbytes of memory.

Sample of an input file for the simulator of both IHON and Ethernet are given in Section C.1 and in Section C.2.

C.1 Input File for IHON Code: Input_IHON.txt

Seeds
907 234 326 104 711 523 883 113 417 656
capacity(in Gb/sec):
10
minlength(minmum length)(in Byte):
40
lengthGST(in Byte):
1200
maxlength(maximum length)(in Byte):
1500
load_GST
0.607
load_SM
0.3
Number_packet_Generated
40000
Number_of_SM_buffer
4
maxNobuffer
4

C.2 Input File for Ethernet Code: Input_Ethernet.txt

Seeds
907 234 326 104 711 523 883 113 417 656
capacity(in Gb/sec):
10
minlength(minmum length)(in Byte):
40
lengthHP(in Byte):
1200
mlength(maximum length)(in Byte):
1500
load_HP
0.49
load_LP
0.4
MaxbufferSize_HP(in MByte):
8
MaxbufferSize_LP(in MByte):
8
Numb_Packet_Generated:
40000

Appendix D

Confidence Interval Calculation In the Simulator

All the results in Chapter 6 are presented with 95% confidence interval accuracy level. The confidence interval of all parameter discussed in this work is calculated based on the formula given in [EHHP14].

Let Θ be unbaised and consistent estimator of a parameter ξ, i.e. $E(\Theta) = \xi$ and $Var(\Theta(n)) \to 0$ when $n \to \infty$. Let X_1,X_2,X_3,...,X_n be n independent and identically distributed observations, and $E(X_i) = \xi$ and $var(X_i) = \delta^2$, i = 1,2,...,n.

Time Average

$$\bar{X} = \frac{1}{T}\int_0^T x(t)dt \tag{D.1}$$

Sample mean

$$\widehat{X} = \frac{1}{n}\sum_{i=1}^{n} X_i \tag{D.2}$$

Sample variance

$$S^2 = \frac{1}{n-1}\sum_{i=1}^{n}(X_i - \widehat{X})^2 = \frac{1}{n-1}\sum_{i=1}^{n} X_i^2 - \frac{n}{n-1}\widehat{X}^2 \tag{D.3}$$

Variance of the sample mean

$$S^2_{\widehat{X}} = \frac{S^2}{n} \tag{D.4}$$

Standard error of the sample mean

$$S_{\widehat{X}} = \frac{S}{\sqrt{n}} \tag{D.5}$$

1 - α confidence interval for $\widehat{X}$ (with unknown variance)

$$(\widehat{X} - t_{\alpha/2,n-1}\,\frac{S}{\sqrt{n}}, \widehat{X} + t_{\alpha/2,n-1}\,\frac{S}{\sqrt{n}}) \tag{D.6}$$

($t_{\alpha/2,n-1}$ is the α quantile of the Student's t-distribution with n-1 degrees of freedom).